Institute of Experimental Cancer Research,

University Ulm

Chair: Prof. Dr. C. Buske

VENTX induced microRNA signatures in normal human hematopoiesis

Thesis submitted for the doctoral degree in Medicine at the Faculty of Medicine

Ulm University, Germany

By

Alexander Grunenberg

Essen

2012

Sitting dean: Prof. Dr. T. Wirth

First examiner: Prof. Dr. C. Buske

Second examiner: Prof. Dr. C. Beltinger

Date of oral examination: 12.07.2013

Table of contents

TABLE OF CONTENTS I

ABBREVIATIONS III

1. INTRODUCTION 1

1.1. Hematopoiesis 1

1.1.1. Embryonic Hematopoiesis 1
1.1.2. Adult Hematopoiesis 3

1.2. Leukemia 7

1.3. Homeobox Genes 12

1.3.1. Hox genes in normal and malignant hematopoiesis 13
1.3.2. Non Hox genes in normal and malignant hematopoiesis 15
1.3.3. VENTX 17

1.4. miRNA 21

1.4.1. miRNA in normal and malignant hematopoeisis 24

1.5. Aim of the study 27

2. MATERIALS AND METHODS 28

2.1. Materials 28

2.1.1. Consumables and and technical equipment 28
2.1.2. Cytokines and antibodies 32
2.1.3. Buffers and stock solutions 32
2.1.4. Kits and reagents for microRNA Profiling 34
2.1.5. Oligonucleotide for standard PCR 35
2.1.6. Oligonucleotide for Real-Time Quantitative PCR 35
2.1.7. Cell lines 35
2.1.8. Human cells 35

2.2. Methods 36

2.2.1. Cell cultivation 36
2.2.2. Thawing and freezing cells 36
2.2.3. Viability test and cell counting 36
2.2.4. Western blot 37
2.2.5. Retroviral constructs 38
2.2.6. Transduction of K562 cells 38
2.2.7. Transduction of cord blood cells 39
2.2.8. Immunophenotyping of transduced cord blood cells 40
2.2.9. Colony forming cell assay 41
2.2.10. Cytospin preparation 42
2.2.11. RNA extraction 42
2.2.12. Measurement of RNA and DNA concentration 43

2.2.13. RT-PCR 43
2.2.14. PCR 43
2.2.15. Agarose gel electrophoresis 44
2.2.16. Extraction of PCR products from agarose gel 45
2.2.17. Sequencing 45
2.2.18. RT- PCR and preamplification of cord blood cells 45
2.2.19. Quantitative Real-Time PCR 47
2.2.20. Search for miRNA target genes 52
2.2.21. Statistical analysis 52

3. RESULTS 53

3.1. Detection of VENTX expression in PG13 cells 53
3.2. Western Blot of PG13 cells 54
3.3. Efficiency of retroviral gene transfer of the AML cell line K562 54
3.4. Efficiency of retroviral gene transfer in cord blood cells 56
3.5. VENTX promotes human myeloid colony formation and inhibits erythroid development *in vitro* 57
3.6. Cytospin 59
3.7. RNA extraction of transduced cord blood cells 60
3.8. MicroRNA profiling of transduced cord blood cells 61
3.9. Sequencing of AML cell lines 72

4. DISCUSSION 77

5. SUMMARY 93

6. REFERENCES 95

7. ACKNOWLEDGEMENT 116

8. CURRICULUM VITAE 117

Abbreviations

AB	antibody
AGM	aorta gonad mesonephros
ALL	acute lymphatic leukemia
AML	acute myeloid leukemia
ANTP	antennapedia
APC	allophycocyanin
BFU-E	Burst Forming Unit Erythrocyte
BM	bone marrow
BMP-4	bone morphogentic protein-4
CB	cord blood
CDS	coding sequence
CFC	colony forming cell
CFU-E	Colony Forming Unit Erythrocyte
CLP	common lymphoid progenitor
CLL	chronic lymphoid leukemia
CML	chronic myeloid leukemia
CMP	common myeloid progenitor
CT	threshold cycle
DEPC	diethylpyrocarbonate
DMEM	Dulbecco's Modified Eagle's Medium
DMSO	dimethylsulfoxide
dNTP	deoxyribonucleotide triphosphate
FAB	French-American-British
FACS	fluorescence activated cell sorting
FBS	fetal bovine serum
Fig.	figure
GAPDH	glyceraldehyde 3-phosphatase dehydrogenase

GFP	green fluorescent protein
HSC	hematopoetic stem cell
IMDM	Iscove's Modified Dulbecco's Medium
IRES	internal ribosomal entry site
LSC	leukemic stem cell
miRNA	microRNA
MIG	MSCV–IRES –GFP
MLL	mixed lineage leukemia
MPP	multipotent progenitor cells
MSCV	murine stem cell virus
PS	penicillin/streptomycin
PCR	polymerase chain reaction
pMIG	MSCV–IRES –GFP plasmid
qRT-PCR	quantitative Real-Time PCR
RIPA	radio-immunoprecipitation assay
RT-PCR	reverse transcription polymerase chain reaction
SD	standard deviation
SFM	serum free medium
SNP	single nucleotide polymorphism
SDS	sodium dodecyl sulfate
Tab.	table
TAE	tris-acetate-EDTA
TBS (T)	tris buffered saline (+ tween)
VCM	virus containing medium
WT	wildtype

1. Introduction

1.1. Hematopoiesis

Blood consists of plasma, electrolytes, hormones and various cellular components. With the exception of a subpopulation of lymphocytes, the individual blood cells have only a limited lifespan and therefore need to be regenerated continuously. Under normal conditions, approximately 3.5 x 10^{11} new blood cells are produced daily in a healthy adult person [40]. This process of blood formation is referred to as hematopoiesis and is structured hierarchically. In the human body, a distinction is made between embryonic and adult hematopoiesis.

1.1.1. Embryonic Hematopoiesis

Hematopoiesis in mice and humans is very similar. For this reason, numerous studies have been conducted in recent decades to evaluate embryonic hematopoiesis in the mouse model [198]. Blood formation in the embryo takes place in various anatomical structures, depending on the embryonic stage (Fig. 1). In all vertebrates, hematopoiesis starts in the yolk sac mesoderm. In terms of its form, the mesoderm can be subdivided into a ventral and dorsal domain, also referred to as Spemann's organizer. It is assumed that mesodermal development is the result of an antagonistic relationship between ventralizing signals on the one hand and factors which stimulate dorsal development on the other [180] [66]. Maternal factors such as the transcription factors from the TGF-ß and FGF families lead to mesoderm induction at the blastula stage. The mesoderm ventralization which is important for embryonic hematopoiesis occurs during gastrulation. Ventralizing homeobox genes from the Vent and Mix families play a role in this [32] [73]. Both families are downstream targets of the BMP-4 signalling pathway. Lack of BMP-4 usually leads to premature embryonic death as a result of mesodermal defects [191] [83], whereas the ectopic expression of BMP-4 after gastrulation leads to increased blood production. Important early markers of hematopoietic mesoderm which are induced by BMP-4 are: GATA-1, GATA-2 and also the transcription factor SCL [117] [126]. The first blood islands subsequently develop from a small cluster of

cells in the ventral mesoderm. These differentiate into both hematopoietic and endothelial cells. The fact that both cell lineages arise simultaneously led to the assumption of a common precursor cell, known as the hemangioblast [194]. From this hemangioblast, the first primitive nucleated erythrocytes develop on day 7-7.5 after fertilization in the mouse. Myeloid precursor cells appear in the yolk sac one day later, and lymphoid precursor cells on day 8.5 post conceptionem [44] [61]. Because it was a long time before any other hematopoietic cell source was identified in the embryo, it was assumed that the yolk sac also supplied hematopoietic stem cells [131]. Further investigations revealed, however, that only HSCs from the AGM region of the embryo at day 10.5 p.c. are capable of reconstructing bone marrow in lethally irradiated adult mice. As a result of this, the AGM region is now considered to be the source of definitive hematopoiesis [30] [127]. Unlike the primitive hematopoiesis in the yolk sac, other specific transcription factors play a decisive role at this point in time. Mice which are deficient in RUNX1, part of the notch1 signalling pathway, die on day 10-12 post conceptionem, despite the fact that they exhibit nearly normal hematopoiesis in the yolk sac [44]. The HSCs produced in the AGM are released into the bloodstream one day later, and also colonize the yolk sac and placenta [37] [144]. The AGM region may not be capable of generating sufficient quantities of HSC on its own to colonize the fetal liver [95]. From day 10-12 post conceptionem, the fetal liver and thymus become involved in hematopoiesis. De novo HSC synthesis in the liver does not occur. Instead, there is expansion of HSCs and differentiation into erythrocytes, myeloid and lymphoid cells. Shortly before birth, the bone marrow takes over hematopoiesis [44] [60].

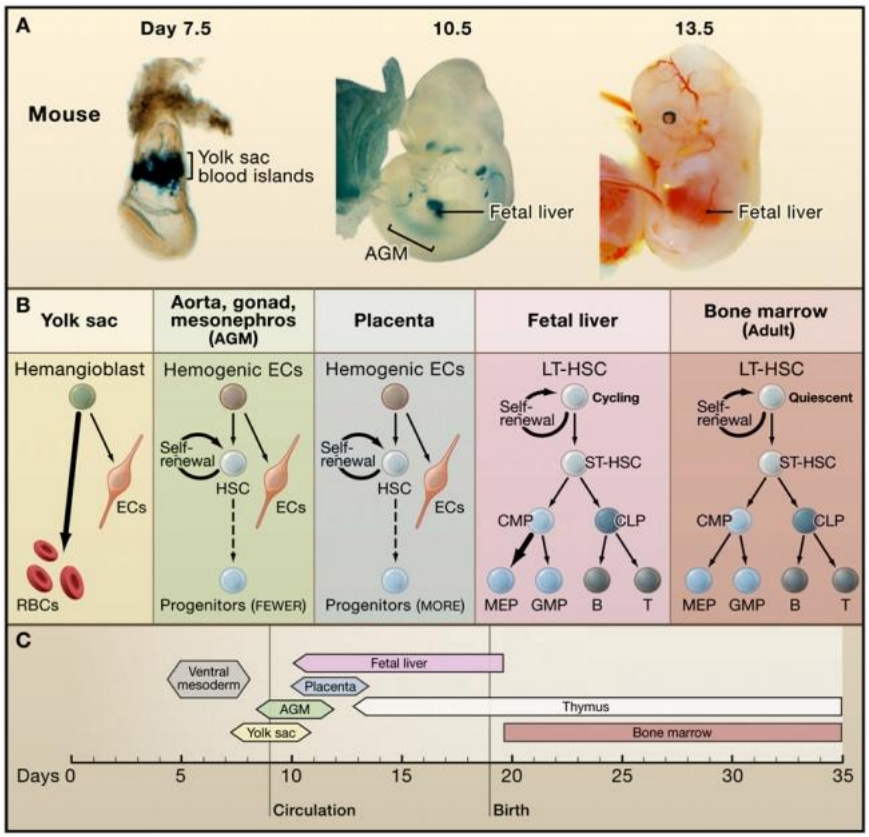

Fig. 1: **Developmental regulation of Hematopoiesis in the Mouse, adapted from [143, p. 632]**
(A) Hematopoiesis occurs first in the yolk sac blood islands and later at the AGM (aorta gonad mesonephros) region, plazenta, and fetal liver. (B) Hematopoiesis in each location favors the production of specific blood lineages, ECs (endothelial cells), RBCs (red blood cells), HSC (hematopoietic stem cell), LT-HSC (long-term hematopietic stem cell), ST-HSC (short-term hematopoietic stem cell), CMP (common myeloid progenitor), CLP (common lymphoid progenitor), MEP (megakaryocyte/erythroid progenitor), GMP (granulocyte/macrophage progenitor). (C) Developmental time windows for shifting sites of hematopoiesis

1.1.2. Adult Hematopoiesis

In all adult mammals, the site of hematopoiesis is the bone marrow. Throughout life, new blood cells are generated in this compartment and released into the peripheral blood. Only lymphopoiesis takes place additionally in other lymphatic tissues. All cells are derived from the pluripotent HSC which represents the top of the haematopoietic hierarchy (Fig. 2). Two properties characterize this cell: its ability to self-renew and its ability to differentiate into all types of blood cells. HSCs include long-term (LT-HSCs), short-term (ST-HSCs) and also the multipotent progenitor cells. Whereas the LT-HSC has a lifetime capacity for self-renewal, this capacity is limited to around eight weeks in the later ST-HSC stage. Multipotent progenitor cells (MPPs) self-renew only for a brief period, if at all, although they have a higher proliferation rate than their predecessors [147] [134] [158]. They represent a bridge

point in hematopoiesis and differentiate into oligolineage restricted progenitors, with common lymphoid progenitors (CLPs) being the precursors for all lymphoid cells, while common myeloid progenitors (CMPs) represent the starting point for the myeloid/erythroid lineages [88] [3]. Interestingly, dendritic cells arise from both CMPs and CLPs [120]. The production of functional, mature blood cells represents the end of the hematopoietic differentiation cascade.

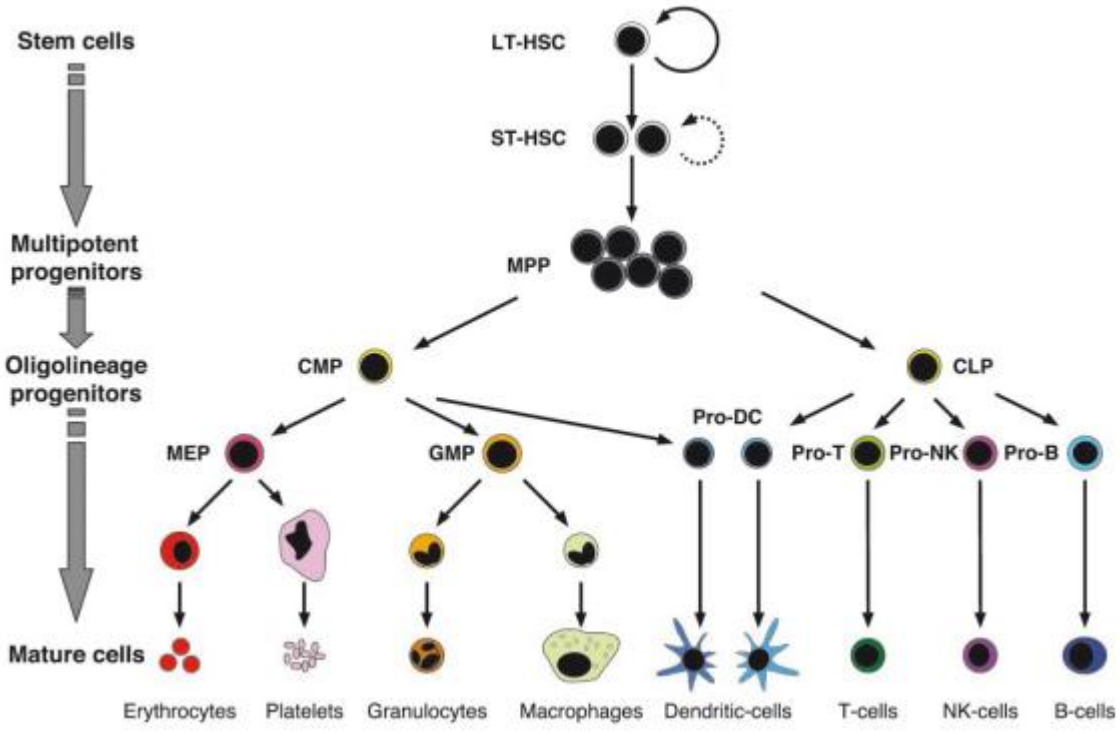

Fig. 2: Classical model of hematopoiesis, modified from [147, p. 11843]
Hematopoietic and progenitor cell lineages. Hematopoietic stem cells (HSCs) can be divided into highly self-renewing long-term (LT) HSCs and short-term (ST) HSCs which ability to self renew is limited and which differentiate into multipotent progenitors (MPP). MPPs do not or briefly self-renew and give rise to the oligolineage-restricted progenitors CMPs or CLPs, which in turn produce mature cells of the myeloid-erythroid lineage or the lymphoid lineage. Both CMPs and CLPs can give rise to dendritic cells. CMP (common myeloid progenitor), CLP (common lymphoid progenitor), MEP (megakaryotic/erythroid progenitors), GMP (myelomonocytic progenitors), DC (dendritic cells), NK (natural killer cells)

Hematopoietic Stem Cells

The existence of hematopoietic stem cells was first demonstrated by a series of experiments in the early 1960s. In lethally irradiated syngenic mice, transplanted bone marrow cells lead to the clonal proliferation of myeloerythroid colonies in the spleen [14]. A balance between self-renewal and lineage commitment is essential

if a sufficient pool of HSCs and a constant supply of new mononuclear blood cells (MBCs) is to be ensured in the long-term. If this homeostasis is disturbed in the form of abnormal HSC development, leukemia may develop [158]. The factors involved in HSC maintenance and differentiation can be divided into intrinsic and extrinsic signals. Known intrinsic factors are PTEN, BMI-1, TEL/ETV-6, p21 and the homeobox gene HOXB4. PTEN-deficient HSCs are more involved in the cell cycle and lead to a decrease in the stem cell pool [163]. Loss of function analyses in mice have shown that the Polycomb group gene BMI-1 represents an essential factor for HSC self-maintenance [78], and the transcription factor TEL/ETV-6 appears to be the first identified selective regulator of stem cell regeneration [71]. In experiments, retroviral overexpression of the homeobox gene HOXB4 showed a significantly increased number of HSCs [4] [22]. The cyclin-dependent kinase inhibitor p21 regulates the transition from G0 to G1 in the HSC cell cycle. In its absence, the number of HSCs decreases and there is an increase in HOXB4-induced stem cell self-renewal in $p21^{-/-}$ mice [29] [129].

In the bone marrow stem cell niche, HSCs are also under the influence of a range of external signalling pathways, with the notch signalling pathway playing an important role. Blockade of the notch signalling pathway leads to increased differentiation of HSCs in vitro and to a decrease in HSCs in vivo [43]. The highly conserved Wnt/ß-catenin signalling pathway also leads to HSC proliferation, whereas inhibitors of this signalling pathway lead to a reduction in vivo [157]. Two other factors which are involved in HSC regulation are the sonic hedgehog and Smad signalling pathways. One of the factors which activates the latter is TGF-ß, a known inhibitor of HSC proliferation [18].

Progenitors

Progenitor cells, regardless of their lineage, have lost the ability to self-renew. The lineage specification mechanisms of stem cells are still only partly understood, but there is a family of transcription factors (TFs), called a transcription factor network (TFN), the antagonizing or cooperative effects of which play an important role in the diversification of hematopoiesis [79].

Erythrocytes, megakaryocytes, eosinophils, neutrophils and monocytes are all derived from the common myeloid progenitor (CMP). In the CMP, the transcription factors PU.1 and GATA-1 are co-expressed and interact physiologically. The increased expression of the zinc finger transcription factor GATA-1 leads to differentiation into eosinophils, erythrocytes and megakaryocytes, the precursors of platelets [142]. Co-expression of GATA-1 and the cofactor FOG (friend of GATA-1) is important for the development of erythrocytes and megakaryocytes, whereas eosinophils express GATA-1 together with C/EBPß (Fig. 3) [152] [186].

Granulocytes and monocytes develop from the granulocyte/monocyte progenitor (GMP), with PU.1 representing an important transcription factor. The ETS family transcription factor PU.1 inhibits GATA-1 function by preventing GATA-1 from binding to relevant DNA sequences and thus promoting both myeloid and lymphoid differentiation (Fig. 3, 4). Whereas high concentrations of PU.1 lead to differentiation into macrophages (deriving from circulating monocytes), less high levels of PU.1 tend to favour lymphocytic development [201] [36]. Whether or not C/EBPα is expressed influences GMP lineage selection. C/EBPα expression is found mainly in granulocytes.The additional expression of PU.1 together with its partner, interferon consensus sequence-binding protein (ICSBP), is of greater relevance for the development of monocytes [203].

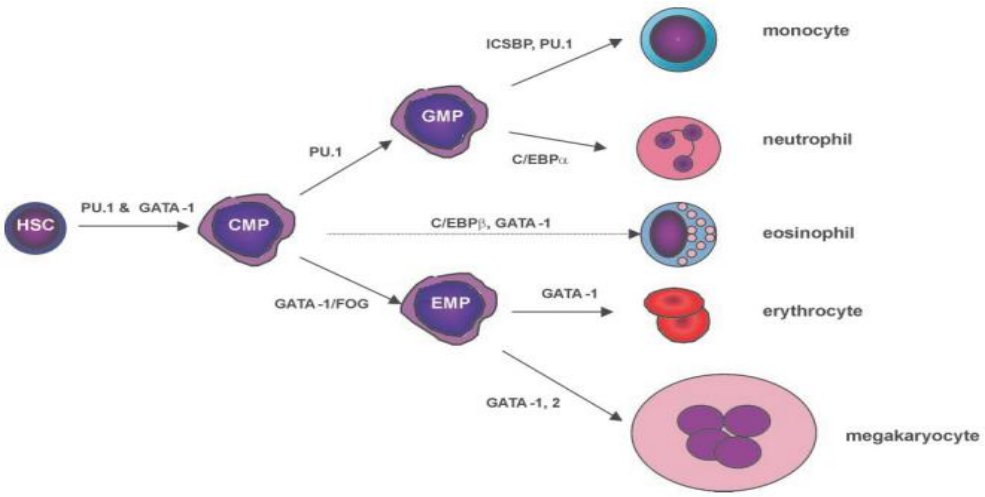

Fig. 3: **Transcriptional regulation of common myeloid precursor (CMP) commitment, adapted from [203, p. 3302]**
CMPs differentiate into either common precursors for granulocytic and monocytic lineages (GMPs) or common precusors for both erythroid and megakaryocytic lineages (EMPs). A separate, possible, pathway leading to eosinophils is depicted by dotted line. Dual expression of PU.1 and GATA-1 leads HSCs to CMPs, but then dominant expression of PU.1 is restricted to GMPs, while unopposed GATA-1 directs differrentiation to EMPs. HSC (hematopoietic stem cell)

Both T and B lymphocytes are derived from the common lymphoid progenitor (CLP). Besides the requirement for the transcription factor PU.1 which has already been mentioned, other characteristics of this progenitor are the surface expression of the IL-7 receptor, combined with a decrease in the G/M potential [38] (Fig. 4). The development of T lymphocytes takes place in the thymus, with the notch1 receptor signalling pathway being a crucial factor for the start of T lymphocyte development, inhibiting the transcription of genes which play a role in B cell development [203]. In contrast, E2A and EBF are initial transcription factors in B lymphocyte differentiation. In the absence of both, B cell differentiation is inhibited [204] [108]. EBF also directly regulates PAX5, another regulator of lymphopoiesis. Absence of this factor also blocks differentiation and can even lead to dedifferentiation of B cells [139].

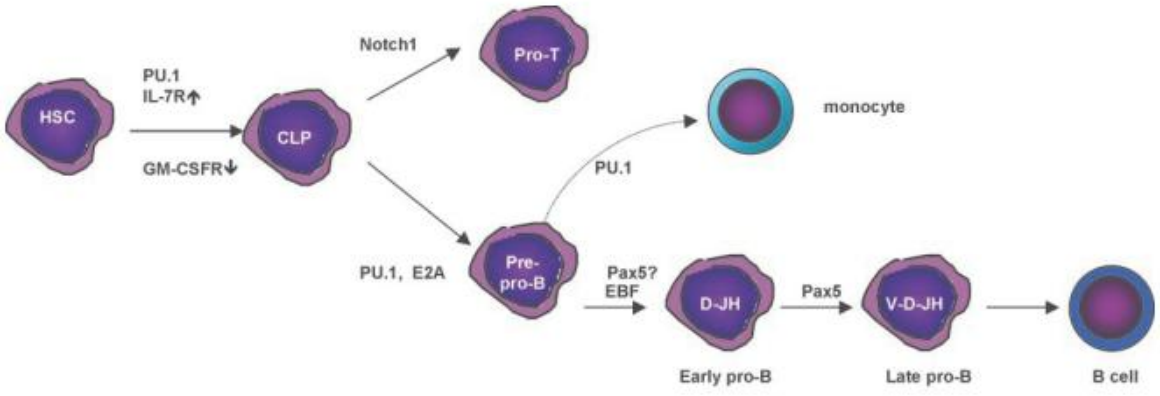

Fig. 4: Transcriptional regulation of common lymphoid precursor (CLP) commitment, adapted from [203, p. 3302]
B lymphocytes and T lymphocytes are derived from a common lymphoid precursor (CLP). The early development of B cell is distinguished into distinct stages by the sequential expression of different transcription factors that direct Ig gene recombination and the expression of B cell specific cell surface phenotyps. A proposed (alternative) differentiation pathway of macrophages from pro-B is also indicated by a dotted line. HSC (hematopoietic stem cell)

1.2. Leukemia

Leukemia is a malignant clonal disease originating from hematopoietic stem – and progenitor cells. The causes are diverse, and also often unclear. Possible triggers are benzene, ionizing rays, viruses and hematological or genetic disorders. A distinction is made between acute and chronic leukemias, depending on the course.

Each type of leukemia is characterized by its own age-specific incidence.The acute leukemias include the acute myeloid and acute lymphoid leukemias (AML and ALL), which generally lead to death within weeks or months if left untreated. The chronic forms of leukemia include chronic lymphoid leukemia, which is classified as an indolent non-Hodgkin's lymphoma, and chronic myeloid leukemia, which is classified as a myeloproliferative disorder.

Acute myeloid Leukemia

Acute myeloid leukemia is a very heterogeneous group of diseases genetically and in terms of phenotype and develops as a result of clonal transformation and proliferation of a multipotent hematopoietic stem cell. As a consequence, physiological hematopoiesis in the bone marrow is impaired by the leukaemia cells. Anaemia, granulocytopenia and thrombocytopenia are consequences of hematopoietic insufficiency. While ALL represents 80 % of acute leukemias in childhood, AML is responsible for 80 % of cases in adults and the median age at diagnosis is 65. There are two commonly used classification schemata for AML. The older FAB system classifies AML mainly according to criteria relating to blast cell morphology (Tab. 1).

Tab. 1: The FAB-classification (French-American-British) [16]

FAB-Subtype	Name	Cytogenetics
M0	minimally differentiated acute myeloblastic leukemia	
M1	acute myeloblastic leukemia, without maturation	
M2	acute myeloblastic leukemia, with maturation	t(8;21)(q22;q22), t(6;9)
M3	acute promyelocytic leukemia	t(15;17)
M4	acute myelomonocytic leukemia	inv(16)(p13q22), del(16q)
M4eo	myelomonocytic together with bone marrow eosinophilia	inv(16), t(16;16)
M5	acute monoblastic leukemia (M5a) or acute monocytic leukemia (M5b)	del (11q), t(9;11), t(11;19)
M6	acute erythroid leukemias	
M7	acute megakaryoblastic leukemia	t(1;22)
M8	acute basophilic leukemia	

The newer, revised WHO classification, on the other hand, incorporates immunophenotypic, cytogenetic and molecular genetic aspects in addition to morphology (Tab. 2).

Tab. 2: WHO Classification of 2008, only major disease categories are listed [67] [188]

Acute myeloid leukemia with recurrent genetic abnormalities:
AML with t(8;21) ; RUNX1-RUNX1T1
AML with inv(16)(p13.1q22) or t(16;16)(p13.1;q22); CBFB-MYH11
APL with t(15;17)(q22;q12); PML-RARA
AML with t(9;11)(p22;q23); MLLT3-MLL
AML with t(6;9)(p23;q34); DEK-NUP214
AML with inv(3)(q21q26.2) or t(3;3)(q21;q26.2); RPN1-EVI1
AML (megakaryoblastic) with t(1;22)(p13;q13); RBM15-MKL1
Acute myeloid leukemia with myelodysplasia-related changes
Therapy-related myeloid neoplasms
Acute myeloid leukemia,not otherwise specified (NOS)
AML with minimal differentiation
AML without maturation
AML with maturation
Acute myelomonocytic leukemia
Acute monoblastic/monocytic leukemia
Acute erythroid leukemia
Pure erythroid leukemia
Erythroleukemia, erythroid/myeloid
Acute megakaryoblastic leukemia
Acute basophilic leukemia
Acute panmyelosis with myelofibrosis

According to the WHO criteria, over 20 % myeloblasts must be present in the bone marrow for a diagnosis of AML. Entities with the genetic abnormalities t(15;17), t(8;21), inv(16) or t(16;16) and some cases of acute erythroid leukaemia are diagnosed as AML irrespective of the blast percentage [41]. Cytogenetically, a distinction can be made between two main subgroups of AML.

The first group, which accounts for almost 50 % of all AML cases, includes AML without chromosome aberrations, which means a normal karyotype. Molecular mutations are frequently found in this category (Fig. 5) [10], the most common of which involves the NPM1 gene which regulates the ARF-p53 tumour suppressor pathway and is present in 50 % of patients with a normal karyotype [47]. This is followed by mutations in the FLT-3 gene which codes for a tyrosine kinase receptor and is not uncommonly associated with NPM1 gene mutations [57] [10].

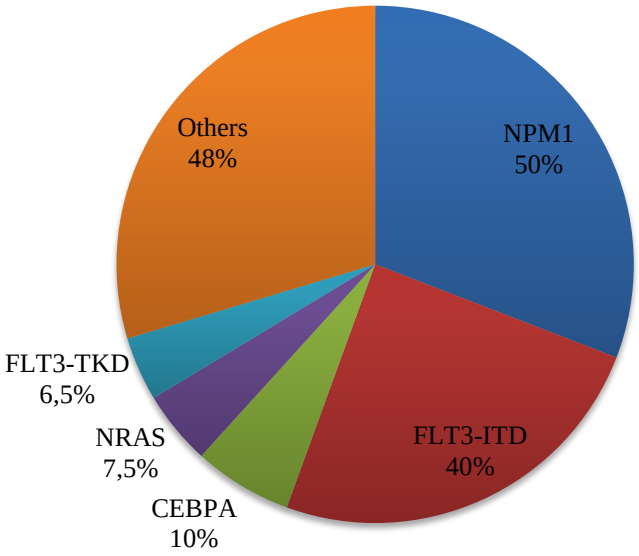

Fig. 5: Frequency of recurrent molecular mutations in normal karyotyp acute myeloid leukemia

The second cytogenetic group includes AML with an abnormal or complex karyotype. The translocation t(8;21) represents a common chromosomal abnormality in AML patients. It occurs in approximately 15 % of AML patients and exhibits an increased incidence in the FAB-M2 subtype. This translocation gives rise to the transcription factor fusion protein RUNX1-RUNX1T1 (also known as AML1-ETO), which promotes the self-renewal of haematopoietic cells and selectively inhibits erythroid and granulocytic differentiation [149] [185]. The rearrangement of chromosome 16 by inversion, inv(16), or its variant t(16;16) are associated with the FAB-M4eo subtype. The resulting fusion protein CBFß-MYH11 leads directly to repression of the tumour suppressor RUNX1(AML1) [112]. Other more frequently occurring alterations at the chromosomal level relate to rearrangements in the MLL gene and the translocation t(15;17) with the fusion protein PML/RARα [111] [170]. A complex karyotype is defined by three or more unrelated cytogenetic abnormalities.

Cancer is the result of a stepwise accumulation of genetic alterations resulting in a transformation from normal into malignant cells [65]. A “two hit” theory exists for AML, which states that at least two classes of mutation must be present for the disease to develop (Fig. 6).

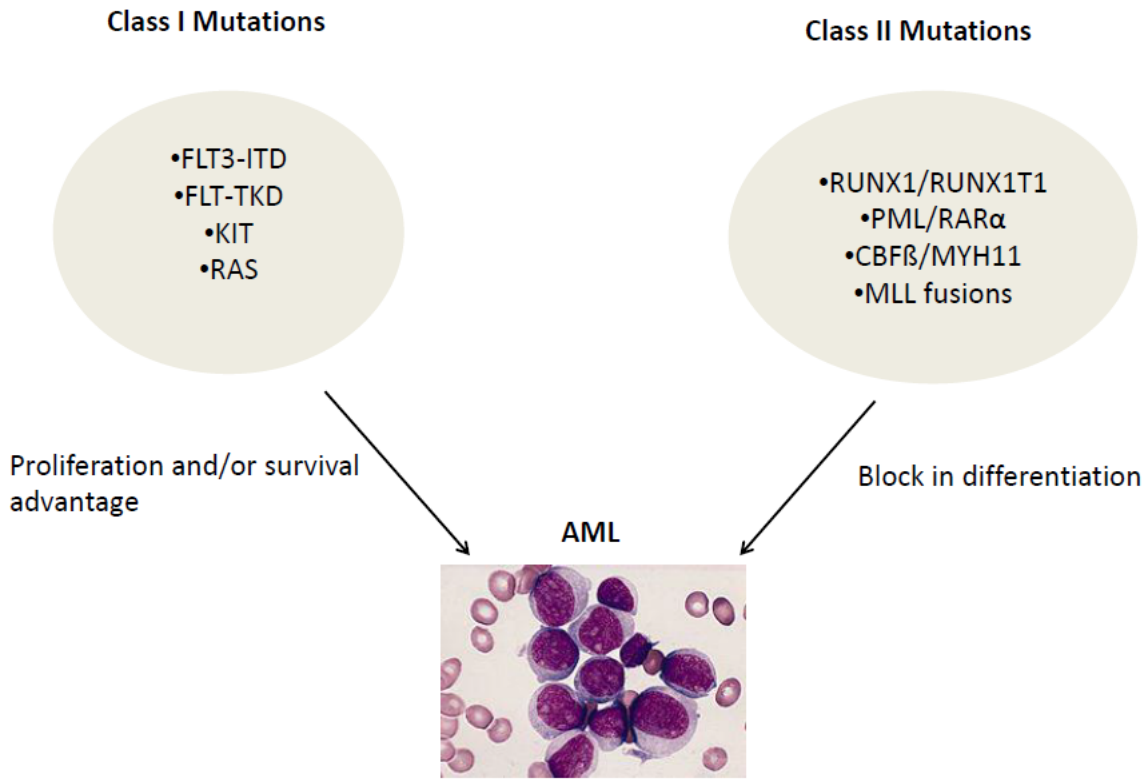

Fig. 6: Cooperating mutations in AML (acute myeloid leukemia), modified from [58, p. 1539]

Class I mutations confer proliferation and survival advantages, but have hardly any influence on cell differentiation. These mutations expressed in isolation cause myeloproliferative disease with normal differentiation. Class II mutations inhibit cell differentiation. When expressed in isolation, they give rise to myelodysplastic syndromes. In summary, what this means is that many of the aforementioned mutations are not capable of inducing AML in isolation, but that cooperation with distinct genetic alterations is required for this [15] [59].

1.3. Homeobox Genes

Homeobox genes represent a major family of transcription factors to which an essential role is attributed in embryogenesis, organogenesis, cell proliferation, cell differentiation and other developmental processes across organisms. The characteristic of this class of genes is the homeobox, a common sequence element of 180 bp which was first identified in the fruit fly Drosophila in 1983. The homeobox codes for a helix-turn-helix motif, or “homeodomain”, which contains 60 amino acids and which interacts sequence-specifically with the DNA of a multitude of other genes, either as an activator or a repressor [125] [55]. The human homeobox gene family is currently divided into 235 functional genes and 65 pseudogenes. These genes are in turn classified into 11 gene classes [72]. ANTP homeobox genes represent the biggest class, of which the best-known members are the 39 Hox genes. In the human body, as in other vertebrates, the Hox genes are arranged in four clusters in accordance with the homology to the genes of the fruit fly Drosophila (HOXA, HOXB, HOXC, HOXD), whereas the fruit fly has only one Hox gene cluster (HOM-C) (Fig. 7). Their main role during embryonic development is the formation of the anteroposterior body axis of the embryo [93]. Older studies in Drosophila showed that homeotic mutants, or individuals with mutations in these genes, exhibit changes in patterns of body parts which are significant in some cases. Such mutants may have four wings rather than two, for example [100] [105].

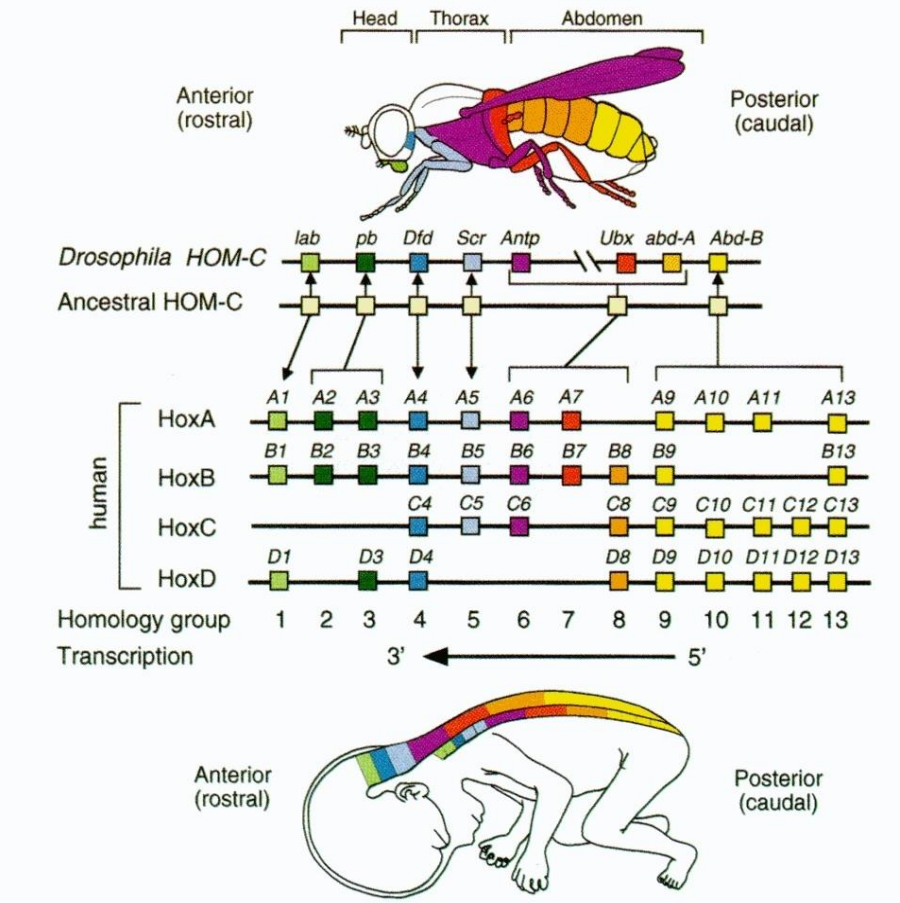

Fig. 7: Genomic organization and colinear expression patterns of Drosophila HOM genes and mammalian Hox genes, adapted from [121, p. 422]
Schematic representation of the Drosophila homeotic complex (HOM-C), the four human Hox complexes and a hypothetical ancestral homeotic complex are displayed showing their possible phylogenic relationships. Each gene is represented by a colored box. The expression domains of HOM/ Hox genes are schematized in a fly and in the CNS and prevertebrae of a human fetus. Within the different HOX clusters each gene can be divided into paralogous groups which is based on the sequence homology of their homeobox regions (shown by same colours). HOM gene abbreviations are: lab (labial), pb (proboscipedia), Dfd (Deformed), Scr (Sex combs reduced) Antp (Antennapedia), Ubx (Ultrabithorax), abd-A (abdominal-A), Abd-B (Abdominal-B)

Another common classification system divides the homeobox genes into two classes according to their arrangement within the genome. The clustered homeobox or Hox genes located on chromosomes 2, 7, 12 and 17 in the human genome belong to the Class I homeobox genes. Class II or non-clustered homeobox (non-Hox) genes are dispersed throughout the genome [145].

1.3.1. Hox genes in normal and malignant hematopoiesis

The significance of the Hox genes in hematopoiesis has been investigated in numerous studies via the overexpression of retroviral vectors in murine hematopoi-

etic stem cells and human umbilical cord blood and using knockout mouse models [145]. Hox genes play a role both in HSC self-renewal and in progenitor cell lineage specification. Their expression is tightly regulated and they exhibit expression of a time-limited nature with regard to their 3‘→ 5‘ chromosomal position during the haematopoietic differentiation cascade [118]. Many Hox genes are expressed in the early stages of hematopoiesis and are then downregulated or silenced during subsequent differentiation. Furthermore, only Hox genes from clusters A, B and C are expressed in early progenitor cells. HOXD genes are not expressed [164] [56]. As already mentioned in section 1.1.2., HOXB4 is a positive regulator of HSC self-renewal, and overexpression in *ex vivo* experiments showed a significantly increased number of HSCs compared with non-transduced cell cultures [4] [22]. HOXA9 is expressed mainly in primitive haematopoietic cells and HOXA9-deficient mice exhibit defects in the differentiation of their haematopoietic cells [7]. The Hox genes with the greatest specificity in their expression pattern are HOXA10, expressed mainly in myelomonocytic cell lines, and HOXC4, which plays a role only in lymphoid progenitor cells [99].

Homeobox genes which are physiologically expressed in non-differentiated cells such as the Hox genes (class I genes) are generally overexpressed in cancer, whereas those homeobox genes which are normally expressed in differentiated cells are downregulated in cancer [1]. The deregulation of Hox genes is of significance both in myeloid and lymphoblastic leukaemia [7] [75]. Sixty per cent of patients with AML, particularly those with a normal karyotype, exhibit an altered pattern of Hox gene expression. The first evidence of the involvement of homeobox genes in leukaemia development was the identification of the HOXB8 (Hox-2.4) Hox gene in the myeloid leukaemia WEHI-3B cell line, the constitutive activation of which leads to inhibition of myeloid cell differentiation [89] [19]. In other studies, the overexpression of individual Hox genes such as HOXB6, HOXA10, HOXA9 or HOXB3 in murine bone marrow cells resulted in leukaemia with long latency [49] [181] [92], there being a significant reduction in the time to development of the full-blown AML phenotype with the coexpression of certain non-Hox homeobox genes (section 1.3.2.) [145]. Furthermore, few Hox genes are associated with leukaemia-specific translocations. Both HOXA9 and HOXD13, which are not expressed constitutively in normal hematopoiesis, form fusion genes with the nucleoporin gene NUP98 and lead to leukaemic transformation [138] [109]. Chromosomal rear-

rangements in the MLL (mixed lineage leukaemia) gene play a role in 5 % of AML cases. This gene is essential for physiological hematopoiesis and is a known upstream regulator of Hox genes [33]. In the majority of cases, however, the cause of aberrant Hox gene expression remains unclear.

1.3.2. Non Hox genes in normal and malignant hematopoiesis

Many non clustered (class II) homeobox genes, are less well characterized in terms of their role than Hox genes. As a rule their gen size is smaller than Hox genes, they are dispersed throughout the genome, and their regulatory effects are more specific and limited mainly to organogenesis and cell differentiation.

One example of the role of the non-Hox homeobox genes in hematopoiesis is the hematopoietically-expressed homeobox protein (HHEX) gene. It is essential both in primitive hematopoiesis at the hemangioblast stage (Fig. 1) and in adult hematopoiesis, in which it influences multipotent progenitor cell differentiation [148]. The HB24 (HLX) homeobox gene displays selective expression in $CD34^+$ bone marrow cells and is downregulated in the subsequent process of hematopoietic cell differentiation [35]. Various experiments have shown that some non-Hox genes function as cofactors for Hox proteins. The three-amino-acid-loop-extension (TALE) proteins PBX and MEIS belong to this group. They interact directly with Hox proteins in order to increase their DNA binding affinity and specificity [130]. Paralogous group 1-10 Hox proteins interact with the divergent homeodomain protein PBX1, whereas paralogous groups 11-13 interact with MEIS1 [167]. Loss-of-function experiments with these Hox cofactors have shown that they influence a range of Hox-dependent pathways, and both PBX1- and MEIS1-deficient embryos display defects in haematopoiesis and are unviable [39] [70]. The deregulated expression of non-Hox cofactors with some Hox genes led to leukemic transformation in mouse models and human myeloid leukemia cells, with non-Hox cofactors being capable of shortening the latency for leukemia development. Although the overexpression of PBX1 and MEIS1 is not sufficient in isolation for leukemia development [7], PBX1 does have oncogenic potential as a fusion protein with E2A via the t(1;19) translocation which is probably caused by dysregulation of certain target genes and which is cytogenetically detectable in 25 % of children with pre-B ALL [101] [84]. MEIS1 is overexpressed in half of patients with AML and was first

identified together with HOXA7 and HOXA9 in myeloid cells of BXH-2 mice [2] [135]. Other non-Hox genes such as CDX2, HOX11 or PMX1 play no role in physiological hematopoiesis, although they are associated with leukemia [145]. CDX2 belongs to the ParaHox A cluster and is an upstream regulator of Hox genes. In adults, its expression is strictly limited to intestinal development, and overexpression leads to intestinal metaplasia [76]. CDX2 is overexpressed in over 90 % of patients with AML (Fig. 8). At the cytogenetic level, CDX2 forms a fusion gene with ETV6, a member of the ETS family (section 1.1.2.), via the t(12;13) translation, although interestingly this gene is incapable of inducing leukaemia itself. The result of this balanced translocation is the ectopic expression of CDX2 in the hematopoietic system where it acts as an oncogene and induces fatal AML in transplanted mice [154].

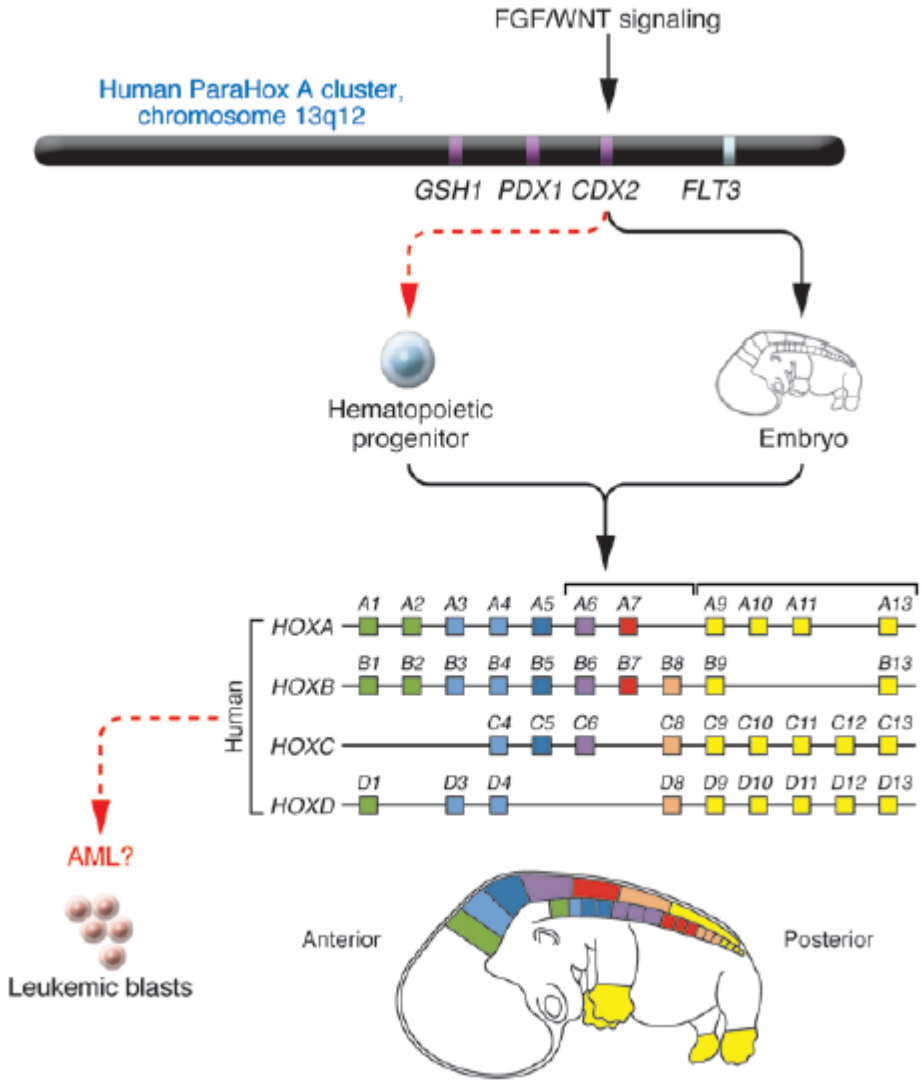

Fig. 8: A model for CDX2-mediated leukemogenesis, adapted from [160,p. 866]
CDX2 is expressed in the posterior primitive streak during embryogenesis, where it directs anteroposterior axial development and elongation by regulating HOX gene expression. Monoallelic expression of CDX2 is observed in 90 % of patients with acute myeloid leukemia (AML) and may perturb hematopoiesis by affecting HOX gene expression (red dashed arrows indicate ectopic expression; black arrows indicate normal expression in embryonic development).

1.3.3. VENTX

The human homeobox gene VENTX (formerly VENTX2/HPX42B) is a non-Hox (class II) homeobox gene and belongs to the large ANTP class of homeobox genes. This is further subdivided into the HOXL subclass, composed mainly of the Hox genes, and the NKL subclass, to which VENTX belongs [133]. This gene is localized at chromosome 10q 26.3 and, for a genome length of 4.03 kbp, has a molecular weight of 28 kDa [133]. The protein structure of VENTX is illustrated in Fig. 9.

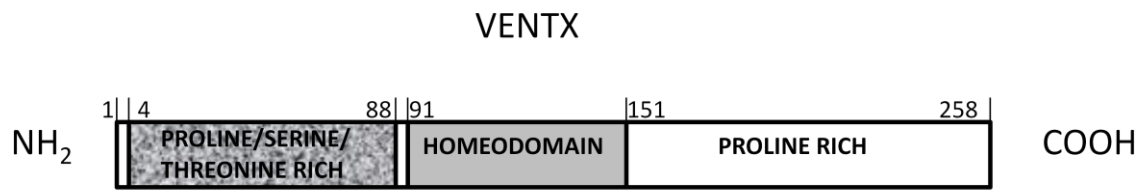

Fig. 9: VENTX protein structure, modified from [133, p. 25]
VENTX contains a high percentage of serine and threonine at the amino terminus, a homeodomain between 91-151 and an overall high frequency of proline. The protein is 258 residues in length. Numbers above represent amino acids positions**.**

VENTX is the human homologue of the Xenopus xvent2b gene. Xvent2b is a member of the multigenic Vent HB gene family which is essential for the formation of the ventral mesoderm and haematopoietic development in Xenopus. This gene family can be further subdivided into two families on the basis of their sequence homology outside the homeodomain. The Vent-1 subfamily in Xenopus includes xvent1, xvent1b and pvi [54] [153] [8]. The Vent-2 subfamily consists of xvent2, xom, xvent2b, Xbr-1, and vox genes [141] [96] [153] [146] [165]. VENTX has 65% identity between its homeodomain and the homeodomain of the xvent2b gene and is the first mammalian gene member of the Vent HB gene family identified to date [133]. Members of the xvent family act as direct and indirect downstream targets for the BMP-4 protein. BMP-4 is the key molecule in the development of the ventral mesoderm which gives rise to hematopoiesis in the embryo following gastrulation (section 1.1.1.). The individual xvent genes from the two Vent subfamilies differ greatly in terms of their expression patterns in time and space during this process. Whereas xvent1b and xvent2b are expressed in the ventral mesoderm, xvent2b is also expressed in the dorsal mesoderm [153]. As a direct target for BMP-4, xvent2b is expressed in an identical manner to BMP-4 throughout embryonic development and is capable of upregulating BMP-4 expression itself via a positive autoregulatory loop [69] (Fig. 10). The cooperative interaction of xvent2b and GATA-2 is required for the activation of xvent1b as an indirect target for the BMP-4 pathway, however [50].

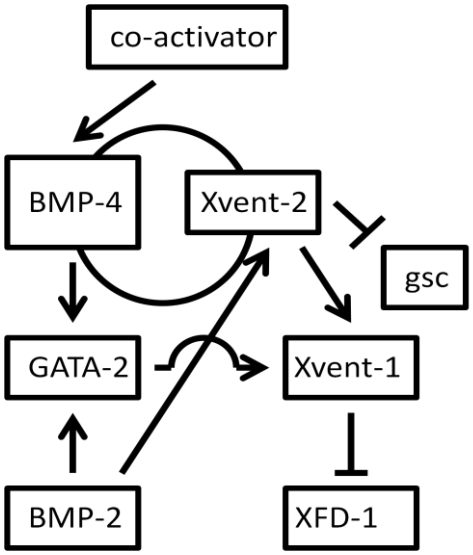

Fig. 10: Genetic cascades involved in the activation and autocatalytic regulation of BMP-4, modified from [166, p. 34372]
While BMP-4 activates Xvent-2 and GATA-2, only Xvent-2 is able to up-regulate BMP-4. BMP-2 protein translated from maternal RNA activates Xvent-2 and triggers the autocatalytic loop, which is subsequently maintained by BMP-4 and Xvent-2 recruiting a yet unknown co-activator. Xvent-2 suppresses gsc. GATA-2 and Xvent-2 activate Xvent-1 which has been shown to repress ventral expression of the dorsal lip-specific winged helix gene XFD-1.

The ectopic expression of members of the Vent HB gene family leads to ventralization in Xenopus and zebra fish embryos. Analogously, VENTX overexpression causes anterior truncation in zebra fish embryos in experiments (Fig. 11).

The role of VENTX in human hematopoiesis has been studied more closely in recent years. Interestingly, it has not been possible to identify a homologue of the Xenopus Vent HB gene family in the mouse, which means that it is not possible to study the function of this gene in the syngenic mouse model. VENTX displays an expression pattern opposite to that of Hox genes which are expressed mainly in immature $CD34^+$ bone marrow cells and are downregulated during subsequent differentiation (section 1.3.1.), there being significantly less expression of VENTX in the $CD34^+$ stem cell compartment than in the more mature $CD34^-/CD38^+$ mononuclear bone marrow cells. Furthermore, VENTX expression levels are significantly higher in myeloid than in lymphoid and erythroid cells. It was possible to confirm this finding via the overexpression of VENTX in retroviral based human cord blood xenograft transplantation model in NOD/SCID mice. Most of the genes which are upregulated by VENTX are those associated with myelopoiesis such as CD11b, CD125 or CD9, whereas genes which are responsible for erythropoiesis, including EPOR, are downregulated. The impaired development of lymphoid cells is attribut-

able to the fact that VENTX represents an LEF1/TCF-associated transcription factor which inhibits the highly conserved Wnt/ß-catenin signalling pathway [155]. This signalling pathway is essential for B cell development [159].

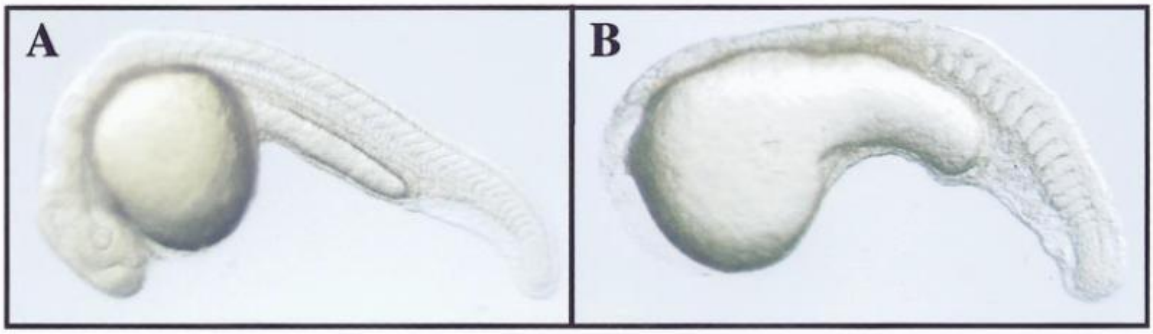

Fig. 11: Ventralization of zebrafish embryos by human *VENTX2* overexpression, adapted from [133, p. 27]
Embryos were injected at the 1- to 4-cell stage with VENTX2 mRNA and photographed after 1 day of development. (A) Uninjected control embryo. (B) VENTX2-injected embryo showing a ventralized phenotype.

Interestingly, there is initial evidence that VENTX is also of relevance in malignant hematopoiesis. The majority of AML patients exhibit significantly increased VENTX expression in studies compared with normal $CD34^+$ and mononuclear bone marrow cells, with AML patients classified as FAB-M2 with the translocation t(8;21) and with a normal karyotype displaying the highest levels of abnormal VENTX expression. In these patients, VENTX expression is particularly high in the $CD34^+$ compartment compared with normal hematopoiesis, which means that the aberrant expression of this gene may contribute to the development of leukemia in some patients [155]. This assumption is based on the existence of the current theory that, in AML, the $CD34^+$ compartment harbours LSCs which are responsible for initiating and maintaining the disease [158]. In addition, knockdown studies of VENTX in human AML cell lines show that this gene is of relevance for the proliferative activity of AML cells [155]. Other studies have shown that VENTX may also function as a putative tumour suppressor in lymphoid malignancies. In CLL, VENTX is significantly downregulated as a negative regulator of cell proliferation, which is associated with changes in the Wnt/ß-catenin signalling pathway [52].

1.4. miRNA

miRNAs are highly conserved endogenous, non-coding RNAs of around 22 nucleotides in length, and represent a young, as yet insufficiently studied, class of gene regulators. Non-coding RNAs are RNA molecules which are not translated into proteins like mRNAs but have a function after transcription. They include rRNAs, tRNAs and small RNAs (miRNAs, siRNAs, piRNAs). miRNAs were first described with the discovery of the function of the lin-4 gene in the Caenorhabditis elegans worm in 1993 [102] [12]. The name miRNA was not coined until 2001, however [200]. miRNAs function as negative gene regulators via a mechanism known as RNA interference which is used to switch off genes in a targeted manner in eukaryotes. In broad terms, the principle consists of the interaction between miRNA and a protein-coding mRNA with the involvement of several enzyme complexes. This causes destruction of the mRNA and translation into a protein is no longer possible [169]. The biogenesis and biological function of miRNA is illustrated in Fig. 12. Interestingly, as one can see in Fig. 12 during typical biogenesis of miRNAs only one strand, the mature miRNA, is loaded in the miRISC complex, whereas the other one is degraded (not shown in this figure). It is called miRNA* or passenger strand. Until recently miRNA* function was believed as merely carrier strand without biological function. However today there is evidence that at least some miRNAs* probably represent potential regulatory molecules with abundant expression [63]. miRNAs are expressed in a large number of organisms and are also involved in a wide range of diseases, including cancer, alongside physiological cell processes such as cell differentiation/proliferation and apoptosis [87]. Over 17,000 miRNA sequences are currently known in more than 140 species, all of which can be looked up on the miRBase online database [128] [90] [62]. By 2009, 400 human miRNAs had been identified in the human genome [13]. According to miRBase number has dramatically increased to 1898 human miRNAs by the end of 2011[128]. miRNAs can be classified into families on the basis of the sequence homology at their 5´ end. The first 2-8 nucleotides at this 5´ end are referred to as the “seed region” and are important for the biological function of miRNAs.

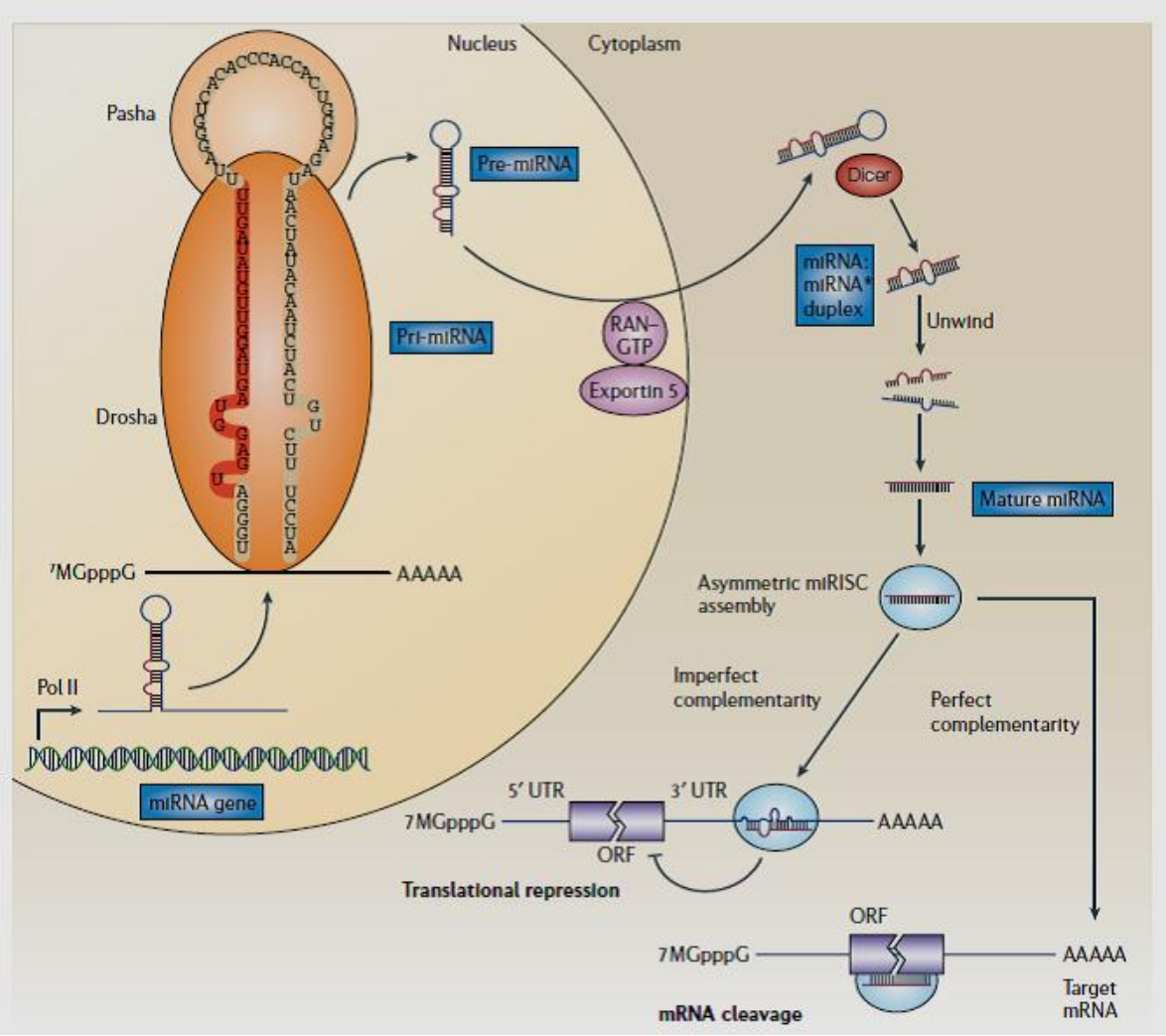

Fig. 12: The biogenesis and function of microRNAs, adapted from [46, p. 261]
MicroRNA (miRNA) genes are generally transcribed by RNA Polymerase II (Pol II) in the nucleus to form large pri-miRNA transcripts, which are capped ($_7$MGpppG) and polyadenylated (AAAAA). These pri-miRNA transcripts are processed by the RNase III enzyme Drosha and its co-factor, Pasha, to release the ~70-nucleotide pre-miRNA precursor product. (Note that the human let-7a-1 miRNA is shown here as an example of a pre-miRNA hairpin sequence. The mature miRNA sequence is shown in red.) RAN–GTP and exportin 5 transport the pre-miRNA into the cytoplasm. Subsequently, another RNase III enzyme, Dicer, processes the pre-miRNA to generate a transient ~22-nucleotide miRNA:miRNA* duplex. This duplex is then loaded into the miRNA-associated multiprotein RNA-induced silencing complex (miRISC) (light blue), which includes the Argonaute proteins, and the mature single-stranded miRNA (red) is preferentially retained in this complex. The mature miRNA then binds to complementary sites in the mRNA target to negatively regulate gene expression in one of two ways that depend on the degree of complementarity between the miRNA and its target. miRNAs that bind to mRNA targets with imperfect complementarity (in general metazoa) block target gene expression at the level of protein translation (lower left). However, recent evidence indicates that miRNAs might also affect mRNA stability (not shown). Complementary sites for miRNAs using this mechanism are generally found in the 3′ untranslated regions (3’ UTRs) of the target mRNA genes. miRNAs that bind to their mRNA targets with perfect (or nearly perfect) complementarity (in general plants) induce target-mRNA cleavage (lower right). miRNAs using this mechanism bind to miRNA complementary sites that are generally found in the coding sequence or open reading frame (ORF) of the mRNA target.

This “seed region” is the determining factor for binding to the 3′ untranslated regions of the target mRNA genes. Within a miRNA family, the 3′ end determines the target specificity of the individual family members [21]. miRNAs represent a

major gene class which accounts for 1-4 % of all expressed genes in humans and regulates the expression of an estimated 30-60 % of human mRNAs. In addition, even individual miRNAs are probably capable of regulating up to 200 gene targets with a wide range of functions [107] [51] [46]. The organization of the miRNA genes in the genome is complex. Around half of all miRNAs lie in the introns of protein-coding genes or non-coding mRNA transcripts [162]. The other half are found either in intergenic regions, within exons of non-coding mRNA genes, or in the 3' ends of coding mRNA genes [140]. miRNAs are also arranged in clusters. A cluster generally includes two or three non-homologous miRNAs. One hypothesis for this is that the clustered miRNAs are functionally related with regard to their gene targets [199]. One example of such a cluster is the miR-17-92 cluster, over-expression of which promotes the proliferation of lung epithelial progenitor cells and inhibits their differentiation [113]. Interestingly, miRNAs are also associated with the Hox gene clusters. In vertebrates, the miRNA miR-196 sequence is localized between the two Hox genes HOX9 and HOX10, and miR-10 between HOX4 and HOX5 [177]. It is known that 50 % of the miRNA genes are localized to chromosome regions which are associated with various types of cancer [23]. miRNAs are consequently considered capable of acting both as tumour suppressors and oncogenes (Fig.13). let-7 family miRNAs act as tumour suppressors by regulating the expression of the Ras oncogene which is mutant in many human tumours [82]. miRNA21, on the other hand, acts as an oncogene in human glioblastoma [27]. On the basis of this causal relationship with carcinogenesis, miRNAs represent a new class of potential therapeutic targets and open up a new field of therapeutic approaches. The development of synthetic RNAs which are complement mature miRNA and are referred to as antagomirs lead efficiently to miRNA inactivation in vivo. At the same time, in the event of loss of miRNAs which function as tumour suppressors, synthesized RNAs might help to replace them and thus to treat specific tumours [94].

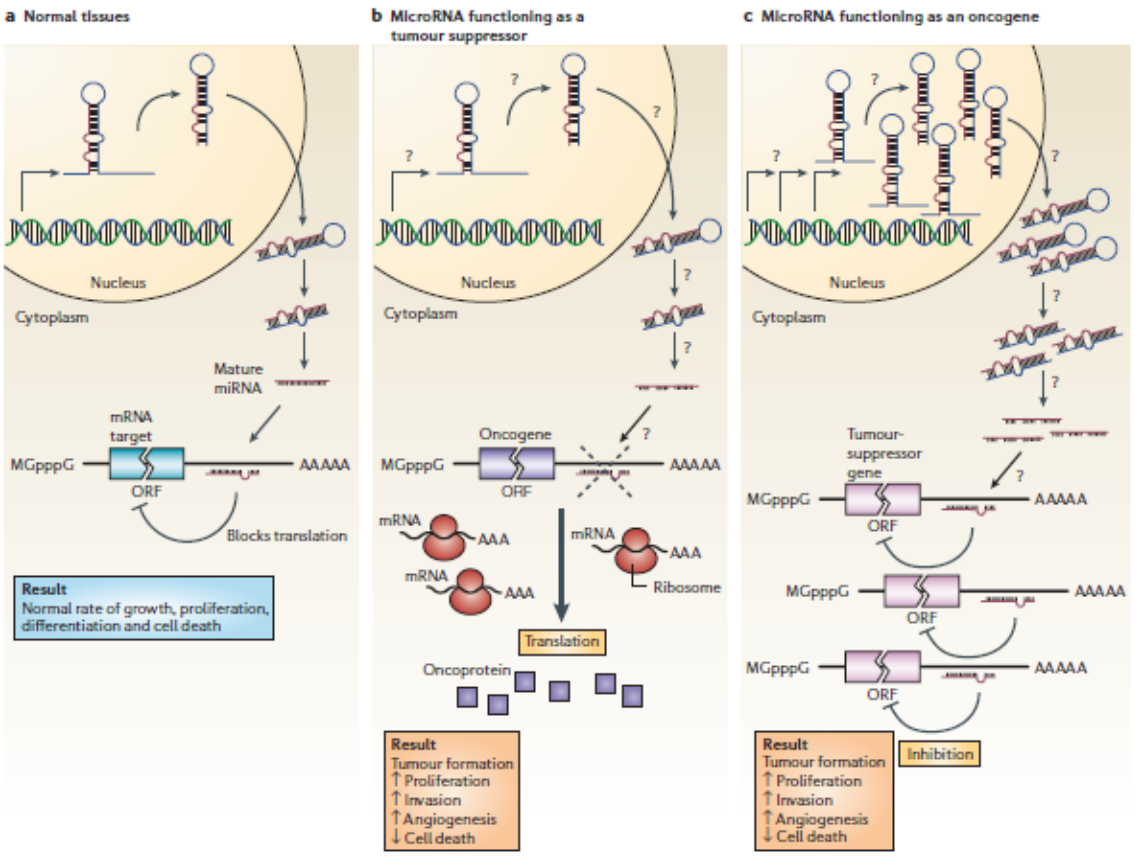

Fig. 13: MicroRNAs can function as tumor suppressors and oncogenes, adapted from [46, p. 263]
a) In normal tissues, proper microRNA transcription,processing and binding to complementary sequneces on the target mRNA results in the repression of target-gene expression through a block in protein translation. The overall result is normal rates of cellular growth, proliferation,differentiation and cell death. b) The reduction or deletion of a miRNA that functions as a tumor suppressor leads to tumour formation. A reduction in or elimination of mature miRNA levels can occur because of defects at any stage of miRNA biogenesis (indicated by question marks) and ultimately leads to inappropiate expression of the miRNA-target oncoprotein (purple squares). The overall outcome might involve increased proliferation,invasiveness or angiogenesis, decreased levels of apoptosis, or undifferentiated or de-differentiated tissue, ultimately leading to tumour formation. c) The amplification or overexpression of a miRNA that has an oncogenic role would also result in tumour formation. In this situation,increased amounts of a miRNA,which might be produced at inappropiate times or in the wrong tissues, would eliminate the expression of a miRNA-target tumour-supressor gene (pink) and lead to cancer progression. Increased levels of mature miRNA might occur because of amplification of the miRNA gene, a constitutively active promoter, increased efficiency in miRNA processing or increased stability of the miRNA (indicating by question marks). ORF (open reading frame)

It may therefore be possible in the future for these antagomirs to be used to inactivate a large number of miRNAs in tumours or to help slow their growth.

1.4.1. miRNA in normal and malignant hematopoeisis

The first evidence of the importance of miRNAs in hematopoiesis came to light in 2004, when it was shown in studies that miRNAs are expressed specifically in hematopoietic cells and they are subject to a specific expression pattern during he-

matopoietic development. As an example, the miRNA miR-181 is expressed primarily in B lymphocytes and their precursor cells, and ectopic overexpression of this miRNA in stem cells or progenitor cells leads to a significant increase in B cell levels in vivo and in vitro [28]. Since this discovery, many other studies have yielded a considerable number of miRNAs with a role in hematopoiesis [68]. A summary of well characterized miRNAs in hematopoiesis is provided in Fig.14.

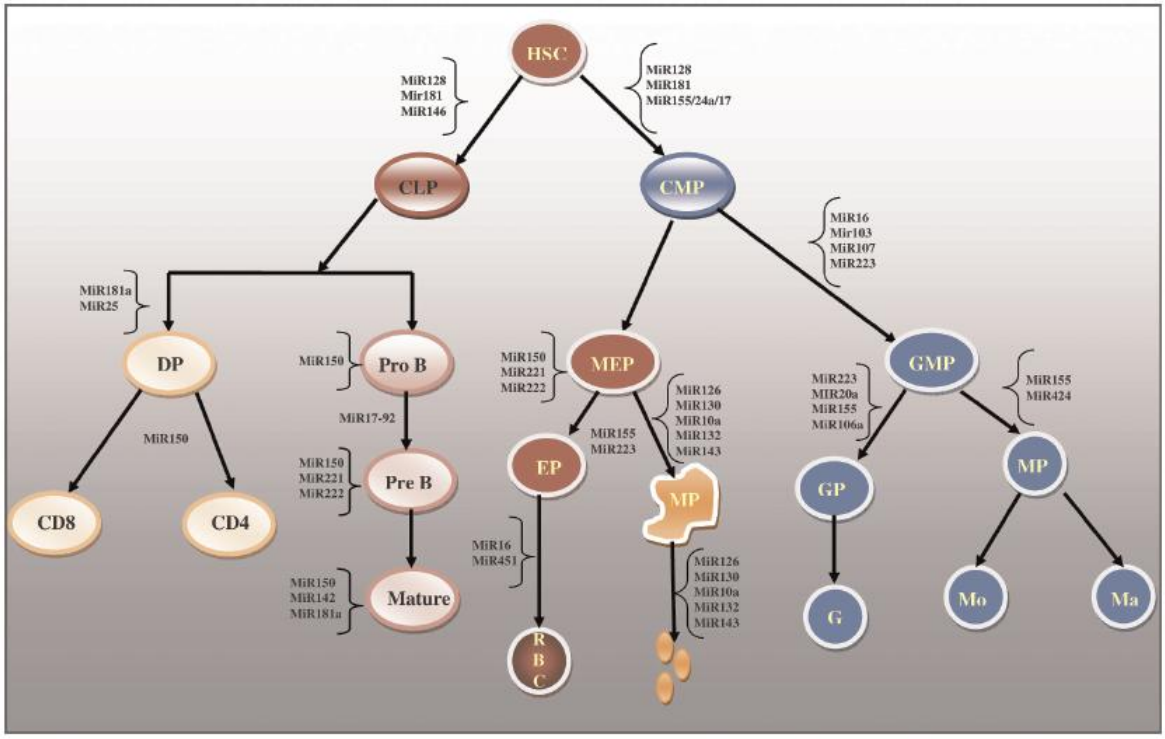

Fig. 14: Role of different microRNAs in normal hematopoiesis, adapted from [17, p. 1278]
Abbreviations: CLP (common lymphoid progenitor), CMP (common myeloid progenitor), DP (double positive) EP (erythroid progenitor), G (granulocyte) GMP, (granulocyte macrophage progenitor), GP (granulocyte progenitor), HSC (hematopoietic stem cells), MEP (macrophage erythroid progenitor), MP (monocyte/macrophage progenitor), Mo (monocyte), Ma (macrophage)

miRNAs regulate hematopoiesis, both as a result of their post-transcriptional inhibition of a wide range of targets and by the fine regulation of transcription factors. PU.1, an important transcription factor for lineage commitment in hematopoietic cells, is a known target of miR-155, for example [189]. The idea that miRNAs are involved in cancer development at all first emerged when it was shown that the two miRNAs, miR-15 and miR-16, are frequently downregulated in CLL patients with the chromosome deletion 13q14 [24]. The upregulation of miR-10 (section 1.4.) correlates with high levels of Hox gene expression in AML patients with a normal karyotype [53]. miR-223, involved in myeloid fate (Fig. 14) of progenitor cells is

epigentically silenced by the AML-ETO1 fusion protein, which is characteristic of AML FAB subtype M2 with the translocation t(8;21) [48]. Physiologically expressed in HSC and downregulated in progenitors overexpression of miR-29a is believed to initiate AML by converting myeloid progenitors into LSC [64]. Increased levels of miR-155 expression are associated with B cell lymphomas [45]. In summary, this small number of examples is intended to illustrate that the deregulated expression of individual miRNAs plays a major role in the development of malignant processes in hematopoiesis.

1.5. Aim of the study

In recent years, numerous advances have been made in our understanding of the molecular network which regulates the self-renewal and differentiation of hematopoietic cells. It has thus been possible to demonstrate that homeobox genes, which play a role in embryonic body formation, also have a relevant part to play in hematopoiesis. As a member of this homeobox gene family, VENTX has been characterized functionally in recent years, demonstrating that it has a significant influence on the differentiation of hematopoietic cells and plays a role in malignant hematopoiesis. Although some target genes of VENTX have already been identified, there is still a need to further elucidate the role of VENTX, including in relation to malignant hematopoiesis. Possible candidate genes include the non-coding miRNAs, which are also of fundamental importance in many physiological processes and are still relatively unstudied. The aim of this work was to examine the influence of VENTX on the expression of miRNAs. To test this, human umbilical cord blood cells was transduced with VENTX or the blank control vector by means of retroviral gene transfer and the expression of several hundred miRNAs was measured quantitatively by TaqMan Low Density Arrays. This allowed the identification of differentially expressed miRNAs between cells aberrantly expressing VENTX and normal controls.

Another separate objective of this work was to investigate, whether VENTX mutations occur in human acute myeloid leukemia cell lines. For this, VENTX was sequenced to exclude mutations resulting in an altered protein structure.

2. Materials and Methods

2.1. Materials

2.1.1. Consumables and and technical equipment

DMEM	PAN Biotech, Aidenbach, Germany
DPBS	PAN Biotech, Aidenbach, Germany
RPMI	PAN Biotech, Aidenbach, Germany
DMSO	Sigma- Aldrich, Taufkirchen, Germany
Ciprobay 400	Bayer, Leverkusen, Germany
FBS	PAN Biotech, Aidenbach, Germany
IMDM	Gibco /Invitrogen, Carlsbad, CA, USA
β- Mercaptoethanol	Gibco /Invitrogen, Carlsbad, CA, USA
Isopropanol	Sigma- Aldrich, Taufkirchen,Germany
Ethanol	Sigma- Aldrich, Taufkirchen,Germany
Trizol	Gibco /Invitrogen, Carlsbad, CA, USA
Polybren (8 mg/ml)	Sigma- Aldrich,Taufkirchen, Germany
Protaminsulfat (5 mg/ml)	Sigma- Aldrich, Taufkirchen, Germany
Methylcellulose M3434	Stem Cell Technologies, Vancouver, Canada
BIT 9500 serum substitute	Stem Cell Technologies, Vancouver, Canada
Penicillin/Streptomycin	PAN Biotech, Aidenbach, Germany
Quick load 100 bp DNA ladder	New England Bio Labs, Ipswich, MA, USA
Quick load 1 kb DNA ladder	New England Bio Labs, Ipswich, MA, USA
Loading dye (6X)	New England Bio Labs, Ipswich, MA, USA
Milk powder	Roth, Karlsruhe, Germany
Trypanblue solution (0.4 %)	Sigma- Aldrich, Taufkirchen, Germany

Myco-1	Appli Chem, Darmstadt, Germany
Myco-2	Appli Chem, Darmstadt, Germany
Chloroform	Appli Chem, Darmstadt, Germany
Gel red	Biotium, Hayward, CA, USA
Agarose	Sigma- Aldrich, Taufkirchen, Germany
7-aminoactinomycin D (7-AAD)	Becton Dickinson, Franklin Lakes, NJ, USA
Hemacolor	Merck, Darmstadt, Germany
Proteaseinhibitor 1	Sigma-Aldrich, Taufkirchen, Germany
Sytox blue	Gibco /Invitrogen, Carlsbad, CA, USA
DEPC- treated water	Applied biosystems, Foster City, CA, USA
Trypsin EDTA	Gibco /Invitrogen, Carlsbad, CA, USA
Phosphatase inhibitor cocktail 1 & 2	Sigma- Aldrich, Taufkirchen, Germany
ECL Western Blotting Detection Reagents	Amersham, Freiburg, Germany
Bradford Reagent	Appli Chem, Darmstadt, Germany
Tween 20	Appli Chem, Darmstadt, Germany
Ladder spectra multicolor	Fermentas, St. Leon Rot, Germany
TEMED	Biorad, Hercules, CA, USA
TBS	Appli Chem, Darmstadt, Germany
Rotiphorese gel A and B	Roth, Karlsruhe, Germany
Ammoniumpersulfat	Sigma-Adrich, Taufkirchen, Germany
BSA	Sigma-Adrich, Taufkirchen, Germany
Bromphenol blue	Merck, Darmstadt, Germany
Triton X-100	Sigma-Adrich, Taufkirchen, Germany
Methanol	Sigma-Adrich, Taufkirchen, Germany
SDS	Appli Chem, Darmstadt, Germany
Syringe filter (0.45 µl und 0.22 µl)	Millipore, Billerica, MA, USA

Gel elektrophoresis chamber	Thermo Fisher Scientific, Waltham, MA, USA
Spectrophotometer Nano Drop 1000	Thermo Fisher Scientific, Waltham, MA, USA
7900 HT Fast Real Time PCR- System	Applied Biosystems, Foster City, CA, USA
PCR-Thermocycler	PeqLAB Biotechnologie,Erlangen,Germany
Water bath	GFL, Burgwedel, Germany
Precision balance CS-200	Ohaus, Nänikon, Switzerland
Cytospin 4 Centrifuge	Thermo Fisher Scientific, Waltham, MA, USA
Centrifuge 5810 & 5415 R	Eppendorf, Leipzig, Germany
FACS Aria III Sorter	Becton Dickinson, Franklin Lakes, NJ, USA
FACS Calibur with Cellquest software	Becton Dickinson, Franklin Lakes, NJ, USA
Neubauer counting chamber	Laboroptik, Friedrichsdorf, Germany
Microscope Axiovert 40 C	Carl Zeiss AG, Jena, Germany
Cell scraper	Corning, NY, USA
Petri dish	Becton Dickinson, Franklin Lakes, NJ, USA
Cell incubator	Binder, Tuftlingen, Germany
CL-1000 Ultraviolet Crosslinker	UVP, Cambridge, Great Britain
50 ml Falcon tube	Becton Dickinson, Franklin Lakes, NJ, USA
15 ml Falcon tube	Sarstedt, Nümbrecht, Germany
Eppendorf tube	Roth, Karlsruhe, Germany
^{137}Cs radiation source	Molsgard Medical, Kopenhagen, Denmark
FACS tube	Becton Dickinson, Franklin Lakes, NJ, USA
Cryo tube	Nunc, Roskilde, Denmark
PCR soft tube	Biozym, Oldenburg, Germany
Cytospin cuvette	Thermo Fisher Scientific, Waltham, MA, USA
Cytospin filter	Thermo Fisher Scientific, Waltham, MA, USA
6-well culture plate	Sarstedt, Nümbrecht, Germany

96-well plate	Applied Biosystems, Foster City, CA, USA
Corning dish	Corning, NY, USA
Cell culture dish (35 mm und 100 mm)	Corning, NY, USA
Blunt end needle	Stem Cell Technologies, Vancouver, Canada
Culture flask (200 ml)	Sarstedt, Newton, NC, USA
Western blot chamber	CBS Scientific, Del Mar, CA, USA
Liquid nitrogen	Chart Biomed, GA, USA
Fridge	Liebherr, Ochsenhausen, Germany
Slide	Roth, Karlsruhe, Germany
Insulin needle	Becton Dickinson, Franklin Lakes, NJ, USA
Needle	Becton Dickinson, Franklin Lakes, NJ, USA
Syringe	Becton Dickinson, Franklin Lakes, NJ, USA
Pipette	Eppendorf, Leipzig, Germany
Vortexer	Scientific Industries, NY, USA
Filter tip	Sarstedt, Newton, NC, USA
High Performance UV-Transilluminator	UVP, Cambridge, Great Britain
Scalpel	Braun, Tuttlingen, Germany
Biophotometer	Eppendorf, Leipzig, Germany
Microwave	Sharp, Hamburg, Germany
Nitrocellulose membrane	Protran, Schleicher & Schüll, Dassel, Germany
Hyperfilm	Amersham, Freiburg, Germany
Hypercassette	Amersham, Freiburg, Germany
Semi-Dry transfer chamber	CBS Scientific, Del Mar, CA, USA

2.1.2. Cytokines and antibodies

rhIL-3	Immunotools, Friesoythe, Germany
rhIL-6	Immunotools, Friesoythe, Germany
rhSCF	Immunotools, Friesoythe, Germany
rhFLT3 Ligand	Immunotools, Friesoythe, Germany
rhG-CSF	Immunotools, Friesoythe, Germany
APC mouse IgG1, κ isotype control AB	Becton Dickinson, Franklin Lakes, NJ, USA
APC mouse anti- human CD 34^+ AB	Becton Dickinson, Franklin Lakes, NJ, USA
Anti VENTX AB	Abcam, Cambridge, United Kingdom
Goat anti mouse IgG-HRP AB	Santa Cruz Biotechnology, CA, USA
Anti ß-Actin AB	Santa Cruz Biotechnology, CA, USA

2.1.3. Buffers and stock solutions

TAE buffer (50X)	2 M Tris (pH 8.0)
	1 M acetic acid
	50 mM EDTA-NA_2 X 2 H_2O
Freezing medium	90 % FBS
	10 % DMSO
TE buffer (100X)	1 M Tris (pH 8.0)
	100 mM EDTA-Na_2 x 2 H_2O
SFM	399 ml IMDM
	100 ml BIT serum substitute
	1 ml mercaptoethanol
	275 µl Ciprobay 400
FACS buffer	PBS
	10 % SFM

100X cytokine cocktail	100 ng/ ml rhFLT3 Ligand
	100 ng/ ml rhSCF
	20 ng/ ml rhIL-3
	20 ng/ ml rhIL-6
	20 ng/ ml rhG-CSF
RIPA buffer	150 mM sodium chloride
	1 % Triton X-100
	0.5 % sodium deoxycholate
	0.1 % SDS (sodium dodecyl sulphate)
	50 mM Tris HCl (pH 7.5)
Laemmli buffer (2X)	4 % SDS
	10 % mercaptoethanol
	20 % glycerol
	0.004 % bromophenol blue
	0.125 M Tris HCl
Tris-glycine buffer (1X)	25.5 mM Tris base (pH 8.3)
	190 mM glycine
	900 ml H_2O
	0.1 % SDS
Transblotting solution	1X Tris glycine buffer
	200 µl mercaptoethanol
Resolving gel (12 %)	30 % acrylamide mix
	1.5 M Tris HCl (pH 8.8)
	10 % SDS
	10 % Ammoniumpersulfat
	TEMED

Stacking gel (5 %)	30 % Acrylamide Mix
	1.5 M Tris HCl (pH 8.8)
	10 % SDS
	10 % Ammoniumpersulfat
	TEMED
Stripping solution	20 ml SDS 10 %
	12.5 ml Tris HCl 0.5 M (pH 6.8)
	0.8 ml mercaptoethanol
	67.5 ml distilled water
TBS (1X)	20 mM Tris-HCl (pH 7.5)
	150 mM NaCl
TBST (1X)	20 mM Tris-HCl (pH 7.5)
	150 mM NaCl
	0.1 % Tween 20

2.1.4. Kits and reagents for microRNA Profiling

PCR x Enhancer System	Gibco/ Invitrogen,Carlsbad,CA, USA
ThermoScript RT-PCR System	Gibco/ Invitrogen, Carlsbad, CA, USA
Platinum *Taq* DNA Polymerase	Gibco/ Invitrogen, Carlsbad, CA, USA
Illustra GFX PCR DNA and Gel Band Purification Kit	GE Healthcare, Uppsala, Sweden
TaqMan MicroRNA Reverse Transcription Kit	Applied Biosystems, Foster City, CA, USA
TaqMan PreAmp Master Mix	Applied Biosystems, Foster City, CA, USA
TaqMan Universal Master Mix NoAmpErase UNG	Applied Biosystems, Foster City, CA, USA
TaqMan Human MicroRNA Array A+B	Applied Biosystems, Foster City, CA, USA

2.1.5. Oligonucleotide for standard PCR

Human

VENTX for	Gibco /Invitrogen, Carlsbad, CA, USA
VENTX rev	Gibco /Invitrogen, Carlsbad, CA, USA
ß-actin for	Gibco /Invitrogen, Carlsbad, CA, USA
ß-actin rev	Gibco /Invitrogen, Carlsbad, CA, USA

2.1.6. Oligonucleotide for Real-Time Quantitative PCR

Human

VENTX	Applied Biosystems, Foster City, CA, USA

Murine

GAPDH	Applied Biosystems, Foster City, CA, USA

2.1.7. Cell lines

Murine

PG13 mouse embryonic fibroblast packaging cell line	ATCC (American Type Culture Collection)

Human

K562 erythroleukemia cell line	ATCC (American Type Culture Collection)
NB-4 promyelocytic leukemia cell line	ATCC (American Type Culture Collection)
MV4-11 myelomonocytic leukemia cell line	ATCC (American Type Culture Collection)
EOL-1 eosinophilic leukemia cell line	ATCC (American Type Culture Collection)
OCI-AML3 acute myeloid cell line	ATCC (American Type Culture Collection)

2.1.8. Human cells

$CD34^+$ cord blood cells (>90 % purity) Donor 19793 (≥1x 10^6) cells Date cryopreserved: 31 August 2010 Cat. No. : 2C-101 Lot No: OF3908	Lonza, Cologne, Germany

2.2. Methods

2.2.1. Cell cultivation

Adherent cell lines were cultivated in DMEM plus 10 % FBS and 1 % PS. Suspension cells were cultivated in RPMI plus 10 % FBS and 1 % PS. The cells were split into 1:10 dilutions every 2-3 days due to their high doubling rate (~ 1 day) and to maintain log phase growth. The human $CD34^+$ umbilical cord blood cells were cultivated in serum free medium (SFM), which was enriched with the following cytokines: 100 ng/ml rhFlt3-ligand, 100 ng/ml rhSCF, 20 ng/ml, rhIL-6, 20 ng/ml, rhIL-3 and 20 ng/ml rhG-CSF. All cell lines were incubated in a humid atmosphere at 37°C at 5 % CO_2.

2.2.2. Thawing and freezing cells

Frozen cells were incubated in a water bath at 37°C while shaking gently and transferred to a Falcon tube directly after thawing. 10-20 ml of medium were added dropwise. After centrifugation at 1100 rpm for 5-10 minutes the cell pellet was washed twice with warm medium to remove residues of DMSO. The cells were then transferred to 10 cm Corning dishes or culture bottles.

If necessary for freezing, the cells were trypsinized and centrifuged under the conditions specified above. 1 ml of freezing medium per 5×10^5 – 5×10^7 cells was pipetted slowly onto the cell pellet. Aliquots of 1 ml were frozen in cryo tubes at -80°C for short-term storage and subsequently to the liquid nitrogen tank for long-term storage.

2.2.3. Viability test and cell counting

Trypan blue dye was used to determine the number and proportion of live cells. Trypan blue is an anionic azo dye which binds onto cell proteins. As a result of defective cell membranes of dead cells, trypan blue penetrates the cytosol of the cells and stains these dark blue. In contrast, living cells will have a clear cytoplasm under the microscope at 10- to 40-fold magnification. In order to count the cells, 10

µl of the cell suspension were diluted with 10 µl of trypan blue (0.4 %) and the cell number per ml was calculated in the Neubauer counting chamber as follows:

Mean value of 4 large quadrants x 2 (dilution factor) x 10^4 (chamber factor)

2.2.4. Western blot

The protein expression of PG13 cells was confirmed by western blot. The cells were washed twice with PBS and, after centrifugation, lysed with 300 µl of RIPA lysis buffer containing protease and phosphatase inhibitors. The samples were incubated on ice for 30 minutes and centrifuged subsequently at 13000 rpm for 15 minutes. The supernatant was transferred to a new Eppendorf tube. Protein lysates were stored at -80°C. The concentration of the extracted proteins was determined using the Bradford method. The basic principle of the method is a shift of the absorption maximum of the acidic solution of Coomassie Brilliant Blue from 470 nm to 595 nm with complex formation with proteins. After the protein concentration had been determined by means of the Bradford assay, 100 µg of the protein was mixed with 2X Laemmli buffer in a ratio of 1:1 and denatured at 95°C for 5 minutes. The samples were cooled down rapidly on ice and subsequently, centrifugation was carried out at 13200 rpm for 2 minutes. The proteins were separated according to their molecular weight by SDS-polyacrylamide gel electrophoresis according to Laemmli. For this a 12 % separation gel was overlayered with a 5 % collection gel. In order to determine the molecular weight, 10 µl of Spectra Multicolor Ladder were applied. Electrophoresis was carried out at 90 V in Tris glycine buffer (1X) for approximately 90 minutes. Using the semi-dry method, the proteins were subsequently transferred to a nitrocellulose membrane at 250 mA for 1.5 hours. Subsequently, to prevent the non-specific binding of primary/secondary antibodies to the membrane, blocking was carried out in 5 % skim milk in 1X TBS while shaking for 1 hour at room temperature. After washing in TBST three times for 10 minutes each time, the membrane was stained with the primary mouse anti-VENTX antibody in a dilution of 1:200 in 2.5 % skim milk while shaking. On the following day the primary antibody was washed off by washing 3 times in TBST, and the membrane was incubated with a secondary antibody (1:2000) for 60 minutes. Subsequently, the membrane was washed again with TBST for 3 x 15 minutes. Detection was carried out using the ECL Western Blotting Detection Kit,

Hypercassette and a Hyperfilm in a darkroom with exposure times of up to half an hour. In order to carry out a positive control with the housekeeping gene ß-actin, the membrane was incubated in stripping solution at 56°C while shaking gently for 30 minutes. After washing four times in TBST for 10 minutes each time, blocking was carried out again in 5 % blocking solution overnight. On the next day after washing the blocking solution, the membrane was stained with a monoclonal anti-ß-actin antibody (1:6000). After washing, the membrane was incubated with the secondary antibody (1:2000) for 1 hour and, subsequently, detection was carried out according to the protocol described above.

2.2.5. Retroviral constructs

In this work the PG13 mouse embryonic fibroblast packaging cell line was used for retroviral gene transfer. This gibbon ape leukemia virus-pseudotyped cell line was already prepared in our group as described previously: “The VENTX cDNA was provided by Paul Moretti (Institute of Medical and Veterinary Science, Adelaide, Australia). The VENTX cDNA was subcloned into the pMSCV-IRES-GFP (pMIG) vector. As a control, the MSCV vector carrying only the IRES-green fluorescent protein cassette (GFP virus) was used. High-titer, helper-free recombinant retrovirus was generated by transfecting the amphotropic Phoenix cell line and subsequently transducing the stable virus producing PG13 cell line” [155]. High-titer single-cell PG13 clones were isolated for each virus and used for either transduction of K562 cells (see section 2.2.6.) or $CD34^+$ umbilical cord blood cells (see section 2.2.7).

2.2.6. Transduction of K562 cells

In order to obtain the highest possible transduction efficiency of $CD34^+$ CB cells, K562 cells were transduced retrovirally to test various conditions using the packaging cell lines PG13 VENTX and PG13 MIG. Tested parameters were: the number of spin infections, different quantities of VCM, or irradiated in comparison to non-irradiated packaging cell lines.

One day before spin infection K562 cells were counted and 5 x 10^4 cells were plated into each well of a 6-well plate. 24 hours later the VCM of the packaging cells was taken and added to the K562 cells using a 0.45 µl syringe filter. After the addition of 2 µl protamine sulphate (5 mg/ml) or 1 µl of polybrene (8 mg/ml) per ml VCM and subsequent centrifugation at 32°C and 1500 rpm for 90 minutes, the supernatant containing VCM was discarded and the cells were resuspended in 500 µl of PBS. In order to differentiate between living and dead cells, cells were stained with 25 µl of 7-ADD. K562 cells were incubated in the dark at 4°C for 15 minutes. After washing with PBS, the cells were resuspended in 250 µl of PBS and the proportion of transduced K562 cells was determined using a FACS Calibur and detecting GFP as a selectable marker.

2.2.7. Transduction of cord blood cells

Human $CD34^+/GFP^+$ umbilical cord blood cells were counted after thawing and cultivated under the conditions specified in section 2.2.1. for 48 hours. 24 hours before the first spin infection the approx. 80 % confluent culture plates of PG13 VENTX and PG13 MIG cells were irradiated using a ^{137}Cs source of irradiation with a total dose of 40 Gy, to prevent overgrowth of the culture.

On the day of the first spin infection, about 5 ml VCM of the packaging cells PG13 VENTX and MIG were pipetted off and added to the umbilical cord blood cells using a 0.45 µl syringe filter. After adding 1 µl of polybrene (8 mg/ml) per ml VCM and 10 µl/ml cytokine cocktail (100 X) the cells were centrifuged at 32°C and 1500 rpm for 90 minutes (Fig. 15).

A second and third spin infection was performed after 6 and 12 hours according, respectively. After each spin infection the CB cells were replated in a Petri dish under the conditions specified above.

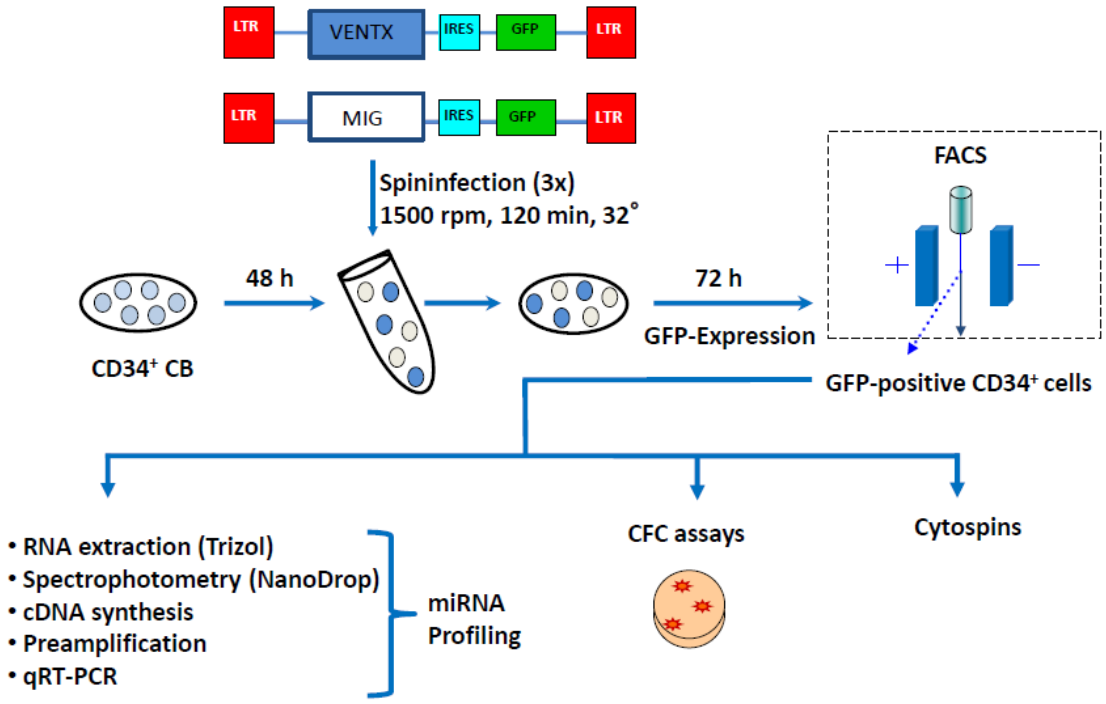

Fig. 15: Experimental design of transducing cord blood cells and following experiments.
LTR (long terminal repeats), IRES (internal ribosomal entry site), GFP (green fluorescent protein), CB (cord blood), FACS (fluorescence activating cell sorting), CFC (colony forming cell), qRT-PCR (quantitative real time polymerase chain reaction), MIG (MSCV-IRES-GFP), MSCV (mouse stem cell virus)

2.2.8. Immunophenotyping of transduced cord blood cells

In order to isolate successfully transduced $CD34^+/GFP^+$ CB cells, FACS sorting was carried out 72 hours after the final spin infection. For this the cells were first counted manually using a Neubauer counting chamber, then they were washed in 3 ml of PBS and transferred to FACS tubes. After centrifugation, the cell pellet was resuspended in PBS (dilution $1x10^6$ cells/100 µl PBS). 100.000 cells were kept in a third tube as an isotype control. The cell samples to be sorted (with the exception of the isotype control) were incubated with anti-human $CD34^+$ APC antibody (antibody: buffer ratio 1:10) for 20 minutes at 4°C. The appropriate APC-conjugated isotype control of the same immunoglobulin class as the anti-human $CD34^+$ antibody (in this case: mouse IgG1, κ APC) was stained and incubated according to the samples described above.

After the antibody incubation period, the FACS tubes were centrifuged at 1100 rpm for 10 minutes, the supernatant was discarded, and the pellet was resuspended in

FACS buffer ($1x10^6$ cells / 200 µl FACS buffer). To stain the dead cells in the samples to be sorted, Sytox blue (1 mM, 0.05 µl per 100 µl FACS buffer) was added. The stained samples were analysed and sorted using a FACS Aria III. The isotype control was used first to rule out non-specific binding and to determine the amount of any background fluorescence or non-specific fluorescence. The negative gate was set on the basis of the population of the isotype control in such a way that 99.98 % of the cells were inside the gate. At least 10.000 events were measured for each sample to ensure that the population could be identified optimally. Once gate delineation of the fluorescence control had been set, the CD34-stained samples were analysed and sorted.

2.2.9. Colony forming cell assay

In order to test the clonogenic potential and the differentiation of the $CD34^+$ umbilical cord cells transduced with VENTX or with the empty control vector, colony-forming assays were carried out in methylcellulose.

Aliquots of 3 ml methylcellulose were thawed overnight at 2-8°C. 1000 $CD34^+/GFP^+$ cells per dish were resuspended in 300 µl of SFM (diluted 10-fold) and subsequently pipetted into 3 ml of methylcellulose. To ensure uniform distribution of the cells in the viscous methylcellulose, the cell mixture was vortexed vigorously. After all air bubbles had disappeared, 1.1 ml of the cell mixture was transferred to 35 mm cell culture plates using a 3 ml syringe and a blunt end needle. For each sample, two 35 mm cell culture plates were prepared and incubated in a 100 mm cell culture plate for 14 days at 37°C and 5% CO_2 together with an uncovered cell culture plate filled with 3-4 ml of sterile water. The water was necessary to maintain humidity.

After 14 days numbers and morphology of the individual erythroid (CFU-E, BFU-E), granulocytic/macrophagocytic (CFU-G, CFU-GM, CFU-M) and the multipotent granulocytic erythroid/macrophagocytic/megakaryocytic (CFU-GEMM) colonies were determined microscopically using counting grids.

2.2.10. Cytospin preparation

For the cytomorphological analysis of $CD34^+/GFP^+$ transduced CB cells, the cells were resuspended in 300 µl PBS after sorting. Subsequently, the cell suspension was transferred to the sample funnels of a Cytospin 4 centrifuge and a thin layer was deposited on the glass slide by centrifugation at 450 rpm for 10 minutes.

The dried samples were stained with the Hemacolor staining kit which produces a stain according to Pappenheim. Staining procedure was carried out in 4 steps. First the slides were placed in fixing solution for one minute subsequently they were stained with red staining reagent for 60 seconds. Staining with blue staining reagent was then carried out for 60 seconds. Finally, the slides were washed with tap water.

2.2.11. RNA extraction

After centrifugation at 1100 rpm the cells were lysed in 1 ml of Trizol and incubated at room temperature for 5-10 minutes to allow nucleoprotein complexes to dissociate completely. After adding 200 µl of chloroform/ml Trizol and vortexing for 10 seconds, further incubation was carried out for 2-3 minutes. Subsequently, centrifugation was carried out at 12000 rpm for 15 minutes at 4°C. Phase separation of the upper phase containing RNA from the lower phase containing phenol was carried out by careful removal and transfer of the upper phase to a new 1.5 ml Eppendorf tube. For the precipitation of RNA 500 µl of isopropanol/ml Trizol were added and the tube inverted for several times. 10-minute incubation at room temperature and repeated centrifugation at 12000 rpm and 4°C followed. The supernatant was discarded and the RNA pellet was washed with 1 ml of 75 % ethanol/ml Trizol and vortexed. After centrifugation at 7500 rpm and 4°C for 10 minutes at room temperature the supernatant ethanol was removed. Residual ethanol was removed by drying the pellet for 5-10 minutes at room temperature. The RNA pellet was dissolved in 20-50 µl of DEPC-treated water depending on the size of the pellet. The dissolved RNA was stored at -80°C.

2.2.12. Measurement of RNA and DNA concentration

Concentrations of RNA and DNA samples were measured in ng/µl using a Nanodrop 1000 spectrophotometer at a wavelength of 260 nm, which represents the absorption peak of nucleic acids. In order to assess the purity of the samples, the ratio of 260/280 nm signal intensity was calculated by simultaneous measurement of the absorption peak of proteins at 280 nm. The RNA sample was regarded as pure with a ratio of 1.7 to 2.0. Significantly lower ratios indicated the presence of proteins or other contaminations.

2.2.13. RT-PCR

Using the enzyme reverse transcriptase, the isolated RNA of PG13 cells and AML cell lines was transcribed into complementary cDNA with the Thermoscript RT-PCR system according to the manufacturer's instructions. Oligo-dT nucleotides for standard PCR or random hexamers for qRT-PCR were used as primers. As a rule 1 µg of RNA was used after photospectrometric measurement to permit semiquantitative statements.

2.2.14. PCR

After RT-PCR of PG13 cells and AML cell lines the polymerase chain reaction was used to amplify specific DNA fragments. Each PCR cycle consisted of three steps. In the first step, the denaturing step, the DNA was heated to 94°C-96°C to break the hydrogen bonds. During primer hybridization the sample was cooled to 55°C-65°C, the exact temperature depending on the GC-content and length of the primers. Elongation ended with the synthesis of the new DNA strain by Taq-polymerase. Ideally, each newly synthesized DNA strain is used as the starting material in the next cycle, so that theoretically each completed cycle would result in the doubling of the DNA amount. PCR was carried out with the Taq DNA polymerase kit. For problematic DNA templates the PCR x Enhancer System was used additionally according to the manufacturer's instructions.

Following reagents were used:

Tab. 3: Reaction components for standard PCR (polymerase chain reaction)

	Volume (µl)
DEPC treated water	18.0-19.0
10 X Buffer	2.5
$MgCl_2$ 50 mM	0.75
dNTP Mix 10mM	0.5
Forward Primer	0.5
Reverse Primer	0.5
Taq Polymerase 5 U/ µl	0.25
Template DNA	1.0-2.0

In this work the polymerase chain reaction was carried out to detect possible mutations in the CDS of the VENTX gene in various immortalized human AML cell lines. The following primer sequences and PCR conditions were selected for the detection of expression of VENTX in these cell lines.

Tab. 4: Primer sequences

Primer	**Primersequence 5‘-3‘**
Ventx forward	GCCATGCGCCTCTCCTCCT
Ventx reverse	CCGCGAGTGTGGGAGTCAGA
ß-Actin forward (loading control)	GGACTTCGAGCAAGAGATGG
ß-Actin forward (loading control)	AGCACTGTGTTGGCGTACAG

Tab. 5: PCR conditions (polymerase chain reaction)

	PCR conditions for VENTX	**PCR conditions for ß-Actin**
Initial denaturing	94°C 5 min	94°C 2 min
Denaturing	94°C 30 sec	94°C 30 sec
Annealing	58°C 30 sec	60°C 30 sec
Extension	72°C 60 sec	72°C 30 sec
Termination	72°C 10 min	72°C 2 min
Cycles	40	30

2.2.15. Agarose gel electrophoresis

Gel electrophoresis was carried out for the detection of PCR products and analytical purposes. A 1 % gel was used by default. Agarose was dissolved in 1X TAE buffer by boiling in the microwave. The DNA was visualized by adding 1 µl of gel red (10000X) per 10 ml TAE buffer (1X). 0.05 µg of a 100 bp or 1 kbp ladder was

used as a marker. Subsequently this mixture was transferred to the electrophoresis chamber with a comb. After the gel had hardened and the comb had been removed, TAE buffer was added to the chamber until the complete gel was covered. Subsequently, 25 µl of PCR product mixed with 5 µl of loading dye (6X) were pipetted into the appropiate wells of the agarose gel. Separation of the individual DNA bands was effected at 60-110 V.

2.2.16. Extraction of PCR products from agarose gel

After gel electrophoresis the corresponding PCR products in the agarose gel were visualized using a UV transilluminator at a wavelength of 365 nm and cut out from the gel using a scalpel. The DNA was isolated with an Illustra GFX PCR DNA and Gel Band Purification Kit according to the manufacturer's instructions.

2.2.17. Sequencing

PCR products were sequenced by GATC Biotech (Constance, Germany). The Sanger dideoxy method was used for sequencing. The obtained sequence was compared with the PubMed reference sequence by the help of the online tool MultAlin [151] [136].

2.2.18. RT- PCR and preamplification of cord blood cells

The extracted RNA of transduced $CD34^+/GFP^+$ CB cells was transcribed using the TaqMan MicroRNA Reverse Transcription Kit as well as specific miRNA stem-loop primers and reagents from the Megaplex primers according to the manufacturer's instructions (Applied Biosystems). For the three biological replicates 405 µg-960 µg of RNA were used, depending on the results of RNA extraction. Identical amounts of RNA were used for both the VENTX and the GFP arms of the same biological replicate. Figure 16 shows the reverse transcription (RT) step. In this step, cDNA is reverse transcribed from total RNA samples. The reverse transcription uses specific miRNA primers and reagents from the Megaplex Primers. The manufactures instructions were followed (Applied Biosystems).

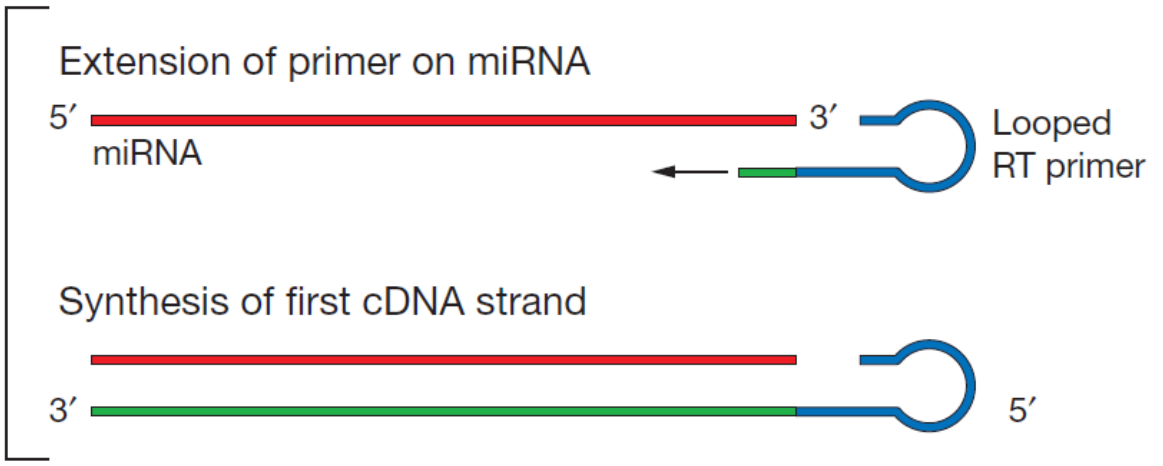

Fig. 16: RT reaction (reverse transcription), adapted from Applied Biosystems [6]

Preamplification was carried out to increase the quantity of the desired cDNA-transduced CB cells for miRNA gene expression analysis. The purpose of this step is to increase the probability of compiling a comprehensive miRNA gene expression profile, even of low-expressed miRNAs. According to Applied Biosystems preamplification does not cause any bias. Figure 17 shows the preamplification reaction. In the preamplification step, PCR products are uniformly amplified from cDNA templates using the Megaplex PreAmp Primers and the TaqMan PreAmp Master Mix. The manufacturer´s instructions were followed (Applied Biosystems).

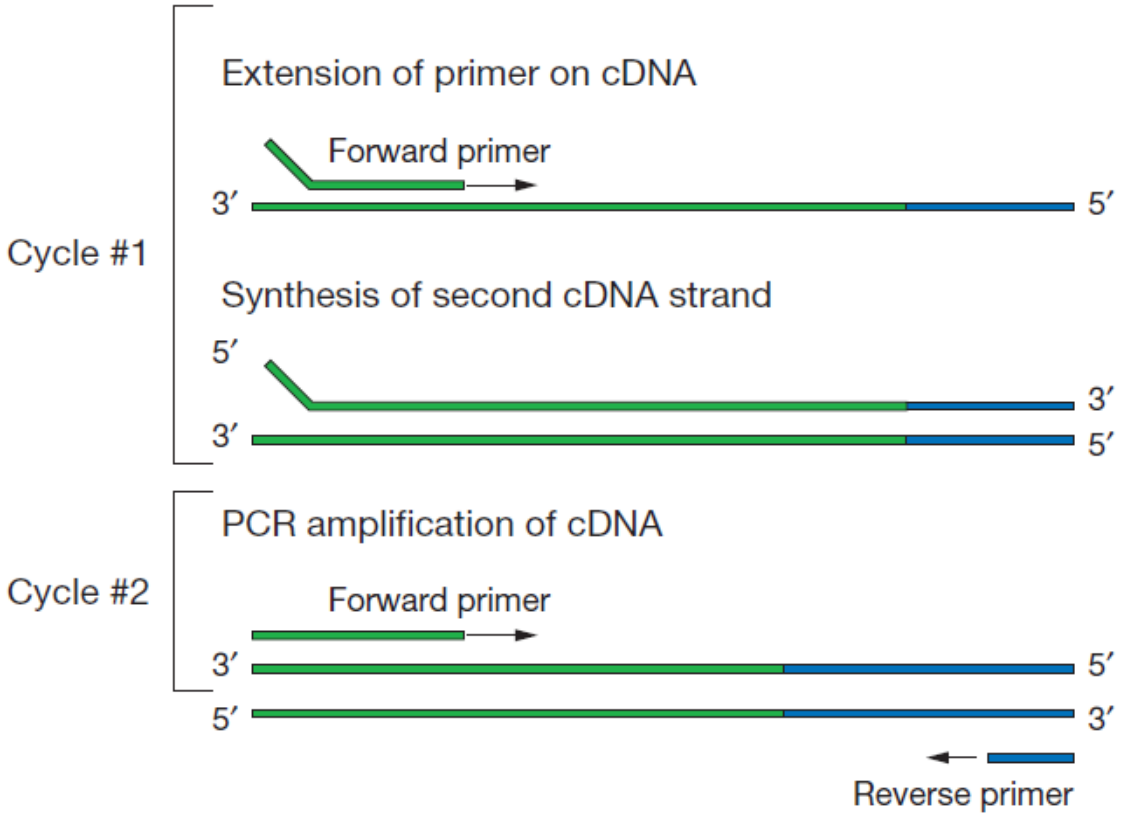

Fig. 17: Preamplification reaction, adapted from Applied Biosystems, PCR (polymerase chain reaction) [6]

2.2.19. Quantitative Real-Time PCR

Quantitative gene expression was determined by TaqMan qRT-PCR. This method is based on a reporter dye being attached to the 5´ end of the DNA sample, and a quencher dye at the 3´ end. If the DNA polymerase degrades the probe with its exonuclease activity, the quencher dye is released and fluorescence is emitted. The point at which the fluorescence exceeds a certain quantity of background fluorescence is designated as the threshold cycle (CT) (Fig. 18).

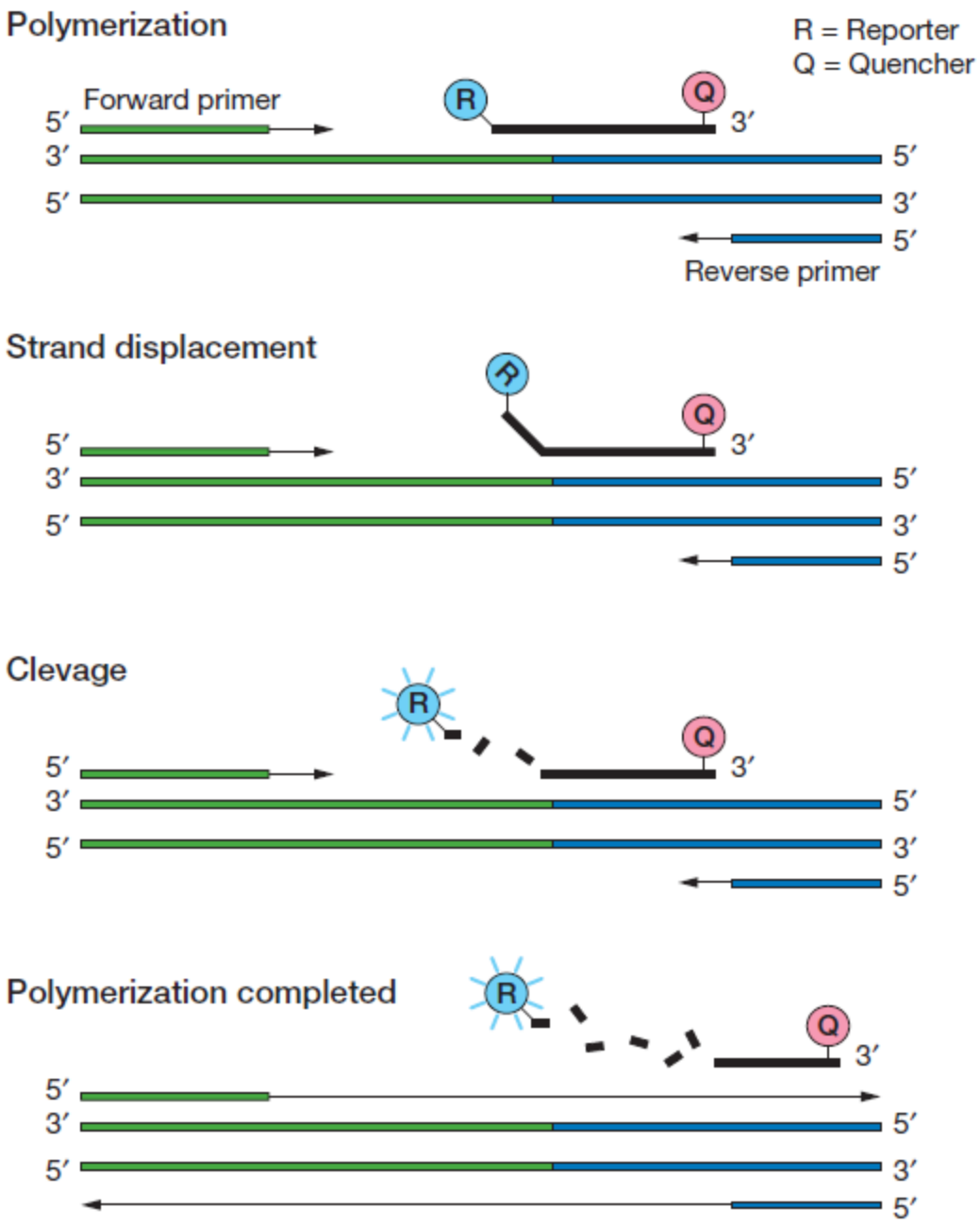

Fig. 18: The 5´ to 3´ nuclease activity of the DNA Polymerase System, adapted from Applied Biosystem [6]

The relative quantification of gene expression was performed by comparison with endogenous controls and evaluated using the RQ Manager (version 1.2.1) software in the 7900 HT Fast Real Time PCR system. Hereby the expression of a target gene is refered to the gen expression of a housekeeping gene and depicts the ΔCT value.

qRT-PCR of PG13 cells

For quantitative expression of VENTX in PG13 cells qRT-PCR was carried out in optical 96-well plates with a maximum of 40 cycles and a total volume of 20 µl. Mouse GAPDH was used as housekeeping gene. Both primers/probes for human VENTX (Hs00797729_s1) and for mouse GAPDH (4352932E) were obtained from Applied Biosystems. Following reagents were used in this experiment:

Tab. 6: Reaction components for quantitative expression of VENTX in PG13 cells

Reagents	Volume (µl)
Taqman Mastermix	10
H_2O	8
Primer (VENTX/GAPDH)	1
cDNA	1
Total	20

Cycles were carried out as following:

Tab. 7: Components of each cycle

Program	
40 cycles	95° for 10 minutes 95° for 15 seconds 60° for 60 seconds

miRNA profiling of cord blood cells

For a comprehensive analysis, TaqMan Human MicroRNA Array Cards A+B (Fig. 19, 20) were used, covering a total of 754 human miRNAs. “In addition, each card contained four control assays – three selected candidate endogenous control assays and one negative control assay. Card A focusses on better characterized miRNAs, while card B contains more recently discovered miRNAs “ [5]. For sample preparation the manufacturer's instructions were followed. The samples prepared in this way were pipetted into the ports of the array cards A and B and subsequently centrifuged at 331 g for 2 x 1 minute. miRNA expression was normalized to endogenous control MammU6 and expression difference between both arms was calculated as following:

1) $CT_{miRNA} - CT_{MammU6} = \Delta CT$

2) $\Delta CT_{VENTX} - \Delta CT_{GFP} = \Delta\Delta CT$

3) $2^{-\Delta\Delta CT}$ = x-times expression difference



Fig. 19: TaqMan Array Human MicroRNA Card A, adapted from Applied Biosystems [5]



Fig. 20: TaqMan Array Human MicroRNA Card B, adapted from Applied Biosystems [5]

2.2.20. Search for miRNA target genes

miRNA sequences of differentially expressed miRNAs between the VENTX and the control arm were obtained from miRBase (version 18) and target prediction was performed by the help of TargetScanHuman Custom (version 5.2) [128] [178]. Targets with conserved 8-mer and 7-mer sites that match the seed region of each miRNA were considered for further analyses. As the TaqMan Human MicroRNA Array A+B cards were using the miR/miR* nomenclature (instead of the newer -5p/-3p), this nomenclature was maintained throughout this study.

2.2.21. Statistical analysis

Data were evaluated with Microsoft Excel using Student´s t-test. P values of <0.05 were considered to be statistically significant.

3. Results

3.1. Detection of VENTX expression in PG13 cells

Quantification of human VENTX was performed in PG13 murine cells to ensure expression of VENTX in transduced CB cells and absence of VENTX expression in the control arm. As endogenous control the murine housekeeping gene GAPDH was used. With a standard number of 40 cycles we detected VENTX expression in the VENTX arm (ΔCT=6.97) whereas as expected there was no VENTX expression detectable in the control arm (Fig. 21).

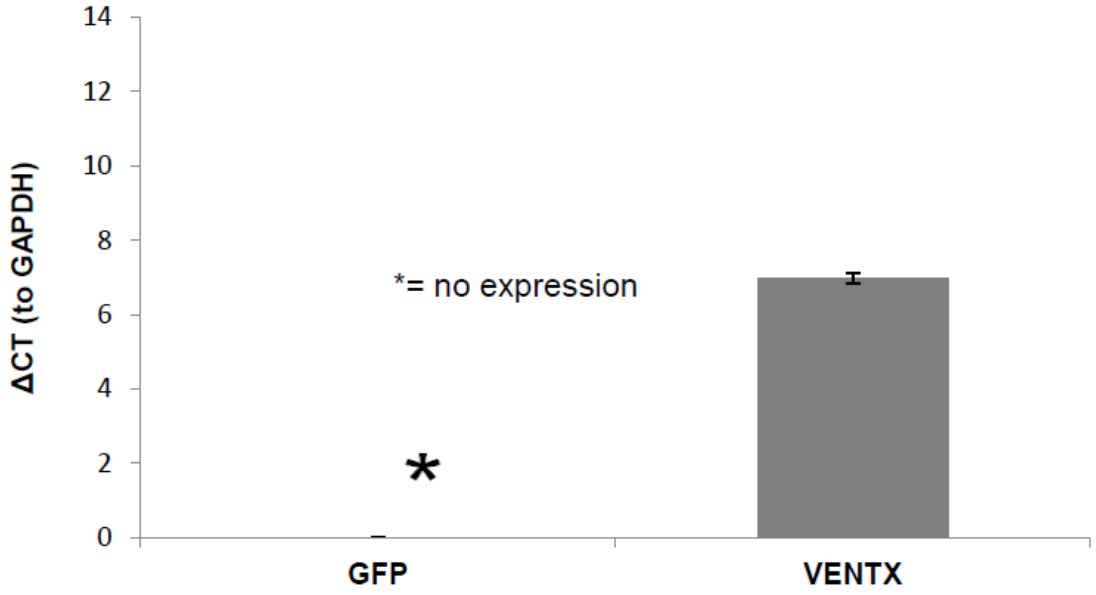

Fig. 21: VENTX was expressed in PG13 cells transduced with VENTX but no expression could be detected in the empty vector control GFP (green fluorescent protein). GAPDH (glyceraldehde 3-phosphatase dehydrogenase) was used as endogenous control. Standard cycle number of 40. Quantitative RT-PCR assay repeatability was determined using triplicates. Bars represent average expression ±SD (standard deviation), CT (threshold cycle)

3.2. Western Blot of PG13 cells

Protein expression of VENTX protein was confirmed by Western Blot analysis using cell lysates from PG13 VENTX and PG13 GFP cells. The 28 kDa VENTX protein was detected by an anti-VENTX mouse antibody, but was not detectable in the GFP control. As a positive control an antibody against ß-actin, a common housekeeping protein was used (Fig. 22).

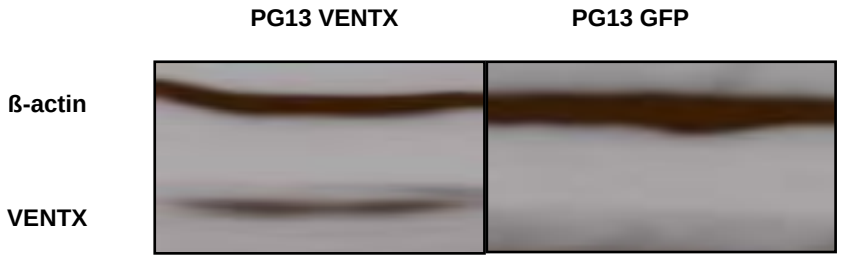

Fig. 22: Western Blot analysis of VENTX protein in PG13 cells. GFP (green fluorescent protein)

3.3. Efficiency of retroviral gene transfer of the AML cell line K562

Transduction of the AML cell line K562 was performed by using VCM of PG13 cells, containing either plasmids with VENTX WT GFP or GFP control. PG13 cells were expanded and subsequently viral production was titered on K562. Hereby, we were able to establish alternative method of retroviral transduction of human CB cells. Tested parameters included the number of spin infections and different quantities of VCM. The highest transduction efficiency was achieved with three spininfections and using 5 ml VCM in both arms. Following this procedure we obtained 30 % transduction efficiency of K562 cells with VENTX compared to 65.7 % with the GFP control. This transduction efficiency was sufficient for performing our subsequent experiments. To ensure high quality and quantity of VCM of PG13 cells throughout all transduction experiments of CB cells each CB experiment was preceeded by the transduction of K562 cells as a direct control. The mean transduction efficiency of K562 cells with the GFP control vector was 67.5 % ± 23.7 compared to VENTX with 39.6 % ± 16.2 (Fig. 23, 24).

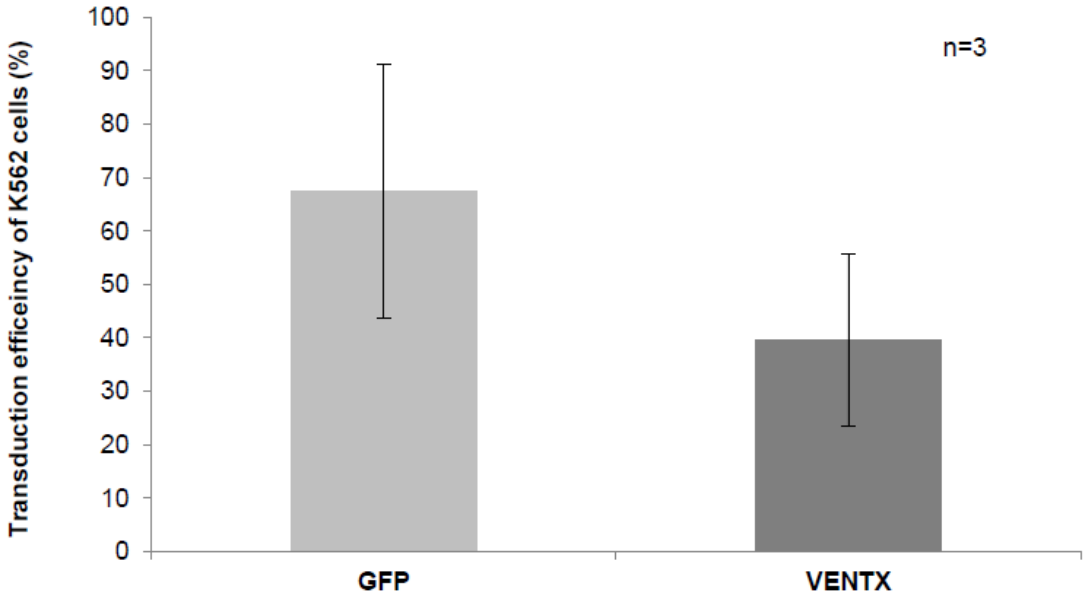

Fig. 23: Efficiency of retroviral transduction in K562 cells. K562 cells were analyzed 2 days after start of transduction. Columns represent average transduction efficiency ±SD (standard deviation), GFP (green fluorescent protein)

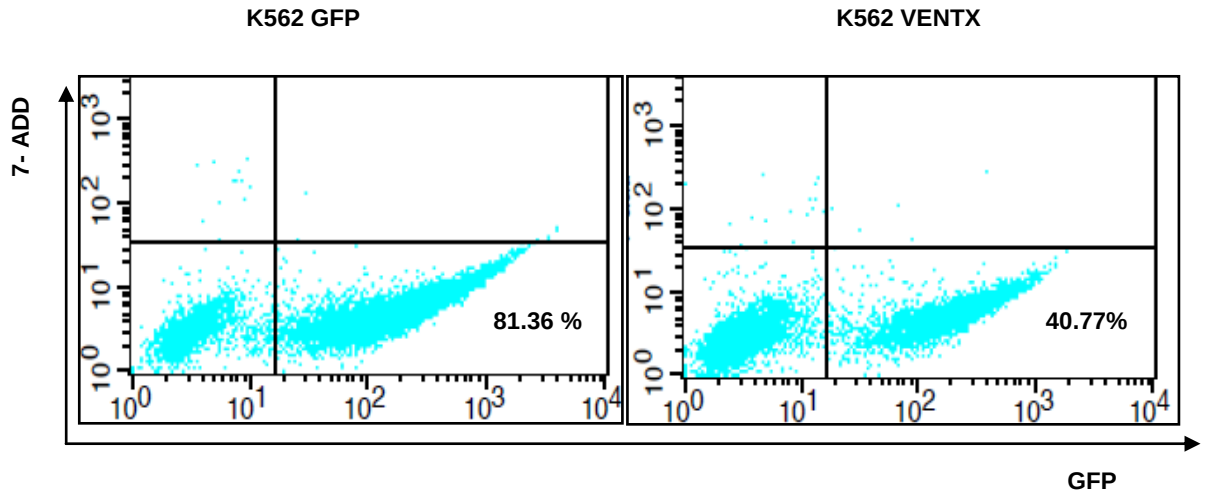

Fig. 24: Representative dot plots showing the transduction efficiency in K562 cells for the GFP control compared to the VENTX retroviral vector. 7-ADD (7-aminoactinomycin), GFP (green fluorescent protein)

3.4. Efficiency of retroviral gene transfer in cord blood cells

In an attempt to characterize potential miRNA gene targets of VENTX in hematopoiesis we retrovirally transduced human CB cells with either VENTX or the empty GFP control vector. Based on our results using K562 cells we performed three subsequent spin infections and used 5 ml VCM in our transduction protocolfor primary cord blood cells. Thereby we achieved a mean transduction efficiency cells of 28.5 % ± 7.3 for the GFP control arm and 12.7 % ± 4.6 for VENTX respectively. Transduction of CB cells was carried out in three independent experiments (Fig. 25, 26).

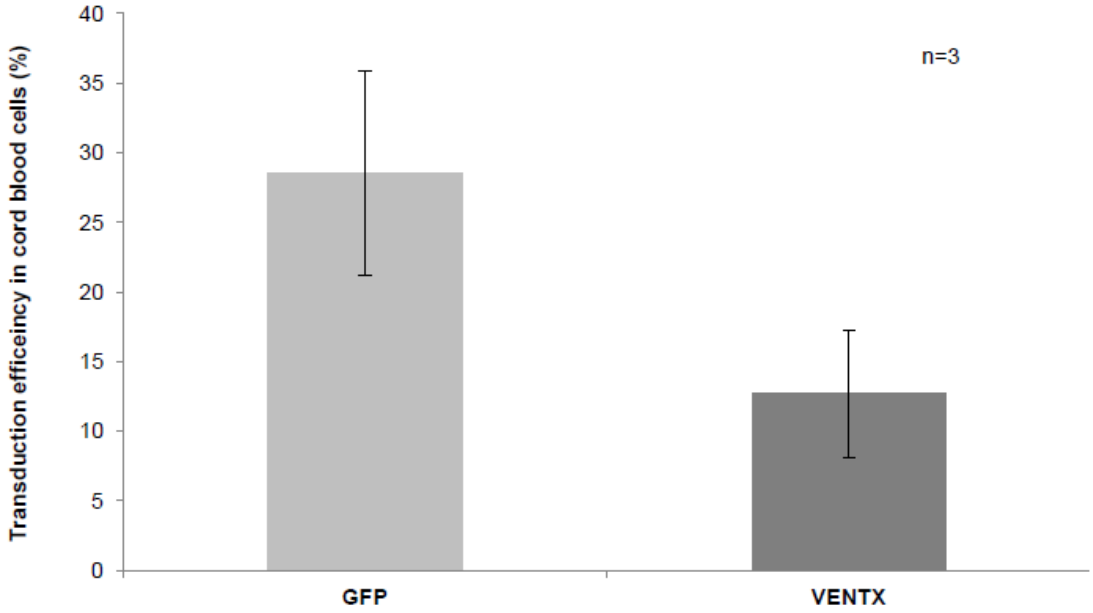

Fig. 25: Efficiency of retroviral transduction of cord blood cells. Columns represent average transduction efficiency ±SD (standard deviation), GFP (green fluorescent protein)

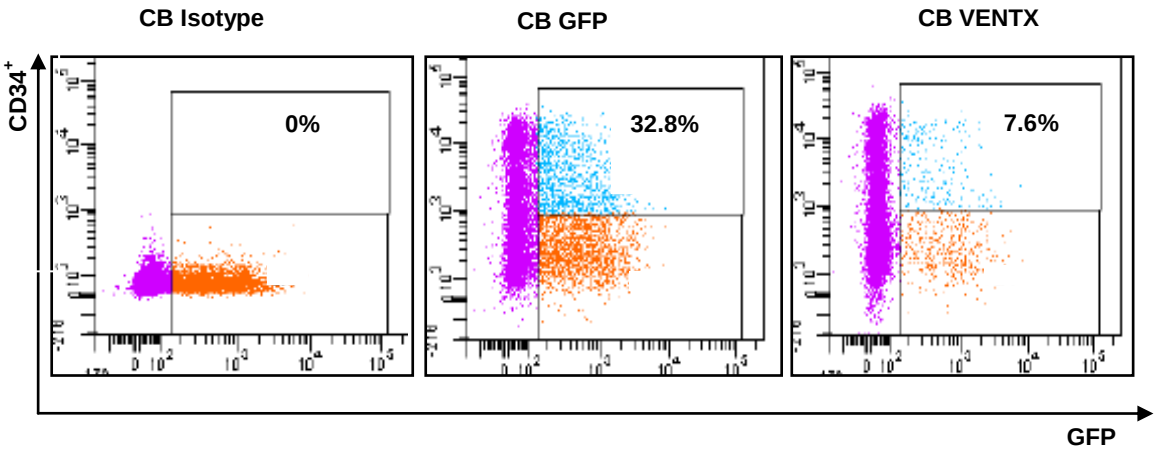

Fig. 26: Representative FACS analysis of the transduction efficiency in cord blood cells. Cord blood cells were analysed 3 days after the last spin infection. Isotype controls were used to measure and exclude non-specific background signals. CB (cord blood), FACS (fluorescence activating cell sorting), GFP (green fluorescent protein)

3.5. VENTX promotes human myeloid colony formation and inhibits erythroid development *in vitro*

In an attempt to test whether and how the constitutive expression of VENTX is perturbing the normal differentiation of clonogenic progenitors, we placed highly purified GFP positive CB cells in methylcellulose and checked colony formation after 14 days. Colonies observed after this period of cultivation comprised primitive CFU-GEMM (Granulocyte, Erythrocyte, Macrophage and Monocyte Colony Forming Unit) colonies as well as the lineage committed progenitors CFU-E (Colony Forming Unit Erythrocyte), BFU-E (Burst Forming Unit Erythrocyte),CFU-G (Colony Forming Unit Granulocyte), CFU-M (Colony Forming Unit Macrophage) and CFU-GM (Colony Forming Granulocyte/Macrophage).

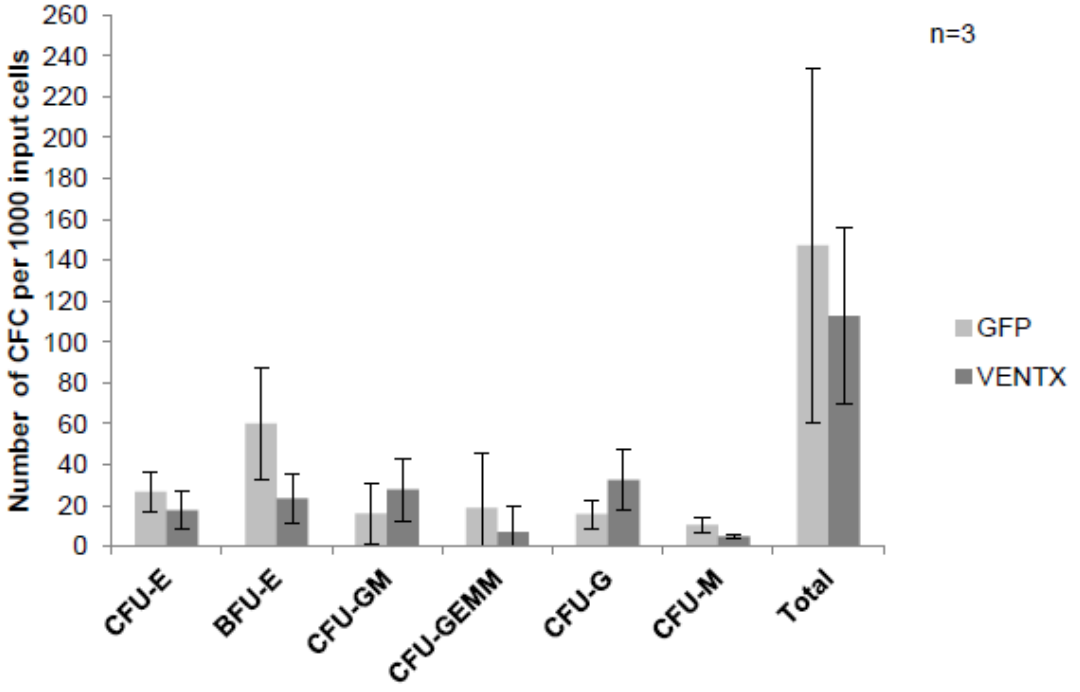

Fig. 27: Mean number of colonies detected after 14 days of culture: CD34$^+$/VENTX/GFP$^+$ cord blood cells compared to CD34$^+$/ GFP$^+$ cord blood cells. Colums represent average cell numbers ±SD (standard deviation), GFP (green fluorescent protein), CFC (colony forming cell), CFU-E (Colony Forming Unit Erythrocyte), BFU-E (Burst Forming Unit Erythrocyte), CFU-GM (Colony Forming Granulocyte/Macrophage), CFU-GEMM (Granulocyte, Erythrocyte, Macrophage and Monocyte Colony Forming Unit), CFU-G (Colony Forming Unit Granulocyte), CFU-M (Colony Forming Unit Macrophage)

Although results were not statistically significant we observed a trend towards a reduced generation of erythroid colonies when CB cells were transduced with VENTX as compared to the GFP control (Fig. 27, 28). These findings were consistent with previous results obtained within our group and showed that the transduction protocol we are using within this work resulted in the same functional changes of the cord blood cells. In addition we also found a 1.5 fold increase in myeloid colony formation in the VENTX arm as compared to the control. The number of BFU-E´s produced in the VENTX transduced cord blood cells was 2.5 fold lower compared to the GFP fraction. Furthermore, we observed a 1.5 fold decrease in CFU-E colonies in the VENTX arm. The total number of CFCs was 1.3 fold lower in VENTX transduced CB cells as compared to the empty vector control.

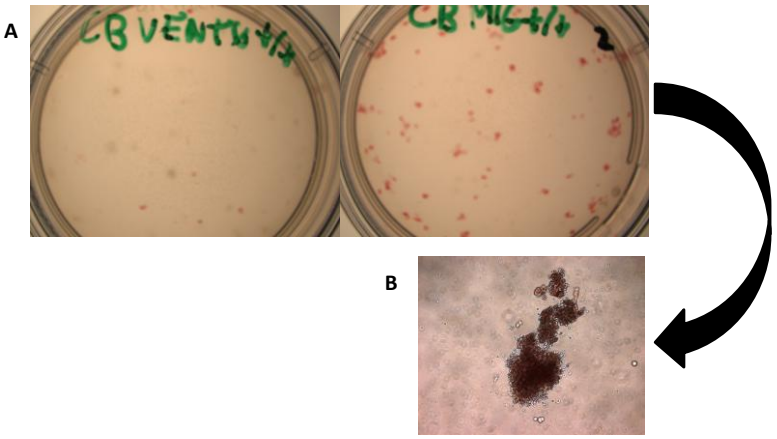

Fig. 28: (A) Macroscopic view of CFC plates showing the difference in growth of erythroid colonies in the GFP fraction (labeled with MIG) compared to VENTX transduced cord blood cells. (B) Microscopic view (40x) from one BFU-E colony.
CFC (colony forming cell), GFP (green fluorescence protein), CB (cord blood)

3.6. Cytospin

Morphology was evaluated using cytospin preparations of sorted $CD34^+$/VENTX/GFP^+ and $CD34^+$/GFP^+ cells. Compared to the GFP control, VENTX transduced CB cells showed more macrophages with a foamy appearance after *in vitro* culture as compared to the GFP control (Fig. 29).

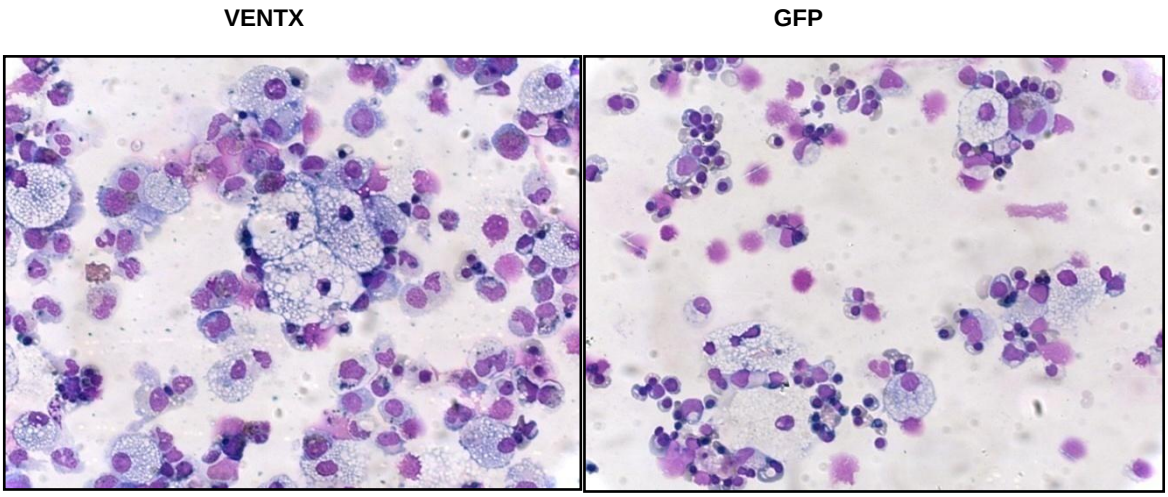

Fig. 29: Pictures of cell morphology after CFC (colony forming cell) assays. Cytospins of transduced $CD34^+$ cord blood cells confirmed the myeloid phenotype of the VENTX transduced cells compared with GFP control. Pictures were taken with 40x magnification. GFP (green fluorescent protein)

3.7. RNA extraction of transduced cord blood cells

For microRNA profiling RNA extraction was performed from highly purified transduced $CD34^+$/VENTX/GFP^+ and $CD34^+$/GFP^+ cord blood cells. Table 8 and 9 show the cell numbers and isolated RNA in ng/µl and the according 260/280 nm ratios both of the VENTX arm and the GFP control (Tab. 8, 9).

Tab. 8: Cell numbers after transduction and RNA concentrations after extraction from $CD34^+$/VENTX/GFP^+ transduced cord blood cells. GFP (green fluorescent protein)

VENTX	Cell Number	[RNA] ng/µl	260/280 ratio
1. experiment	316487	383	1.87
2. experiment	157740	176	1.69
3. experiment	660213	1314	1.79

Tab. 9: Cell numbers after transduction and RNA concentrations after extraction from $CD34^+$/GFP^+ transduced cord blood cells. GFP (green fluorescent protein)

GFP	Cell Number	[RNA] ng/µl	260/280 ratio
1. experiment	308246	414	1.85
2. experiment	441279	135	1.69
3. experiment	520373	320	1.83

3.8. MicroRNA profiling of transduced cord blood cells

The microRNA gene expression profiling with TaqMan Human Array Cards was performed from three independent experiments. A total of 2262 unique assays specific to human miRNAs (meaning 754 assays per each experiment) either for GFP and VENTX transduced CB cells, including endogenous controls and negative controls were obtained. There was a significantly different expression of five miRNAs when profiles from GFP and VENTX transduced cord blood cells were compared. Fig. 30 gives an overview of these miRNAs. For all five miRNAs we found 1720 potential gene targets.

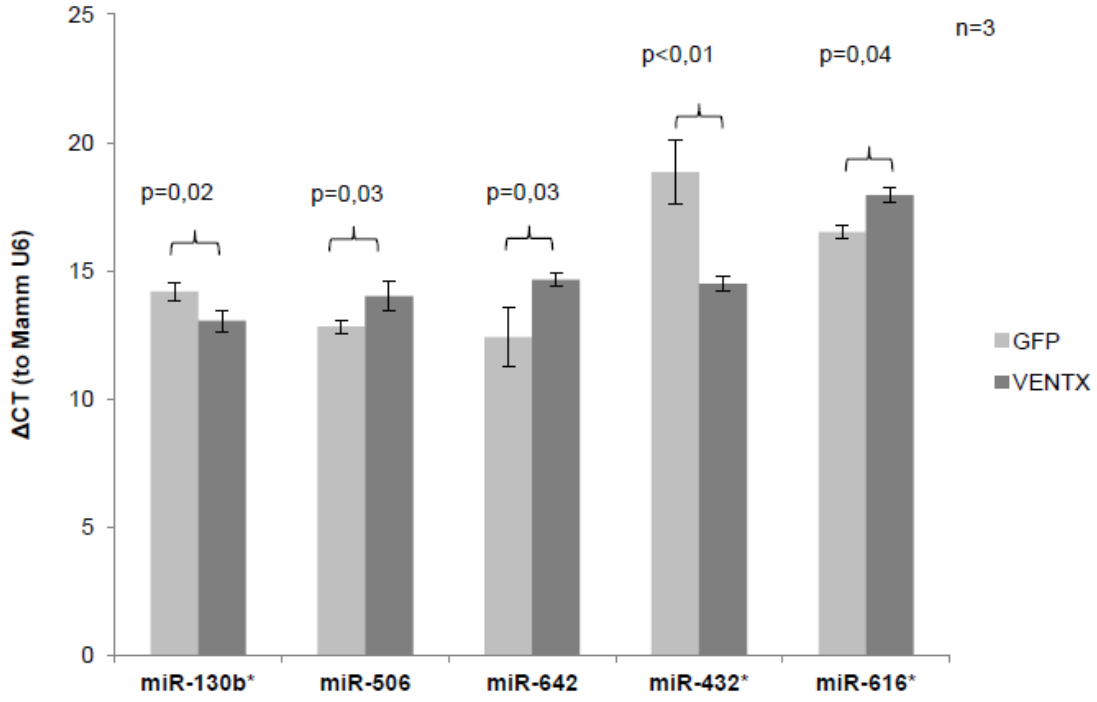

Fig. 30: Five miRNAs showed significant differences in the expression patterns between GFP vector control and the VENTX arm. MammU6 (endogenous control). Note that ΔCT values are inversely correlated to expression levels. Bars represent average expression ±SD (standard deviation). GFP (green fluorescent protein), CT (threshold cycle).

miR-130b*

Figure 31 shows results detected for miR-130b*. miR-130b* is localized on chromosome 22q 11.21 with a genomic size of 82 nucleotides. It is important to note that this localization is referred to the whole stemloop (pre-miRNA) and this annotation also applies for miRNAs listed below. The average ΔCT value in the GFP fraction was 14.17 ± 0.33 versus an average ΔCT in the VENTX fraction of 13.03 ± 0.41(p=0.02). According to this, the expression of miR-130b* was 2.2 fold higher in the VENTX fraction as compared to the vector control.

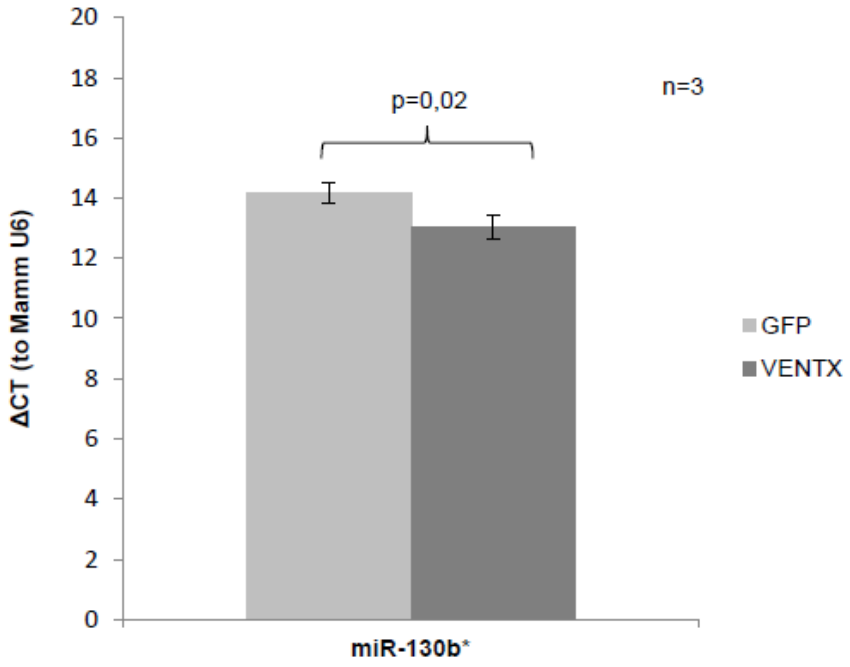

Fig. 31: Diagramm showing the different expression of miR-130b* between GFP and VENTX transduced cord blood cells, p=0.02. MammU6 (endogenous control). Note that ΔCT values are inversely correlated to expression levels. Bars represent average expression ±SD (standard deviation). GFP (green fluorescent protein), CT (threshold cycle).

By the help of TargetScanCustom Human (section 2.2.20.) we found 349 potential gene for miR-130b*. The first 25 potential gene targets are listed in Tab. 10. MiRNAs act as single stranded RNA in the regulation of gene expression. The dominant strand is called the mature miRNA strand, whereas the other one is known as the passenger strand or miRNA*, which is either degraded or also acts as a regu-

lator of transcription.Taqman Human Array Cards also contained the mature strand miR-130b. In this case expression of miR-130b was 3.6 fold lower in the VENTX fraction compared to the GFP fraction. However this result was not statistically significant. The average ΔCT value in the GFP fraction was 9.41 ± 1.23 versus an average ΔCT in the VENTX fraction of 11.25 ± 2.75 (p=0.35).

Tab. 10: The top twenty five putative targets of miR-130b* identified with TargetScanHuman Custom

Target gene	Gene name
ANKRD50	ankyrin repeat domain 50
BCAT1	branched chain aminotransferase 1, cytosolic
CHIC1	cysteine-rich hydrophobic domain 1
HOXA13	homeobox A13
UNC5D	unc-5 homolog D (C. elegans)
MAF	v-maf musculoaponeurotic fibrosarcoma oncogene homolog (avian)
DIO2	deiodinase, iodothyronine, type II
ASH1L	ash1 (absent, small, or homeotic)-like (Drosophila)
CLEC5A	C-type lectin domain family 5, member A
IGF1	insulin-like growth factor 1 (somatomedin C)
LENG8	leukocyte receptor cluster (LRC) member 8
PHACTR2	phosphatase and actin regulator 2
PURA	purine-rich element binding protein A
ABLIM1	actin binding LIM protein 1
ACCN2	amiloride-sensitive cation channel 2, neuronal
ACOX1	acyl-Coenzyme A oxidase 1, palmitoyl
ACSL4	acyl-CoA synthetase long-chain family member 4
ACVR1C	activin A receptor, type IC
AICDA	activation-induced cytidine deaminase
AK2	adenylate kinase 2
ANKRD28	ankyrin repeat domain 28
AP1B1	adaptor-related protein complex 1, beta 1 subunit
ARHGEF9	Cdc42 guanine nucleotide exchange factor (GEF) 9
ARL5B	ADP-ribosylation factor-like 5B
ASCL1	achaete-scute complex homolog 1 (Drosophila)

miR-506

Figure 32 shows the results detected for miR-506. Its genomic localization is on chromosome Xq 27.3 with a genomic size of 124 nucleotides. The average ΔCT value in the GFP fraction was 12.8 ± 0.26 versus an average ΔCT in the VENTX fraction of 14.00 ± 0.57. This was statistically significant (p=0.03). Gene expression of miR-506 of the VENTX fraction was 2.3 fold lower compared to the GFP control. Taqman Human Array Cards did not contain the passenger strand miR-506*.

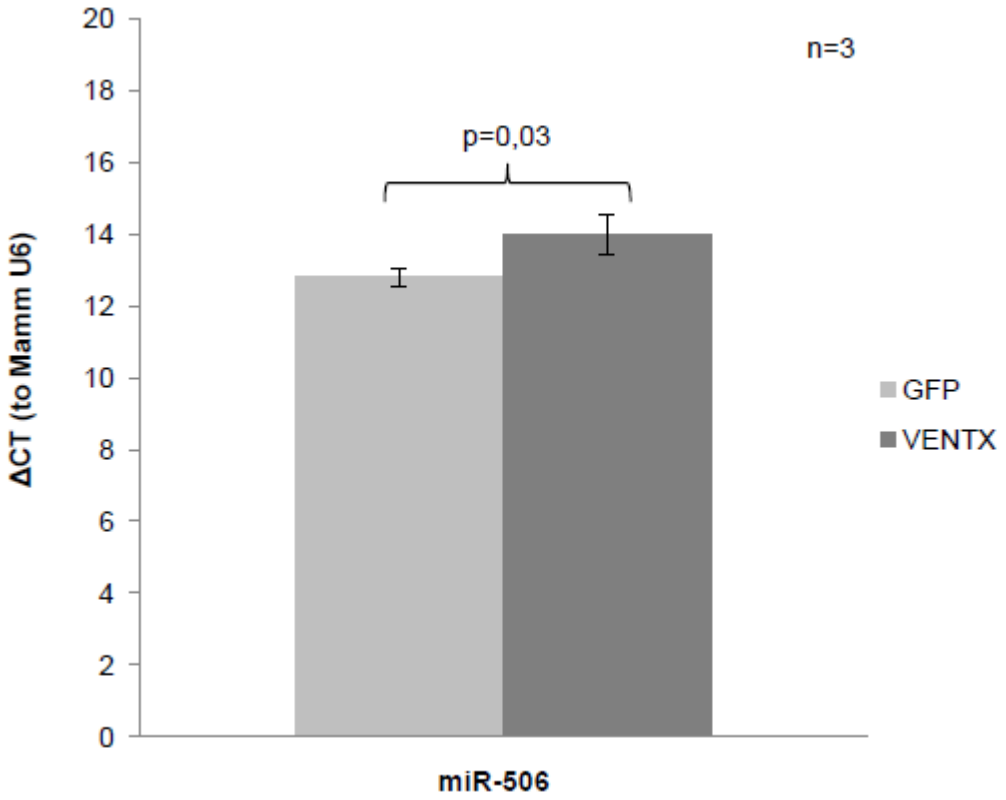

Fig. 32: Diagramm showing different miR-506 expression between GFP and VENTX transduced cord blood cells, p=0.03. MammU6 (endogenous control). Note that ΔCT values are inversely correlated to expression levels. Bars represent average expression ±SD (standard deviation). GFP (green fluorescent protein), CT (threshold cycle).

We observed 464 potential targets for miR-506 using the TargetScanHuman Custom program. The first 25 stated potential gene targets are listed in Tab. 11.

Tab. 11: The top twenty five putative targets of miR-506 identified with TargetScanHuman Custom

Target gene	Gene name
EYA4	eyes absent homolog 4 (Drosophila)
PIK3C2A	phosphoinositide-3-kinase, class 2, alpha polypeptide
ASPA	aspartoacylase (Canavan disease)
LAMC1	laminin, gamma 1 (formerly LAMB2)
AGXT2L1	alanine-glyoxylate aminotransferase 2-like 1
B4GALT1	UDP-Gal:betaGlcNAc beta 1,4- galactosyltransferase, polypeptide 1
LRRC1	leucine rich repeat containing 1
PTBP2	polypyrimidine tract binding protein 2
FZD4	frizzled homolog 4 (Drosophila)
CHIC1	cysteine-rich hydrophobic domain 1
LRRC58	leucine rich repeat containing 58
FRMD4B	FERM domain containing 4B
FRMD8	FERM domain containing 8
MYO10	myosin X
EDEM1	ER degradation enhancer, mannosidase alpha-like 1
SERTAD2	SERTA domain containing 2
TUB	tubby homolog (mouse)
PPARA	peroxisome proliferator-activated receptor alpha
FLOT2	flotillin 2
EVI5	ecotropic viral integration site 5
COL4A1	collagen, type IV, alpha 1
BMPR1B	bone morphogenetic protein receptor, type IB
ROD1	ROD1 regulator of differentiation 1 (S. pombe)
RAG1AP1	recombination activating gene 1 activating protein 1
CHSY1	chondroitin sulfate synthase 1

miR-642

Figure 33 shows the detected results of the expression of miR-642. The genomic localization of miR-642 is on chromosome 19q 13.32 with a genomic size of 97 nucleotides. The average ΔCT value in the GFP fraction was 12.4 ± 1.15 versus an average ΔCT in the VENTX fraction of 14.65 ± 0.25 (p=0.03). This miRNA was 4.8 fold lower expressed in the VENTX compared to the GFP control arm. TaqMan Human Array Cards did not contain the passenger strand miR-642.

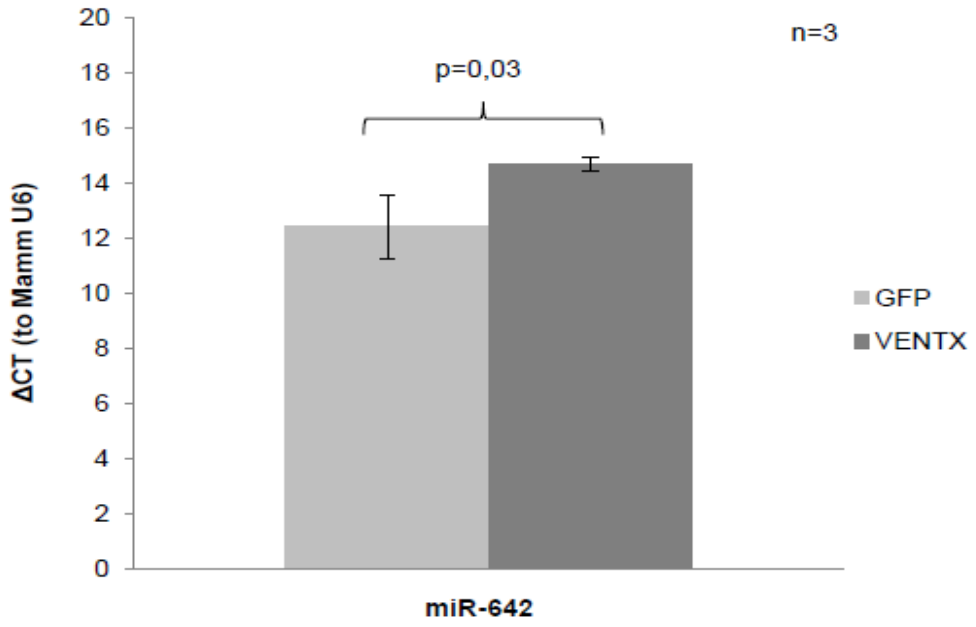

Fig. 33: Diagramm showing different miR-642 expression between GFP and VENTX transduced cord blood cells, p=0.03. MammU6 (endogenous control). Note that ΔCT values are inversely correlated to expression levels. Bars represent average expression ±SD (standard deviation). GFP (green fluorescent protein), CT (threshold cycle).

Using the TargetScanHuman program we obtained 170 potential gene targets. The first 25 potential gene targets are listed in table 12.

Tab. 12: The top twenty five putative targets of miR-642 identified with TargetScanHuman Custom

Target gene	Gene name
SHROOM4	shroom family member 4
MOBKL2C	MOB1, Mps One Binder kinase activator-like 2C (yeast)
SP8	Sp8 transcription factor
DNAL1	dynein, axonemal, light chain 1
C21orf91	chromosome 21 open reading frame 91
PVRL1	poliovirus receptor-related 1 (herpesvirus entry mediator C)
SLC5A3	solute carrier family 5 (inositol transporters), member 3
KRT85	keratin 85
PAQR7	progestin and adipoQ receptor family member VII
SYT11	synaptotagmin XI
SUZ12	suppressor of zeste 12 homolog (Drosophila)
INADL	InaD-like (Drosophila)
PTPN7	protein tyrosine phosphatase, non-receptor type 7
BCAS1	breast carcinoma amplified sequence 1
FAM46A	family with sequence similarity 46, member A
LUZP1	leucine zipper protein 1
INA	internexin neuronal intermediate filament protein, alpha
KAT2A	K(lysine) acetyltransferase 2A
DDX6	DEAD (Asp-Glu-Ala-Asp) box polypeptide 6
INOC1	INO80 complex homolog 1 (S. cerevisiae)
ZDHHC5	zinc finger, DHHC-type containing 5
TNS1	tensin 1
FAM5C	family with sequence similarity 5, member C
MAP3K2	mitogen-activated protein kinase kinase kinase 2
SFRS6	splicing factor, arginine/serine-rich 6

miR-432*

Figure 34 shows the results detected in the expression of miR-432*. The miR-432* gene is localized on chromosome 14q 32.2 with a genomic size of 94 nucleotides. The average ΔCT value in the GFP fraction was 18.84 ± 1.23 versus an average ΔCT in the VENTX fraction of 14.49 ± 0.27 ($p<0.01$), with the highest gene expression difference between both arms. This resulted in a 20.5 fold higher gene expression in the VENTX arm. TaqMan Human Array Cards did not contain the mature miRNA strand miR-432.

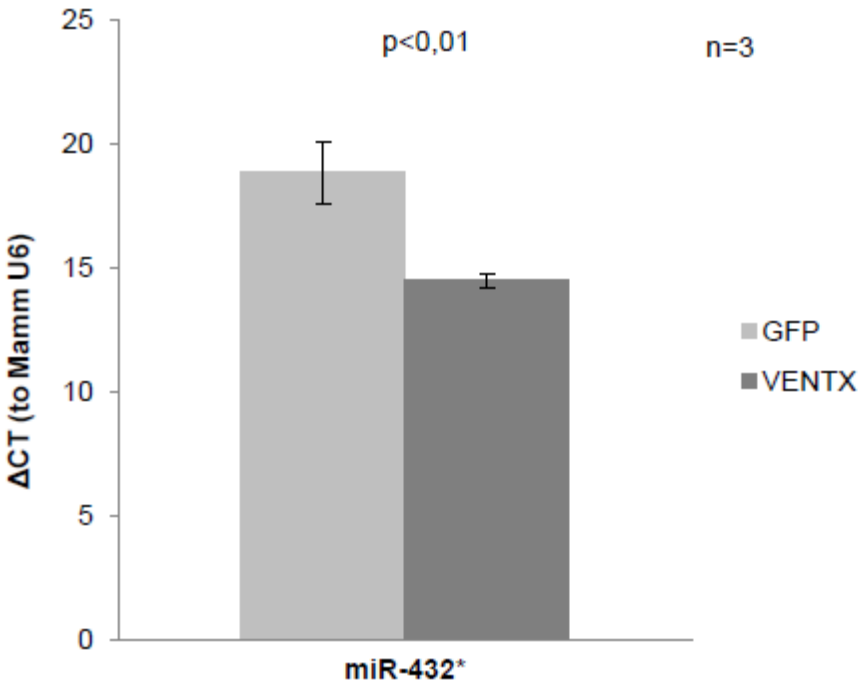

Fig. 34: Diagramm showing different hsa-miR-432* expression between GFP and VENTX transduced cord blood cells, p<0.01. MammU6 (endogenous control). Note that ΔCT values are inversely correlated to expression levels. Bars represent average expression ±SD (standard deviation). GFP (green fluorescent protein), CT (threshold cycle).

126 potential gene targets were found by TargetScanHuman Custom. The first 25 stated potential gene targets are listed in Tab. 13.

Tab. 13: The top twenty five putative targets of miR-432* identified with TargetScanHuman Custom

Target gene	Gene name
GSG1L	GSG1-like
SH3TC2	SH3 domain and tetratricopeptide repeats 2
FAM169B	family with sequence similarity 169, member B
HOXD10	homeobox D10
PCGF3	polycomb group ring finger 3
BCORL1	BCL6 co-repressor-like 1
CLPB	ClpB caseinolytic peptidase B homolog (E. coli)
DCLRE1B	DNA cross-link repair 1B (PSO2 homolog, S. cerevisiae)
DYNLL1	dynein, light chain, LC8-type 1
EPB41	erythrocyte membrane protein band 4.1 (elliptocytosis 1, RH-linked)
FAM168A	family with sequence similarity 168, member A
FLJ30851	hypothetical LOC653140
GPM6A	glycoprotein M6A
GPR162	G protein-coupled receptor 162
HLF	hepatic leukemia factor
HTR4	5-hydroxytryptamine (serotonin) receptor 4
LARP5	La ribonucleoprotein domain family, member 5
LOC402665	hCG1651476
NUCB1	nucleobindin 1
PCDHGA1	protocadherin gamma subfamily A, 1
PCDHGA10	protocadherin gamma subfamily A, 10
PCDHGA11	protocadherin gamma subfamily A, 11
PCDHGA12	protocadherin gamma subfamily A, 12
PCDHGA2	protocadherin gamma subfamily A, 2
PCDHGA3	protocadherin gamma subfamily A, 3

miR-616*

Figure 35 shows the results detected for miR-616*. miR-616* is localized on chromosome 12q 13.3 with a genomic size of 97 nucleotides. The average ΔCT value in the GFP fraction was 16.5 ± 0.28 versus an average ΔCT in the VENTX fraction of 17.95 ± 0.31 (p=0.04). According to this, the expression of miR-616* was 2.7 fold lower in the VENTX fraction compared to the empty vector control. Taqman Human Array Cards also contained the mature strand miR-616. The average ΔCT value in the GFP fraction was 14.34 ± 1.54 versus an average ΔCT in the VENTX fraction of 14.33 ± 0.90. However this result was not statistically significant (p= 1.00). This explains why the expression results for the mature strand miR-616 were nearly exact the same between both test arms.

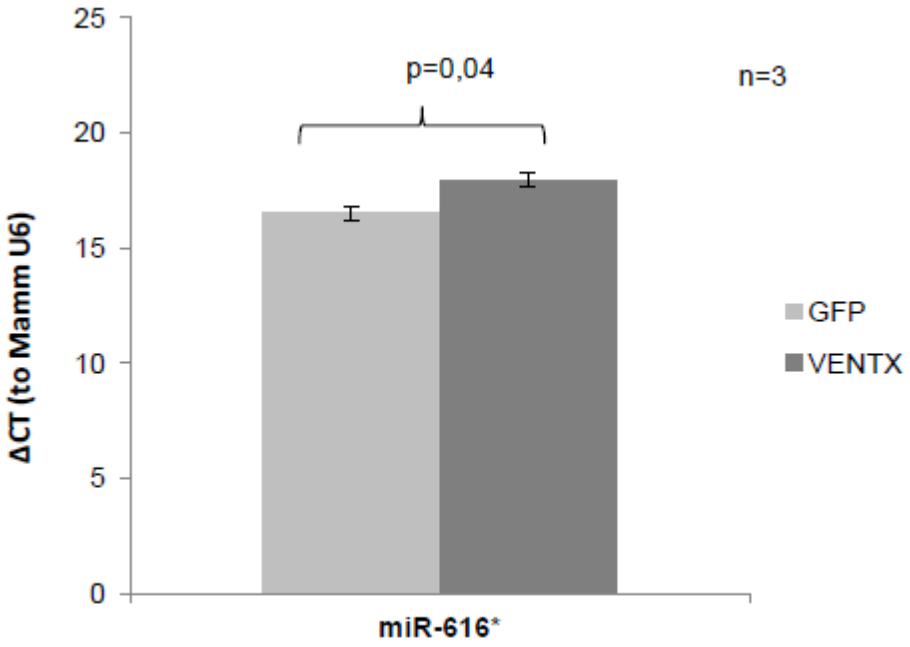

Fig. 35: Diagramm showing different miR-616* expression between GFP and VENTX transduced cord blood cells, p=0.04. MammU6 (endogenous control). Note that ΔCT values are inversely correlated to expression levels. Bars represent average expression ±SD (standard deviation). GFP (green fluorescent protein), CT (threshold cycle).

The miR-616* showed the highest number of 611 potential gene targets.The top twenty five putative targets of miR-616* identified with TargetScanHuman Custom are shown in Tab. 14.

Tab. 14: The top twenty five putative targets of miR-616* identified with TargetScanHuman Custom

Target gene	Gene name
XIAP	X-linked inhibitor of apoptosis
PHTF2	putative homeodomain transcription factor 2
SCAMP1	secretory carrier membrane protein 1
FOXK1	forkhead box K1
CNOT6L	CCR4-NOT transcription complex, subunit 6-like
KIAA0494	KIAA0494
NUFIP2	nuclear fragile X mental retardation protein interacting protein 2
PHF20L1	PHD finger protein 20-like 1
PLEKHH2	pleckstrin homology domain containing, family H member 2
RC3H1	ring finger and CCCH-type zinc finger domains 1
RER1	RER1 retention in endoplasmic reticulum 1 homolog (S. cerevisiae)
C2orf69	chromosome 2 open reading frame 69
CREBZF	CREB/ATF bZIP transcription factor
CUGBP2	CUG triplet repeat, RNA binding protein 2
FAM80B	family with sequence similarity 80, member B
ITGB8	integrin, beta 8
RP5-1000E10.4	suppressor of IKK epsilon
SLAIN1	SLAIN motif family, member 1
ZDHHC2	zinc finger, DHHC-type containing 2
C1orf96	chromosome 1 open reading frame 96
C6orf106	chromosome 6 open reading frame 106
PRPF40A	PRP40 pre-mRNA processing factor 40 homolog A (S. cerevisiae)
PSIP1	PC4 and SFRS1 interacting protein 1
USP7	ubiquitin specific peptidase 7 (herpes virus-associated)
ABCD2	ATP-binding cassette, sub-family D (ALD), member 2

3.9. Sequencing of AML cell lines

Recent data obtained in our group indicate that VENTX is highly expressed in normal myeloid cells and in AML cases with t(8;21) or normal karyotype. Consistent with these findings above it was observed, that VENTX showed a significantly higher expression in malignant myeloid cells as compared to lymphoid cells with the highest expression in K562, NB4 and EOL1 cell lines. In an attempt to address the question why VENTX is highly expressed in malignant AML cell lines we screened the five AML cell lines K562, NB4, MV4-11, EOL1 and OCI-AML3, originally derived from patients with myeloid leukemia for possible mutations in their protein coding sequence (CDS) of VENTX. Tab. 15 shows characteristics of the used AML cell lines.

Tab. 15: Acute myeloid leukemia cell lines, ATCC (American Type Culture Collection)

Cell line	Cell type	Chromosomal aberration	Origin
K562	Erythroleukemia	human hypotriploid karyotype without sharp mode - 61-68<3n>XX, -X, -3, +7, -13, -18, +3mar, del(9)(p11/13), der(14)t(14;?)(p11;?), der(17)t(17;?)(p11/13;?), der(?18)t(15;?18)(q21;?q12), del(X)(p22)	ATCC
NB4	Promyelocytic leukemia	human hypertriploid karyotype with 3% polyploidy - 78(71-81)<3n>XX, -X, +2, +6, +7, +7, +11, +12, +13, +14, +17, -19, +20, +4mar, der(8)t(8;?)(q24;?), der(11)t(11;?)(?->::11p15->11q22.1::11q13->22.1:), der(12)t(12;?)(p11;?), 14p+, t(15;17)(q22;q11-12.1), der(19)t(10;19)(q21.1;p13.3)x2	ATCC
MV4-11	Myelomonocytic leukemia	human hyperdiploid karyotype - 48(46-48)<2n>XY, +8, +18, +19, -21, t(4;11)(q21;q23)	ATCC
OCI-AML3	Acute myeloid leukemia	human hyperdiploid karyotype - 48(45-50)<2n>X/XY, +1, +5, +8, der(1)t(1;18)(p11;q11), i(5p), del(13)(q13q21), dup(17)(q21q25) - sideline with r(Y)x1-2 - hemizygous for RB1	ATCC
EOL-1	Eosinophilic leukemia	human hyperdiploid karyotype with 7.5% polyploidy - 50(48-51)<2n>,XY, +4, +6, +8, +19, del(4)(q12)x2, del(9)(q22) - del(4) effects cryptic FIP1L1-PDGFRA fusion	ATCC

We chose primers which encompassed the whole VENTX CDS. The VENTX CDS is 777 nucleotides long and consists of 3 exons. Using the PCR x Enhancer System we were able to detect VENTX expression in the following AML cell lines NB-4, MV4-11 and EOL-1. Interestingly, we could not detect VENTX expression in K562 and OCI-AML3 cell lines (Fig. 36). We used ß-actin as a loading control.

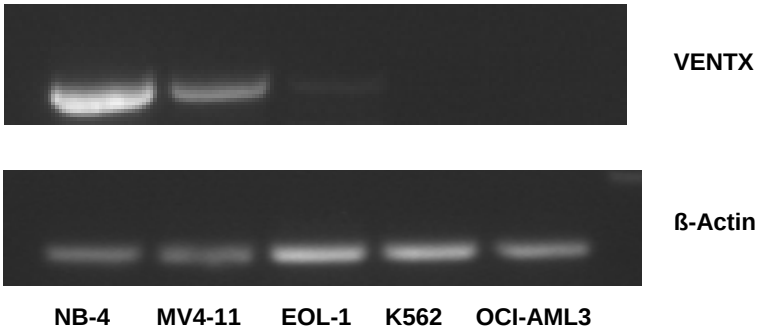

Fig. 36: VENTX expression in five acute myeloid leukemia cell lines. No VENTX expression was detected in K562 and OCI-AML3.

After this, we extracted the VENTX product and sent it to GATC Biotech for sequencing. We compared the sequences we obtained from GATC Biotech with the PubMed VENTX CDS by means of multiple sequence alignment using the online tool MultAlin (version 5.4.1).

Expression of VENTX in the NB4 cell line

The NB-4 cell line is established from the bone marrow of a 23-year-old woman with acute promyelocytic leukemia and t(15;17) translocation. It was not possible to detect the whole VENTX CDS in this cell line with the chosen primers owing to difficulties with sequencing of the beginning of our sequence. This is a common issue and can be attributed to the fact that sequencing around primer binding sites is often difficult. We were able to evaluate the NB-4 CDS between nucleotides 58-777, however. For this coding sequence, no differences were found between our sequence and the PubMed reference sequence, apart from a single polymorphism (SNP) at position 144 (Fig. 37). According to the USCS Genome Browser, this

SNP is named rs2998143 [187]. Its minor allele is adenine and it has an average global distribution of 0.391. Guanine, the major allele, has a frequency of 0.609. It is a synonymous SNP, meaning that no change in the amino acid occurs. In this case, our sequence contains the nucleotide guanine (G) instead of adenine (A) (Fig. 37). At the protein level, both sequences code for the amino acid proline.

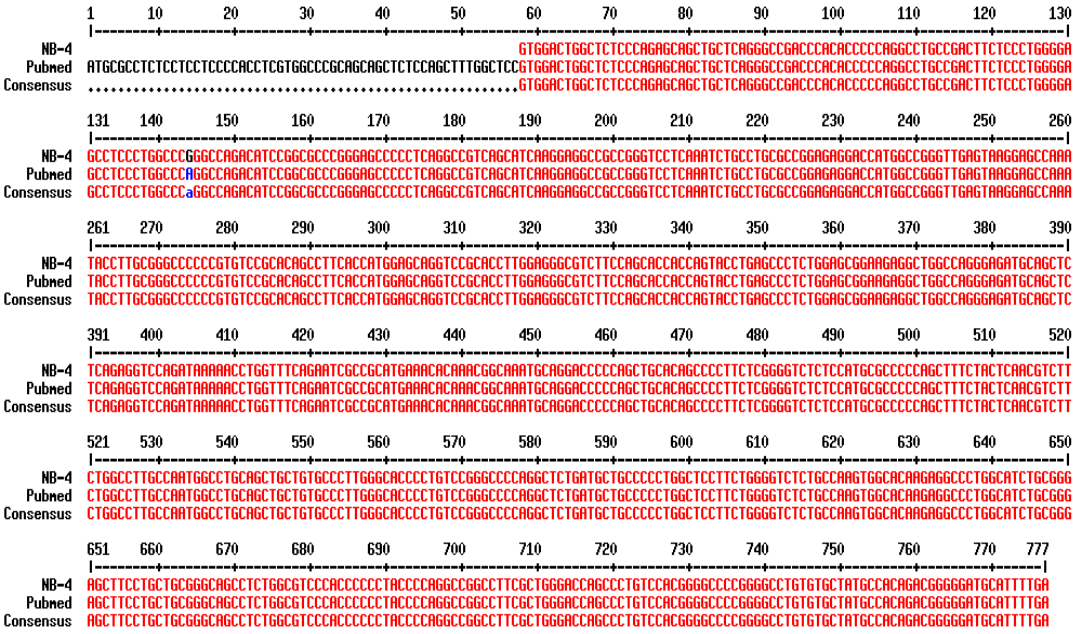

Fig. 37: Coding sequence alignment of acute myeloid leukemia cell line NB-4 VENTX sequence with VENTX sequence of PubMed. Note the difference at position 144 between both sequences

Expression of VENTX in the MV4-11 cell line

High VENTX expression was also observed in the MV4-11. This cell line is established from the peripheral blood of a 10-year-old male with biphenotypic B-myelomonocytic leukemia and t(4;11) translocation. The same obstacles as with the NB-4 cell line did not allow us to make a comparison between MV4-11 and the PubMed VENTX sequence for the whole sequence. In this case, we were able to align both sequences between nucleotides 58-777 (Fig. 38). Interestingly, we observed the presence of the same SNP rs2998143 as mentioned above at position 144.

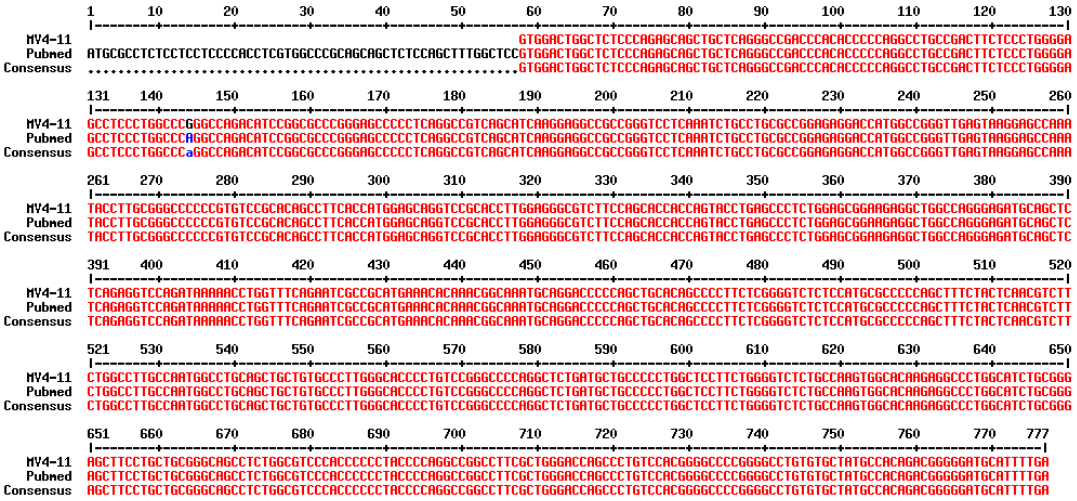

Fig. 38: Coding sequence alignment of acute myeloid leukemia cell line MV4-11 VENTX sequence with VENTX sequence of PubMed. Note the difference at position 144 between both sequences

Expression of VENTX in the EOL-1 cell line

We also analyzed the expression of VENTX in the EOL-1 cell line. VENTX was almost undetectable on PCR gel (Fig. 36), so that the sequence we received back from GATC Biotech did cover less of the CDS compared to the other two cell lines described above. This cell line was established from the peripheral blood of a 33-year-old man with acute myeloid eosinophilic leukemia (AML) following hypereosinophilic syndrome. In this case, we were able to align both sequences between nucleotides 54-740. We found two differences in the multiple alignment of our sequence compared to the PubMed VENTX sequence. First, at position 144, we saw the same SNP rs2998143 as we had observed in the other two cell lines mentioned above. The second difference was found at position 420, where our sequence contained the nucleotide adenine (A) instead of the guanine (G) in the PubMed sequence (Fig. 39). At the protein level, both sequences code for the amino acid glutamine. According to the USCS Genome Browser, it is not a SNP but a silent mutation. This is probably attributable to the fact that, until now, only two bigger cohorts, each containing 60 samples, have been screened. In theory, it seems to be possible that, with larger numbers of samples screened, it might also be found to be a SNP.

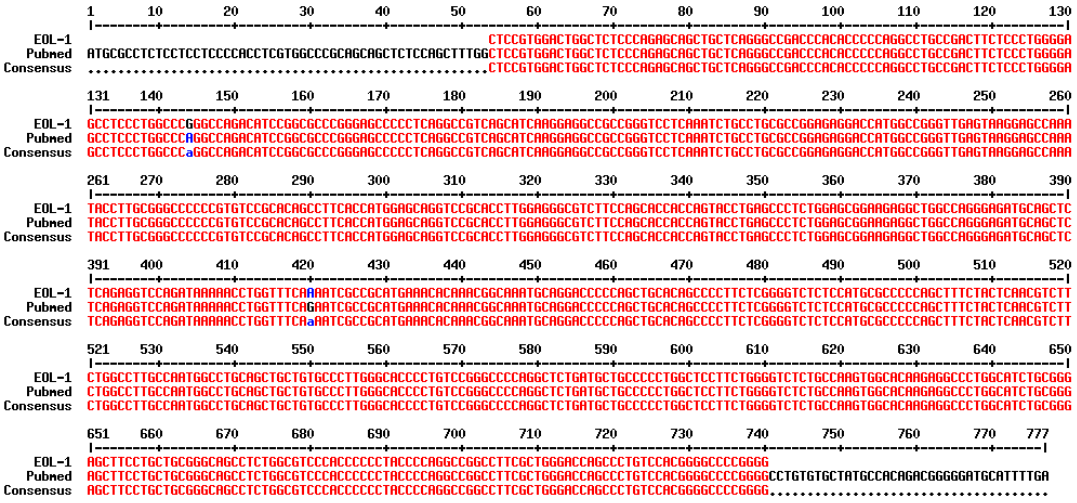

Fig. 39: Coding sequence alignment of acute myeloid leukemia cell line EOL-1 VENTX sequence with VENTX sequence of PubMed. Note the difference at position 144 and 420 between both sequences

Expression of VENTX in the K562 and OCI-AML3 cell line

No expression of VENTX was observed in the K562 cell line, a cell line established from the pleural effusion of a 53-year-old female with chronic myelogenous leukemia in terminal blast crisis, which means that it was not possible to screen this cell line for possible CDS alterations. There was also no expression of VENTX detected in the OCI-AML3 cell line (Fig. 36). This cell line was established from the peripheral blood of a 57-year-old man with acute myeloid leukemia (AML FAB-M4).

4. Discussion

Previously, it was shown that the human Vent-like homeobox gene VENTX, a putative homolog of the early developmental Xenopus xvent2 gene, acts as a novel regulatory hematopoietic gene. Furthermore, it was demonstrated that VENTX is aberrantly expressed in $CD34^+$ leukemic stem cell (LSC) candidates in human AML, predominantly in t(8;21)-positive and normal karyotype (NK) AML. Gene expression profiling, pathway analysis, as well as functional assays showed that enforced expression of VENTX in normal $CD34^+$ cells initiates expression of genes associated with myeloid development and promotes generation of myeloid cells *in vivo*, paralleled by downregulation of lymphoid genes and suppression of lymphoid engraftment. Lentivirally mediated knock-down of VENTX in human AML cell lines significantly impaired leukemic cell growth, indicating that VENTX is a key protein for human leukemic cell growth [155]. On the other hand it has been possible to show that via transactivation of the tumor suppressors p53 and $p16^{ink4a}$, VENTX regulates the cell cycle and acts as an inhibitor of cell proliferation in lymphoid cell populations. In this context, VENTX is involved in senescence pathways, which play an important role in tumor prevention. In fact, VENTX downregulation in lymphocytes is associated with a significant decrease in the concentrations of the aforementioned tumor suppressor proteins [192]. This fact is consistent with a recent publication which showed that VENTX expression is downregulated in CLL patients. VENTX was also referred to as a possible tumor suppressor in this cellular context, which, as a LEF/TCF-associated transcription factor, inhibits the canonical Wnt/ß-catenin signaling pathway when expressed normally [52]. The functional effects of VENTX therefore seem to be context-dependent. As VENTX seems to play a role in normal as well as malignant hematopoiesis we wanted to continue studies on its functional role and took a closer look at potential molecular changes focusing on miRNAs.

In an attempt to characterize potential molecular changes that are caused by VENTX and that might play a role in VENTX-associated leukemias, we performed profiling of the miRNA transcriptome from cord blood cells transduced with VENTX and used cord blood cells transduced with the empty vector as a control.

In this study we successfully established a spin infection protocol of retroviral transduction of human CB cells. This resulted in a significant amount of transduced CB cells, which was mandatory for the completion of miRNA profiling.

In order to show that we were able to reproduce the functional results obtained by Rawat et al. we performed CFC assays using our transduction protocol. In line with the findings published by Rawat et al. we could demonstrate a decrease in the formation of erythroid colonies and an increase in the formation of myeloid from cord blood cells that constitutively expressed VENTX as compared to the empty vector control [155]. The latter result confirms the findings of the Wu et al. study group, which was able to demonstrate that VENTX expression is upregulated during monocyte-to-macrophage differentiation and represents an important prerequisite for terminal macrophage differentiation. At the molecular level, this was attributed to the fact that VENTX regulates the expression of key proteins, including the M-CSF receptor. In this study, VENTX also appeared to play an essential role in the pro-inflammatory response of terminally differentiated macrophages. In knockdown experiments involving VENTX in macrophages, a significant decrease was detected in secreted pro-inflammatory cytokines such as TNF-α, IL-6 and IL-8 [193].

We were able to collect enough material to perform low density arrays from three independent cord blood experiments. In each of these three separate experiments, the expression values of 754 miRNAs were detected, including endogenous and negative controls. For five miRNAs, a significant difference in expression was observed between retrovirally VENTX- and GFP-transduced cord blood cells ($p<0.05$). miRNAs which, according to their expression levels, showed statistically significant changes in their expression, were miR-130b* ($p=0.02$), miR-506 ($p=0.03$), miR-642 ($p=0.03$), miR432* ($p<0.01$) and miR-616* ($p=0.04$).

Based on a literature search in PubMed, these five miRNAs were initially studied in previous publications to gain a first idea of their possible function. Publications were searched irrespectively of which miRNA strand was significantly expressed differentially in this study. In this context, it is important to recall that both the mature miRNA strand and the passenger miRNA* strand arise from a common pre-miRNA precursor strand at the start of their biogenesis and represent separate molecules only after their separation (Fig. 40). Until recently, miRNAs*, regardless

in which species, were thought not to have any biological function, and the generally accepted theory was that these would be degraded after separation of the mature miRNA strand [85] [46]. Therefore publications on the function of miRNAs* are still rare. A paradigm shift can be seen, however. There is now growing evidence that at least some miRNAs* definitely function as mature miRNAs and have a biological function [63]. The molecular background for the expression of one or both of the known miRNA strands is still largely unclear. There is some evidence, however, that, depending on the thermodynamic stability of the 5' and 3' strand in the stem loop structure of the pre-miRNA, the cell uses the strand with lower stability as miRNA and breaks down the other more stable strand. It is also known according to expression analyses that, depending on the tissue, miRNA and miRNA* can also be co-expressed simultaneously and that the ratio of miRNA to miRNA* can vary significantly during different developmental processes [161] [81]. In our study we found five miRNAs which, according to their expression levels, showed statistically significant changes in their expression: both the two mature miRNA strands miR-506 and miR-642 and the three miRNA* strands miR-130b*, miR-432* and miR-616*.

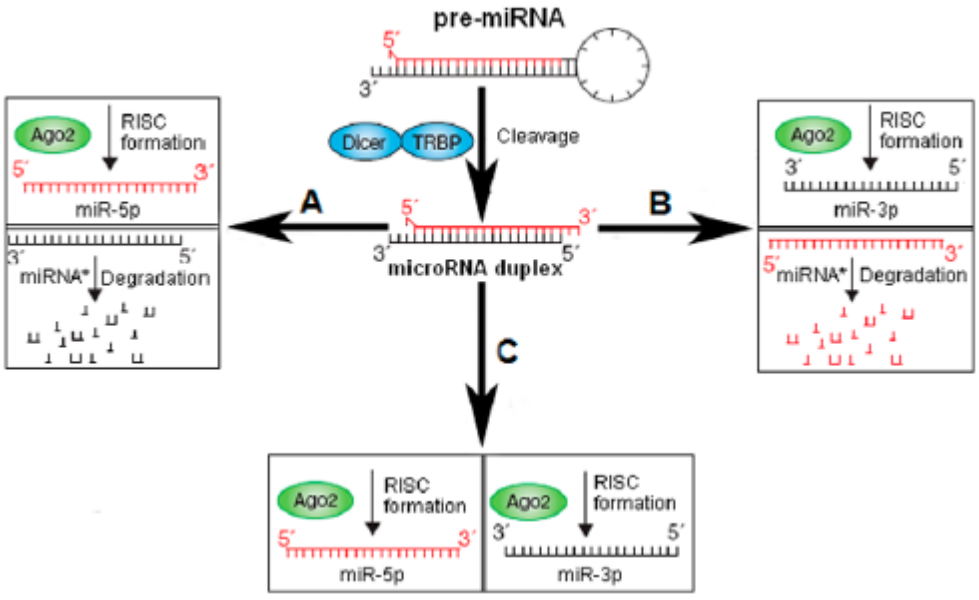

Fig. 40: The selection of mature miRNA strand and the fate of its passenger strand, adapted from [63, p. 11387] (A) The mature miRNA sequence is miR-5p, and its passenger sequence is miRNA* (star) which is degraded. (B) The mature miRNA sequence is miR-3p, and its passenger sequence is miRNA*. (C) Both the miR-5p and the miR-3p are mature miRNA sequences that guide RICS (RNA-induced silencing complex) to silence target mRNAs through mRNA cleavage, translational repression or deadenylation.

miR-130b* was expressed 2.2 times higher in VENTX-transduced umbilical cord blood cells than in the GFP control (p=0.02). In contrast, expression of the mature miRNA miR-130b was 3.5 times lower in the VENTX fraction than in the GFP control, although the difference was not statistically significant (p=0.35). This miRNA-130b* seems to be differentially expressed in patients with gastric cancer. In a study analyzing the miRNA profiles from patients with gastric cancer miRNA-130b* was significantly higher expressed in those patients with stomach cancer as compared to the control [196]. More data are available about the mature miRNA, miR-130b. It was recently reported that miR-130b overexpression in gastric cancer is associated with a decrease in the expression levels of the known tumor suppressor, RUNX3 [98]. In one publication, it was also reported that miR-130b promotes the growth of cancer stem cells, i.e. those cells that initiate and maintain tumor growth and self-renewal, in hepatocellular carcinoma [116]. Interestingly, in combination with miR-15b, miR-130b even serves as a potential biomarker for the detection of hepatocellular carcinoma and, according to early results, appears to be superior to serum α-fetoprotein (AFP) in the early stages of the disease. AFP is the only tumor marker in widespread clinical use at present in hepatocellular carcinoma [110]. Epigenetic silencing of miR-130b is associated with the development of chemotherapy resistance in ovarian cancer [195]. Besides its role in solid tumors, miR-130b is also involved in malignant hematopoiesis. Yeung et al. showed that miR-130b gene expression is upregulated both in the peripheral blood mononuclear cells of adult T-cell leukemia (ATL) patients and in adult T-cell leukemia cell lines transformed by human T-cell lymphotropic virus 1 (HTLV-1). In this context, miR-130b overexpression gives rise to a decrease in tumor suppressor gene expression for tumor protein 53-induced nuclear protein 1 (TP53INP1), a key protein in the induction of cell cycle arrest and apoptosis [197]. Pathognomonic in classic CML is the Philadelphia chromosome t(9;22), which codes for the BCR-ABL fusion gene. This fusion gene generates a protein with constitutive tyrosine kinase activity and thus leads to malignant transformation of the pluripotent stem cells of the bone marrow. In this process, the BCR-ABL fusion gene also upregulates oncogenic miRNAs such as miR-130a/b, which downregulates the expression of the negative growth regulator, CCN3, conferring a growth advantage to the leukemic cells [175]. As a final example, it should be mentioned that miR-130b overexpression reduces the sensitivity of multiple myeloma cells to glucocorticosteroid receptors and thus

impairs the efficacy of glucocorticosteroids in the treatment of multiple myeloma [179]. Overall these previous publications show that miR-130b might confer survival advantage to tumour cells. In our study, the expression of miR-130b was 3.5 times lower expressed in VENTX-transduced umbilical cord blood than in the control arm, although the difference was not statistically significant. More in-depth studies in known VENTX-overexpressing AML subtypes would be helpful to verify a potential role of miR-130b expression in certain AML subtypes.

In our experiments, miR-506 was another miRNA, which showed a differential expression: it was 2.3 times lower expressed in VENTX-transduced umbilical cord blood cells as compared to the control ($p=0.03$). Banales et al. could recently show that the expression of miR-506 is increased in the biliary epithelium of patients with primary biliary cirrhosis. This upregulation was associated with a decrease in the Cl^-/ HCO_3^--anion anion exchanger 2 (AE2), which plays an important role in maintaining intracellular pH homeostasis and in the secretin-mediated release of bicarbonate. The authors conclude from their data that miR-506 might represent a potential therapeutic target in patients with primary biliary cirrhosis [11]. Unlike with miR-130b, the role of miR-506 in tumor development is not yet clear. So far, there is evidence that miR-506 acts as a tumor suppressor. Zhao et al., for example, observed reduced miR-506 gene expression levels in malignantly transformed human bronchial epithelial cells (16HBE-T) compared to normal human bronchial epithelial cells (16HBE), whereas the mRNA levels of N-RAS, one of the best known oncogenes, were increased [202]. N-RAS mutations also occur in a proportion of AML patients (section 1.2.). There are also reports which ascribe oncogenic properties to miR-506 in other cellular contexts. Firstly, it has been shown that miR-506 overexpression confers resistance to hydroxycamptothecin, a topoisomerase I inhibitor chemotherapy agent, in human bowel cancer cells. The peroxisome proliferator–activated receptor PPARα plays an important role in this process. The latter is an intracellular steroid receptor which is integrated into various biological signaling pathways and is negatively regulated by miR-506 [184]. That PPARα is a direct target of miR-506 is also confirmed by the results of this study (Tab. 11). Within the miRNA-506-514 cluster, miR-506 is also overexpressed in almost all subtypes of malignant melanoma and experimental inhibition of this cluster is associated with a decrease in melanoma growth and apoptosis induction [172]. So

far, there are no data on the role of miR-506 in normal or malignant hematopoiesis.

The third miRNA which showed a differential expression profile was miR-642. miR-642 was 4.8 times lower expressed in VENTX transduced CB cells than in the GFP control ($p=0.03$). So far, there are no reports related to this miRNA.

The expression of miR-432* was highly differential between VENTX transduced CB cells and CB cells transduced with the empty vector control ($p<0.01$). Expression of this miRNA was 20.5 times higher in VENTX-transduced umbilical cord blood cells than in the vector control. So far, only little is known about the function of this miRNA. miRNA profiling from white blood cells of schizophrenia patients compared with healthy subjects was used to try and establish potential blood biomarkers for schizophrenia. Among these, seven miRNAs with different expression levels were detected, including miR-432 with a 1.4 times reduction in gene expression. It should be stressed, however, that the reliability of individual miRNAs as predictors for this disease is insufficient. In fact, only examination of a number of differentially expressed miRNAs in lymphocytes provides greater diagnostic specificity in schizophrenia [97]. McDaneld et al. also reported, following miRNA profiling during various developmental stages of porcine muscle, that miR-432 takes on an important role in early fetal muscle development and its expression decreases continuously again in later developmental stages [124].

The last significantly differentially expressed miRNA was miR-616*, with a 2.7 times lower expression in VENTX-transduced cells ($p=0.04$). Expression of the mature miRNA, miR-616, was almost exactly the same in the two fractions, with no statistically significant difference ($p=0.03$). Like the miR130b*, miR-616* was also significantly overexpressed in patients with gastric cancer compared with healthy gastric tissue [196]. Ma et al. showed that miR-616, i.e. the mature miRNA, promotes androgen-independent growth in prostate cancer cells. This is of relevance because in its early stages prostate cancer can be treated with hormone therapy before it starts to become increasingly hormone-insensitive and then progresses in a hormone-independent form. At the molecular level, miR-616 inhibits the expression of the tumor suppressor TFPI-2. Reexpression of this tumor suppressor in prostate cancer cells in which miR-616 is overexpressed leads to growth inhibition in these cells and maintains the androgen-independent phenotype of the cells

[116]. It has also been reported that miR-616 belongs to a number of miRNAs which have a high binding affinity to the mRNA of HLA-G and may regulate this. HLA-G is not expressed in many tissues, but plays an important role in materno-fetal tolerance in pregnancy. HLA-G expression is also found in tumors, autoimmune diseases and in hematopoietic cells [26].

In the next step, the potential target genes of the five aforementioned miRNAs, and in this case only the strands of the miRNAs which were differentially expressed in a statistically significant manner, were determined using the online tools miRBase and TargetScanHuman Custom. Because of the large number of potential targets, only the first 25 target genes listed for each miRNA (section 3.8.) have been considered for further discussion. All 125 possible target genes were analyzed in respect to their functional role on the basis of the PubMed literature search. For illustration purposes, however, only those potential target genes for which a role in physiological/malignant hematopoiesis or a connection with VENTX can be demonstrated will be discussed below.

One miR-130b* target gene which must be discussed is the homeobox gene HOXA13. It belongs to the clustered or class I homeobox genes which are grouped into the HoxA-D clusters (section 1.3.). In particular, the HoxA cluster genes play a role in the self-renewal of hematopoietic stem cells and progenitor cell lineage specification. It was recently reported that HOXA13 exclusively promotes differentiation into monocytes/macrophages *in vitro*, whereas cells that have been transduced by the other HoxA genes, besides differentiating into monocytes/macrophages, have also been observed to develop into granulocytes [9]. Based on the findings of this study, the role played by VENTX in this situation via increased expression of miR-130b* is still unclear. Furthermore, the CFC assays in this study and published data show that VENTX, via factors which are still unclear, definitely promotes granulocyte development [155]. In malignant hematopoiesis HOXA13 was identified as a fusion partner of the nucleoporin gene NUP98. NUP98 is a known gene in hematopoietic malignancies with 11p15 translocations and fuses with a large number of other genes, including other homeobox genes (section 1.3.1.). In addition, it has been observed that HOXA13 expression is significantly higher in monocytic leukemia cell lines than in other leukemia cell lines

[176]. Su et al. also observed isolated HOXA13 overexpression induced by translocation of the HoxA cluster in one patient with T-ALL [173].

As another miR-130b* target gene, insulin-like growth factor (IGF-1) also plays a significant role in hematopoiesis. As an endocrine hormone, IGF-1 is an important growth factor and its production is stimulated principally in the liver by growth hormone (GH). IGF-1 receptors are to be found on all cells of hematopoietic origin. *In vitro*, IGF-1 stimulates the growth of the erythroid precursor cells BFU-E and CFU-E. *In vivo*, it has also been possible to demonstrate in rats that parenteral administration of IGF-1 increases erythropoiesis [20] [86]. Interestingly, the results of this study showed a markedly smaller number of BFU-E´s and CFU-E´s in VENTX-transduced cells compared with the vector control *in vitro*, although the difference was not statistically significant, confirming previous results by the results [155]. One possible explanation for this would be that VENTX, via increased miR-130b* expression, down-regulates IGF-1 and consequently influences erythropoiesis negatively. This is contradicted, however, by the fact that IGF-1 does not have an isolated effect on erythropoiesis, but also promotes granulopoiesis, for example [168]. Logically, the overexpression of miR130b* induced by VENTX with consecutive down-regulation of IGF-1 should therefore also suppress granulopoiesis. But, in fact, VENTX promotes myeloid differentiation. Besides the role of IGF-1 in physiological hematopoiesis, evidence also exists that this factor has an influence in malignant hematopoiesis. For example, IGF-1 has mitogenic effects on malignant cell lines such as HL-60 (promyelocytic leukemia cell line), AML-193 (acute myeloid cell line) and K562 (erythroleukemia cell line). In addition, a decrease in IGF-1 receptor levels is observed during the subsequent differentiation of these cell lines, which suggests that IGF-1 maintains these cells in an undifferentiated state [168].

ANKRD28 (ankyrin repeat domain 28) is the last gene target of miR-130b* that will be discussed here. Just like HOXA13, ANKRD28 has also been identified as an additional fusion partner of the NUP98 gene. This gene fusion has been identified in a patient with myelodysplastic syndrome/acute myelogenous leukemia. Under normal circumstances, ANKRD28 is found only in the cell nucleus, whereas in this case ANKRD28 was also found in the cytoplasm. This change in location may play a part in disease development [77]. Jonge et al. was recently able to show, that ANKRD28 is also expressed differentially between AML $CD34^+$ and BM $CD34^+$

cells. High expression levels of ANKRD28 in AML patients with a normal karyotype were also associated with a significantly poorer outcome. In this study, ANKRD28 was found to have an independent prognostic value in relation to prognostic markers that are already clinically established, such as FLT-3 ITD, NPM1 or CEBPA [34]. Interestingly, VENTX expression levels are also particularly high in AML patients with a normal karyotype, which means that, via increased miR-130b* expression, ANKRD28 might be regulated differently in this case than in normal $CD34^+$ BM cells.

Three interesting miR-506 gene targets will be discussed in detail below. FZD4 (frizzled homolog 4), a receptor for Wnt ligands, is part of the Wnt signaling pathway, which is illustrated in Fig. 41. This well-characterized cell signaling pathway is an essential factor for embryonic development and is dysregulated in many tumors. In hematopoiesis, the highly conserved Wnt/ß-catenin signaling pathway leads to HSC proliferation and progenitor cell self-renewal, whereas inhibitors of this signaling pathway lead to a reduction *in vivo* [156] [157]. In normal hematopoiesis, FZD4 is highly expressed in $CD34^+$ cells and increases the Wnt3a-induced stability of ß-catenin in myeloid progenitor cells. It is now widely thought that excessive Wnt signaling is also of significance in the pathogenesis of a range of hematological neoplasms. Published data show that primary AML blasts display increased FZD4 expression compared with normal bone marrow cells. This suggests that the induction of FZD4 leads to increased Wnt signaling in AML and increases the self-renewal of AML cells [183]. It is conceivable that VENTX, via down-regulation of miR-506 expression, might cause induction of FZD4 and increased Wnt signaling indirectly. It should be pointed out, however, that VENTX is also known to form a transcription complex with LEF1, which inhibits LEF1/TCF-mediated transcription and thereby reduces Wnt signaling [52].

.

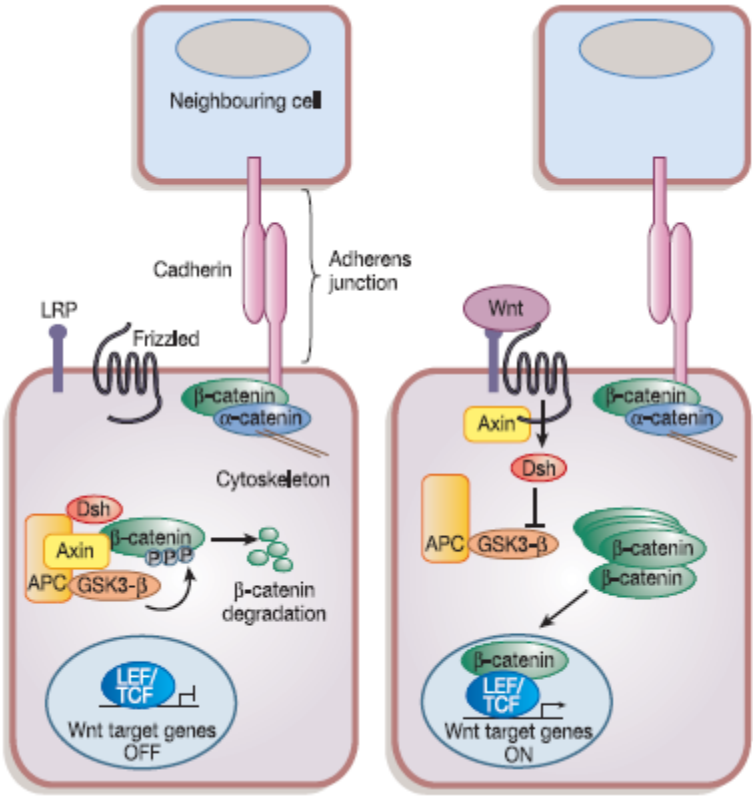

Fig. 41: The canonical Wnt signaling pathway, adapted from [156, p. 843]
In the absence of Wnt signaling (left panel), ß-catenin is in a complex with axin, APC and GSK3-ß, and gets phosphorylated and targeted for degradation. ß-catenin also exists in a cadherinbound form and regulates cell-cell adhesion. In the presence of Wnt signaling (right panel), ß-catenin is uncoupled from the degradation complex and translocates to the the nucleus, where it binds Lef/Tcf transcription factors, thus activating target genes.

The transcription factor RUNX1 is an important factor in embryonic hematopoiesis which also regulates HSC differentiation into mature blood cells (section 1.1.1.). RUNX1 is one of the most frequently mutated genes in AML. Possibly the most common mutation of this gene is found in the chromosomal translocation t(8;21), which is found in 15 % of AML patients and displays an increased incidence in the M2 subtype according to the FAB Classification [185] [149]. Genetic changes in the RUNX1 gene result in loss of function in this gene and are considered responsible for RUNX1-related leukemias. Leukemia was not able to develop spontaneously in studies in RUNX1-deficient mice, however. This observation is attributed to the fact that RUNX1-deficient HSCs are not able to maintain their capacity for self-renewal indefinitely and it can be assumed from this that additional genetic changes are necessary in the pathogenesis of leukemia. In fact, a gene was recently identified with EVI5 (ecotropic viral integration site 5) that prevents stem cell exhaustion in RUNX1-deficient mice and was also overexpressed in 44 % of AML

patients with the FAB-M2 subtype [80]. EVI5 was identified as a miR-506 gene target in this study. It should be pointed out again in this context that VENTX expression in AML is extended to the most primitive progenitors and stem cells and that VENTX is highly expressed in AML patients with a normal karyotype and the FAB-M2 subtype [155]. VENTX overexpression with down-regulation of miR-506 may therefore be responsible for activation of EVI5.

With 65 % homeodomain homology, VENTX is a putative homolog of the Xenopus xvent2b gene and belongs to the VENT HB gene family. This family is essential for the formation of the ventral mesoderm and hematopoietic development in Xenopus [133]. Members of this family act as direct and indirect downstream targets for the BMP-4 protein which is the key molecule in the development of the ventral mesoderm and gives rise to hematopoiesis in the embryo following gastrulation (sections 1.1.1. and 1.3.3.). Interestingly, xvent2b in Xenopus is capable of up-regulating BMP-4 expression itself via a positive autoregulatory loop (Fig. 10) [69]. BMP-4 exerts its regulatory effects via a range of BMP receptors. Accordingly, it is known from studies in mice that, after BMP-4 binding, the receptor BMPRII heterodimerizes with a type I receptor such as BMPRIb (bone morphogenetic protein receptor, type Ib) and as a result is activated and can initiate a large number of possible signaling cascades [31]. BMPRIb was identified as a miR-506 gene target in this study. Assuming that the same findings apply to VENTX as to xvent2b, it would be interesting to test whether VENTX, through the down-regulation of miR-506, might be capable of inducing BMP-4 expression and, as a result, its own expression via a positive regulatory loop.

Just one potential target gene of miR-642 will be discussed below. This is the gene SUZ12 (suppressor of zeste 12 homolog). This gene belongs to the Polycomb-group family of proteins which were first identified in the fruit fly *Drosophila* and which are of significance as epigenetic gene silencers, including of the Hox genes, in embryonic and tissue development. They are also important factors in the self-renewal of embryonic and adult stem cells and are involved in tumor development. The Polycomb-group protein family can be broadly divided into Polycomb repressive complex 1 (PRC1), the best-known member of which is the oncogene BMI1, and Polycomb repressive complex 2 (PRC2), composed mainly of the genes EED, EZH2 and SUZ12 [171]. Loss-of-function mutations in mouse studies have shown

that loss of SUZ12 is associated with increased stem cell activity and may, via the regulation of other genes, promote the differentiation of myeloid and lymphoid progenitor cells [119]. On the basis of the data currently available, the role of SUZ12 in malignant hematopoiesis is unclear. On the one hand, Kroeze et al. reported that SUZ12, unlike EZH2, a member of the same family, does not play a particular role in myeloid neoplasms [91]. Instead, SUZ12 is found to be dysregulated in solid tumors such as colon carcinoma, breast cancer or carcinoma of the liver. On the other hand, it has been shown that SUZ12 is overexpressed in bone marrow cells of CML patients in blast crisis and is also involved in the pathogenesis of mantle cell lymphoma [150] [122]. The extent to which VENTX, via down-regulation of miR-642, is capable of intervening in the aforementioned physiological and pathological processes of SUZ12 is an open question.

In this study, miR-432* was the fourth miRNA expressed differentially between VENTX- and GFP-transduced umbilical cord blood cells. In this context, it seems worthwhile to discuss the functional role of two of the first 25 possible target genes of this miRNA that have been studied. HOXD10 is a member of the class I homeobox gene family and is part of the HoxD cluster which, unlike HoxA-C, is not expressed in physiological hematopoiesis. Furthermore, there is no evidence at present that HOXD10 plays a role in malignant hematopoiesis. On the contrary, it is known that HOXD10, by modulating the expression of a range of genes, inhibits angiogenesis, while HOXD10 expression decreases in tumor blood vessels [137]. This finding is consistent with other publications which suggest that HOXD10 acts as a tumor suppressor in breast cancer cells and in stomach cancer [25] [190]. There are no publications to date which link VENTX and miR-432* overexpression and the resulting regulation of HOXD10 gene expression. The functional role of VENTX has previously been described normal and malignant hematopoiesis. The transcriptional corepressor gene, BCORL1 (BCL6-co-repressor-like-1), as another target gene of miR-432*, has recently been identified as a new potential tumor suppressor gene in AML. Functionally, BCORL1 interacts with histone deacetylases and inhibits the expression of E-cadherin [182]. In a clinical trial involving 173 AML patients, mutations in the BCORL1 gene were identified in six percent of cases [106]. VENTX overexpression in individual subtypes of AML may thus, via overexpression of miR432*, contribute to different expression in the BCORL1 gene.

Finally, we should discuss two target genes of miR-616* which, according to the results of the experiments in this study, was expressed at lower levels in VENTX-transduced umbilical cord blood cells than in the vector control. XIAP (X-linked inhibitor of apoptosis) represents a potential target gene of this miRNA. It belongs to a family of proteins with eight members with anti-apoptotic properties ascribed to it. The best-characterized member of this family, XIAP promotes cell survival via direct inhibition of apoptotic caspases. It has also been possible to show that XIAP overexpression results in the increased transcription of a range of genes of major signaling pathways. It has been shown, for example, that XIAP serves as a link between BMP receptors and downstream molecules. The inhibition of XIAP binding to the type I BMP receptor, which was also a target gene of miR-506, thus partly prevents the differentiation of the ventral mesoderm. In this context it is likely, that the role of XIAP in the BMP pathway is not linked to its anti-apoptotic function [42]. It is interesting to speculate that via down-regulation of miR-506, VENTX increases XIAP expression and consequently promotes its own expression as a result of increased BMP signaling through a positive autoregulatory loop. Many patients with AML display XIAP expression and, in a trial in 53 children with de novo AML, expression of this gene correlated significantly with an inferior 3-year relapse-free survival rate and inferior response to chemotherapy [174]. These results are consistent with data from a trial with 30 adult patients with de novo AML. In this trial, 43.3 % of the patients displayed XIAP overexpression and 91.7 % of these had a poor response to chemotherapy [74]. VENTX might be involved in these cases via regulation of miR-506. PSIP1 (PC4 and SFRS1 interacting protein, formerly LEDGF) should also be mentioned as a target gene of miR-506. According to publications, this gene fuses with the NUP98 gene in certain cases of AML. This has already been mentioned in connection with two target genes of miR-130b*. Until 2011, 25 potential NUP98 partners had been identified. The NUP98/PSIP1 fusion gene codes for the two transcription factors p75 and p52 and, according to the data currently available, can be considered a marker for poor prognosis in AML [132] [114].

In summary it is striking that a large number of potential gene targets for the miRNAs discussed above, are involved not only in normal but also in malignant hematopoiesis. To which extent VENTX exerts its physiological and pathological role via the regulation of these miRNAs remains to be determined. Because the number of

potential target genes for each miRNA is considerably higher than the number discussed here, it can not be excluded that other target genes of these miRNAs play a key role for VENTX mediated effects. It should also be pointed out that, with the current online tools such as TargetScan, miRanda, PicTar, etc., various algorithms are available for miRNA target prediction. The tool used in this study, TargetScan-Human Custom, includes new miRNAs which are still relatively unknown in the target search and is a follow-on from TargetScan. TargetScan was the first tool available for human miRNA target prediction with a false-positive target prediction rate of 22-31 %. It has been possible to reduce this initially high false-positive rate in subsequent versions [104] [103]. Despite this apparently very high false-positive rate for human miRNA target prediction, it should be pointed out that the seed complementarity method makes TargetScan one of the tools with the lowest false-positive rates for human miRNA targets [123].

The functional role of the five miRNAs expressed differentially in this study in hematopoiesis should be evaluated in more in-depth investigations. In this study, the expression levels of the three miRNAs miR-506, miR-642 and miR-616* were significantly lower in the VENTX arm than in the control arm. Retroviral or lentiviral overexpression of these miRNAs should be carried out in order to shed further light on their function. Vice versa the expression of the miRNAs miR-130b* and miR-432* overexpressed in the VENTX arm should be reduced by means of lentivirally mediated shRNA knockdown to test their functional relevance.

Aberrant expression of VENTX levels has to be shown to be extended to the most primitive progenitor compartment, which is thought to harbor the candidate leukemic stem cells and makes VENTX a potential leukemogenic factor in this context [155]. Why so many human homeobox genes are expressed aberrantly in malignant hematopoiesis has been unclear in most cases until now. One exception is the MLL (mixed lineage leukemia) rearranged AML, which accounts for 5 % of AML cases. This gene is essential for physiological hematopoiesis and is a known upstream regulator of Hox genes [33]. In the majority of cases, however, the cause of aberrant Hox gene expression remains unclear. The molecular mechanisms leading to aberrant expression of VENTX in some AML subtypes is unclear at present. To exclude mutations as a possible reason for aberrant expression of VENTX, the coding sequence (CDS) of VENTX was analysed for possible muta-

tions in human malignant myeloid cell lines in which the VENTX expression levels were significantly higher than in $CD34^+$ bone marrow progenitor cells [155]. In the first experiments, conducted under various PCR conditions, none of the respective VENTX CDSs were detectable in the five AML cell lines examined. One possible reason for this may have been the GC content, which is high in the CDS with 66 %. As a consequence, the PCR x Enhancer System was used, which allows efficient amplification of GC-rich templates. In fact, this made it possible to study three of the five AML cell lines for mutations in the VENTX coding sequence. However, it was not possible, to detect and sequence CDSs of VENTX in the K562 cell line, which was reported to highly express VENTX [155]. The expression of OCI-AML3 cell line was not detectable in this study either. In NB-4, MV4-11 and EOL-1, it was possible to sequence and analyze a large proportion of the CDSs of VENTX successfully. The initial sequences of all three cell lines exhibited a large number of undetermined bases which made it impossible to produce an alignment between the VENTX PubMed sequence and the sequences obtained in the respective cell lines in the initial regions of their CDSs (Fig. 37, 38, 39). These sequencing problems at and just after the primer binding site are normal and not attributable to methodological errors. In order to be able to cover the complete CDS of VENTX, the primer would consequently have to be located further outside the CDS, as it was done in this study. It should be noted, however, that functionally important protein domains are rarely located at the very beginning or end of a given gen. As a result of the poor PCR amplification, it was not possible to detect the end of the VENTX CDS in the EOL-1 cell line either (Fig. 39). Interestingly, all three cell lines displayed a single nucleotide polymorphism at the same point in their CDS (rs2998143). According to the data from the USCS Genome Browser, this SNP occurs with a frequency of 61 % in the populations screened so far. A silent mutation was observed in the EOL-1 cell line. Importantly VENTX has only been examined for SNPs in two larger populations of 60 individuals each. It is therefore theoretically possible, that this might also be an SNP when tested in a larger number of subjects. According to the results of this study, there is therefore no evidence of relevant mutations in the VENTX CDS in the screened AML cell lines with the limitations imposed by the aforementioned points. Another reason for aberrant VENTX expression could originate from promoter methylation, gene amplification

or overexpression of upstream regulators of VENTX such as BMP-4. This would be important to test, but was beyond of this study.

5. Summary

In recent years, it has been possible to identify VENTX, a member of the homeobox gene family, as a new regulator gene in normal and malignant hematopoiesis. Intensive research is currently focusing on the precise molecular mechanisms via which VENTX influences hematopoiesis. In an attempt to characterize potential molecular changes that are caused by VENTX and that might play a role in VENTX-associated leukemias, we performed profiling of the miRNA transcriptome from cord blood cells retrovirally transduced with VENTX and used cord blood cells transduced with the empty vector as a control. In this study, we established an alternative protocol of retroviral transduction of human cord blood cells. *In vitro* assays were performed as a control and to demonstrate that we were able to use this method to reproduce our previous results. Thus, we confirmed again that VENTX stimulates myelopoiesis, while erythropoiesis is inhibited. By retroviral transduction of human cord blood cells, gene expression profiles of 754 microRNAs in VENTX-associated hematopoiesis were tested and analyzed for the first time. MicroRNAs which, according to their expression levels, showed statistically significant changes in their expression, were miR-506, miR-642, miR-130b*, miR-432* and miR-616*. So far nothing is known about the function of these microRNAs in normal and malignant hematopoiesis. We identified a number of potential gene targets of these miRNAs that, are known to be involved in normal and malignant hematopoiesis. The extent to which VENTX is involved in both physiological and pathological processes via the regulation of these miRNAs remains to be determined on the basis of more in-depth studies. If these miRNAs will prove to be important for the biology of VENTX-associated leukemias, one potential approach to antagonize the oncogenic effect of VENTX would be the application of “anti-miRNA-associated oligonucleotides”.

In the second part of this thesis project the VENTX protein-coding sequence was sequenced in a number of acute myeloid leukemia cell lines to identify potential mutations, which might explain aberrant expression of VENTX in malignant hematopoiesis. Despite the fact that we were unable to analyze the complete coding sequence of tested cell lines, the findings of this study provide no indication of relevant mutations that might explain the aberrant expression of VENTX in human

acute myeloid leukemia. These sequencing efforts are naturally only an initial step and experiments should be extended to acute myeloid leukemia patient samples to finally exclude VENTX mutations in this disease. It would also be important to study whether promoter methylation, gene amplification or overexpression of upstream regulators of VENTX contribute to its aberrant expression in acute myeloid leukemia.

6. References

1. Abate-Shen C: *Deregulated homeobox gene expression in cancer: cause or consequence?*: Nat Rev Cancer, 2002. **2**: 777-785.

2. Afonja O, Smith JE, Cheng DM: *MEIS1 and HOXA7 genes in human acute myeloid leukemia*: Leuk Res, 2000. **24**: 849-855.

3. Akashi K, Traver D, Miyamoto T, Weissman IL: *A clonogenic common myeloid progenitor that gives rise to all myeloid lineages*: Nature, 2000. **404**: 193-197.

4. Antonchuk J, Sauvageau G, Humphries RK: *HOXB4-induced expansion of adult hematopoietic stem cells ex vivo*: Cell, 2002. **109**: 39-45.

5. Applied Biosystems: http://www3.appliedbiosystems.com/cms/groups/mcb_marketing/documents/generaldocuments/cms_054742.pdf (2012/01/31).

6. Applied Biosystems: http://tools.invitrogen.com/content/sfs/manuals/cms_053965.pdf (2012/02/01).

7. Argiropoulos B, Humphries RK: *Hox genes in hematopoiesis and leukemogenesis*: Oncogene, 2007. **26**: 6766-6776.

8. Ault KT, Dirksen ML, Jamrich M: *A novel homeobox gene PV.1 mediates induction of ventral mesoderm in Xenopus embryo*: Proc Natl Acad Sci USA, 1996. **93**: 6415-6420.

9. Bach C, Buhl S, Mueller D, Garcia-Cuellar MP, Maethner E, Slany RK: *Leukemogenic transformation by HOXA cluster genes*: Blood, 2010. **115**: 2910-2918.

10. Bacher U, Schnittger S, Haferlach T: *Molecular genetics in acute myeloid leukemia*: Curr Opin Oncol, 2010. **22**: 646-655.

11. Banales JM, Saez E, Uriz M, Sarvide S, Urribarri AD, Splinter P, Tietz Bogert PS, Bujanda L, Prieto J, Medina JF, Larusso NF: *Upregulation of mir-506 leads to decreased AE2 expression in biliary epithelium of patients with primary biliary cirrhosis*:Hepatology, 2012. **56**: 687-697.

12. Bartel DP: *MicroRNAs: genomics, biogenesis, mechanism, and function*: Cell, 2004. **116**: 281-297.

13. Bartel DP: *MicroRNAs: target recognition and regulatory functions*: Cell, 2009. **136**: 215-233.

14. Becker AJ, Mc CE, Till JE: *Cytological demonstration of the clonal nature of spleen colonies derived from transplanted mouse marrow cells*: Nature, 1963. **197**: 452-454.

15. Bell DR, Van Zant G: *Stem cells, aging, and cancer: inevitabilities and outcomes*: Oncogene, 2004. **23**: 7290-7296.

16. Bennett JM, Catovsky D, Daniel MT, Flandrin G, Galton DA, Gralnick HR, Sultan C: *Proposals for the classification of the acute leukaemias. French-American-British (FAB) co-operative group*: Br J Haematol, 1976. **33**: 451-458.

17. Bhagavathi S, Czader M: *MicroRNAs in benign and malignant hematopoiesis*: Arch Pathol Lab Med, 2010. **134**: 1276-1281.

18. Blank U, Karlsson G, Karlsson S: *Signaling pathways governing stem-cell fate*: Blood, 2008. **111**: 492-503.

19. Blatt C, Aberdam D, Schwartz R, Sachs L: *DNA rearrangement of a homeobox gene in myeloid leukaemic cells*: EMBO J, 1988. **7**: 4283-4290.

20. Blatt J: *IGF1 and leukemia*: Pediatr Hematol Oncol, 2000. **17**: 199-201.

21. Brennecke J, Stark A, Russell RB, Cohen SM: *Principles of microRNA-target recognition*: PLoS Biol, 2005. **3**: e85.

22. Buske C, Feuring-Buske M, Abramovich C, Spiekermann K, Eaves CJ, Coulombel L, Sauvageau G, Hogge DE, Humphries RK: *Deregulated expression of HOXB4 enhances the primitive growth activity of human hematopoietic cells*: Blood, 2002. **100**: 862-868.

23. Calin GA, Dumitru CD, Shimizu M, Bichi R, Zupo S, Noch E, Aldler H, Rattan S, Keating M, Rai K, Rassenti L, Kipps T, Negrini M, Bullrich F, Croce CF: *Frequent deletions and down-regulation of micro- RNA genes miR15*

and miR16 at 13q14 in chronic lymphocytic leukemia: Proc Natl Acad Sci USA, 2002. **99**: 15524-15529.

24. Calin GA, Sevignani C, Dumitru CD, Hyslop T, Noch E, Yendamuri S, Shimizu M, Rattan S, Bullrich F, Negrini M, Croce CM: *Human microRNA genes are frequently located at fragile sites and genomic regions involved in cancers*: Proc Natl Acad Sci USA, 2004. **101**: 2999-3004.

25. Carrio M, Arderiu G, Myers C, Boudreau NJ: *Homeobox D10 induces phenotypic reversion of breast tumor cells in a three-dimensional culture model*: Cancer Res, 2005. **65**: 7177-7185.

26. Castelli EC, Moreau P, Oya e Chiromatzo A, Mendes-Junior CT, Veiga-Castelli LC, Yaghi L, Giuliatti S, Carosella ED, Donadi EA: *In silico analysis of microRNAS targeting the HLA-G 3' untranslated region alleles and haplotypes*: Hum Immunol, 2009. **70**: 1020-1025.

27. Chan JA, Krichevsky AM, Kosik KS: *MicroRNA-21 is an antiapoptotic factor in human glioblastoma cells*: Cancer Res, 2005. **65**: 6029-6033.

28. Chen CZ, Li L, Lodish HF, Bartel DP: *MicroRNAs modulate hematopoietic lineage differentiation*: Science, 2004. **303**: 83-86.

29. Cheng T, Rodrigues N, Shen H, Yang Y, Dombkowski D, Sykes M, Scadden DT: *Hematopoietic stem cell quiescence maintained by p21cip1/waf1*: Science, 2000. **287**: 1804-1808.

30. Cumano A, Godin I: *Ontogeny of the hematopoietic system*: Annu Rev Immunol, 2007. **25**: 745-785.

31. Danesh SM, Villasenor A, Chong D, Soukup C, Cleaver O: *BMP and BMP receptor expression during murine organogenesis*: Gene Expr Patterns, 2009. **9**: 255-265.

32. Davidson AJ, Zon LI: *Turning mesoderm into blood:the formation of hematopoietic stem cells during embryogenesis*: Curr Topp Dev Biol, 2000. **50**: 45-60.

33. De Braekeleer M, Morel F, Le Bris MJ, Herry A, Douet-Guilbert N: *The MLL gene and translocations involving chromosomal band 11q23 in acute leukemia*: Anticancer Res, 2005. **25**: 1931-1944.

34. de Jonge HJ, Woolthuis CM, Vos AZ, Mulder A, van den Berg E, Kluin PM, van der Weide K, de Bont ES, Huls G, Vellenga E, Schuringa JJ: *Gene expression profiling in the leukemic stem cell-enriched CD34+ fraction identifies target genes that predict prognosis in normal karyotype AML*: Leukemia, 2011. **25**: 1825-1833.

35. Deguchi Y, Kehrl JH: *Selective expression of two homeobox genes in CD34-positive cells from human bone marrow*: Blood, 1991. **78**: 323-328.

36. DeKoter RP, Singh H: *Regulation of B lymphocyte and macrophage development by graded expression of PU.1*: Science, 2000. **288**(5470): 1439-1441.

37. Delassus S, Cumano A: *Circulation of hematopoietic progenitors in the mouse embryo*: Immunity, 1996. **4**: 97-106.

38. Dias S, Xu W, McGregor S, Kee B: *Transcriptional regulation of lymphocyte development*: Curr Opin Genet Dev, 2008. **18**: 441-448.

39. DiMartino JF, Selleri L, Traver D, Firpo MT, Rhee J, Warnke R, O'Gorman S, Weissman IL, Cleary ML: *The Hox cofactor and proto-oncogene Pbx1 is required for maintenance of definitive hematopoiesis in the fetal liver*: Blood, 2001. **98**: 618-626.

40. Dingli D, Pacheco JM: *Modeling the architecture and dynamics of hematopoiesis*: Wiley Interdiscip Rev Syst Biol Med, 2010. **2**: 235-244.

41. Döhner H, Estey EH, Amadori S, Appelbaum FR, Buchner T, Burnett AK, Dombret H, Fenaux P, Grimwade D, Larson RA, Lo-Coco F, Naoe T, Niederwieser D, Ossenkoppele GJ, Sanz MA, Sierra J, Tallman MS, Lowenberg B, Bloomfield CD: *Diagnosis and management of acute myeloid leukemia in adults: recommendations from an international expert panel, on behalf of the European LeukemiaNet*: Blood, 2010. **115**: 453-474.

42. Dubrez-Daloz L, Dupoux A, Cartier J: *IAPs: more than just inhibitors of apoptosis proteins*: Cell Cycle, 2008. **7**: 1036-1046.

43. Duncan AW, Rattis FM, DiMascio LN, Congdon KL, Pazianos G, Zhao C, Yoon K, Cook JM, Willert K, Gaiano N, Reya T: *Integration of Notch and Wnt signaling in hematopoietic stem cell maintenance*: Nat Immunol, 2005. **6**: 314-322.

44. Dzierzak E, Speck NA: *Of lineage and legacy:the development of mammalian hematopoietic stem cells*: Nat Immunol., 2008. **9**: 129-136.

45. Eis PS, Tam W, Sun L, Chadburn A, Li Z, Gomez MF, Lund E, Dahlberg JE: *Accumulation of miR-155 and BIC RNA in human B cell lymphomas*: Proc Natl Acad Sci USA, 2005. **102**: 3627-3632.

46. Esquela-Kerscher A, Slack FJ: *Oncomirs - microRNAs with a role in cancer*: Nat Rev Cancer, 2006. **6**: 259-269.

47. Falini B, Mecucci C, Tiacci E, Alcalay M, Rosati R, Pasqualucci L, La Starza R, Diverio D, Colombo E, Santucci A, Bigerna B, Pacini R, Pucciarini A, Liso A, Vignetti M, Fazi P, Meani N, Pettirossi V, Saglio G, Mandelli F, Lo-Coco F, Pelicci PG, Martelli MF: *Cytoplasmic nucleophosmin in acute myelogenous leukemia with a normal karyotype*: N Engl J Med, 2005. **352**: 254-266.

48. Fazi F, Racanicchi S, Zardo G, Starnes LM, Mancini M, Travaglini L, Diverio D, Ammatuna E, Cimino G, Lo-Coco F, Grignani F, Nervi C: *Epigenetic silencing of the myelopoiesis regulator microRNA-223 by the AML1/ETO oncoprotein*: Cancer Cell, 2007. **12**: 457-466.

49. Fischbach NA, Rozenfeld S, Shen W, Fong S, Chrobak D, Ginzinger D, Kogan SC, Radhakrishnan A, Le Beau MM, Largman C, Lawrence HJ: *HOXB6 overexpression in murine bone marrow immortalizes a myelomonocytic precursor in vitro and causes hematopoietic stem cell expansion and acute myeloid leukemia in vivo*: Blood, 2005. **105**: 1456-1466.

50. Friedle H, Knochel W: *Cooperative interaction of Xvent-2 and GATA-2 in the activation of the ventral homeobox gene Xvent-1B*: J Biol Chem, 2002. **277**: 23872-23881.

51. Friedman RC, Farh KK, Burge CB, Bartel DP: *Most mammalian mRNAs are conserved targets of microRNAs*: Genome Res, 2009. **19**: 92-105.

52. Gao H, Le Y, Wu X, Silberstein LE, Giese RW, Zhu Z: *VentX, a novel lymphoid-enhancing factor/T-cell factor-associated transcription repressor, is a putative tumor suppressor*: Cancer Res, 2010. **70**: 202-211.

53. Garzon R, Garofalo M, Martelli MP, Briesewitz R, Wang L, Fernandez-Cymering C, Volinia S, Liu CG, Schnittger S, Haferlach T, Liso A, Diverio D, Mancini M, Meloni G, Foa R, Martelli MF, Mecucci C, Croce CM, Falini B: *Distinctive microRNA signature of acute myeloid leukemia bearing cytoplasmic mutated nucleophosmin*: Proc Natl Acad Sci USA, 2008. **105**: 3945-3950.

54. Gawantka V, Delius H, Hirschfeld K, Blumenstock C, Niehrs C: *Antagonizing the Spemann organizer: role of the homeobox gene Xvent-1*: EMBO J, 1995. **14**: 6268-6279.

55. Gehring WJ, Qian QY, Billeter M, Furukubo-Tokunaga K, Schier AF, Resendez-Perez D, Affolter M, Otting G, WuthrichK: *Homeodomain-DNA recognition*: Cell, 1994. **78**: 211-223.

56. Giampaolo A, Sterpetti P, Bulgarini D, Samoggia P, Pelosi E, Valtieri M, Peschle C: *Key functional role and lineage-specific expression of selected HOXB genes in purified hematopoietic progenitor differentiation*: Blood, 1994. **84**: 3637-3647.

57. Gilliland DG, Griffin JD: *Role of FLT3 in leukemia*: Curr Opin Hematol, 2002. **9**: 274-281.

58. Gilliland DG, Griffin JD: *The roles of FLT3 in hematopoiesis and leukemia*: Blood, 2002. **100**: 1532-1542.

59. Gilliland DG, Jordan CT, Felix CA: *The molecular basis of leukemia*: Hematology Am Soc Hematol Educ Program, 2004: 80-97.

60. Godin I, Cumano A: *The hare and the tortoise: an embryonic haematopoietic race*: Nat Rev Immunol, 2002. **2**: 593-604.

61. Godin I, Dieterlen-Lievre F, Cumano A: *Emergence of multipotent hemopoietic cells in the yolk sac and paraaortic splanchnopleura in mouse embryos, beginning at 8.5 days postcoitus*: Proc Natl Acad Sci USA, 1995. **92**: 773-777.

62. Griffiths-Jones S, Saini HK, van Dongen S, Enright AJ: *miRBase: tools for microRNA genomics*: Nucleic Acids Res, 2008. **36**: D154-158.

63. Guo L, Lu Z: *The fate of miRNA* strand through evolutionary analysis: implication for degradation as merely carrier strand or potential regulatory molecule?* : PLoS One, 2010. **5**: e11387.

64. Han YC, Park CY, Bhagat G, Zhang J, Wang Y, Fan JB, Liu M, Zou Y, Weissman IL, Gu H: *microRNA-29a induces aberrant self-renewal capacity in hematopoietic progenitors, biased myeloid development, and acute myeloid leukemia*: J Exp Med, 2010. **207**: 475-489.

65. Hanahan D, Weinberg RA: *The hallmarks of cancer*: Cell, 2000. **100**: 57-70.

66. Harland R, Gerhart J: *Formation and function of Spemann´ s organizer.* Annu: Rev. Cell Dev. Biol., 1997. **13**: 611-617.

67. Harris NL, Jaffe ES, Diebold J, Flandrin G, Muller-Hermelink HK, Vardiman J, Lister TA, Bloomfield CD: *The World Health Organization classification of neoplastic diseases of the hematopoietic and lymphoid tissues. Report of the Clinical Advisory Committee meeting, Airlie House, Virginia, November, 1997*: Ann Oncol, 1999. **10**: 1419-1432.

68. Havelange V, Garzon R: *MicroRNAs: emerging key regulators of hematopoiesis*: Am J Hematol, 2010. **85**: 935-942.

69. Henningfeld KA, Friedle H, Rastegar S, Knochel W: *Autoregulation of Xvent-2B; direct interaction and functional cooperation of Xvent-2 and Smad1*: J Biol Chem, 2002. **277**: 2097-2103.

70. Hisa T, Spence SE, Rachel RA, Fujita M, Nakamura T, Ward JM, Devor-Henneman DE, Saiki Y, Kutsuna H, Tessarollo L, Jenkins NA, Copeland NG: *Hematopoietic, angiogenic and eye defects in Meis1 mutant animals*: EMBO J, 2004. **23**: 450-459.

71. Hock H, Meade E, Medeiros S, Schindler JW, Valk PJ, Fujiwara Y, Orkin SH: *Tel/Etv6 is an essential and selective regulator of adult hematopoietic stem cell survival*: Genes Dev, 2004. **18**: 2336-2341.

72. Holland PW, Booth HA, Bruford EA: *Classification and nomenclature of all human homeobox genes*: BMC Biol, 2007. **5**: 47.

73. Huber TL, Zon LI: *Transcriptional regulation of blood formation during Xenopus development*: Semin Immunol, 1998. **10**: 103-109.

74. Ibrahim AM, Mansour IM, Wilson MM, Mokhtar DA, Helal AM, Al Wakeel AM: *Study of Survivin and X-Linked Inhibitor of Apoptosis Protein (XIAP) Genes in Acute Myeloid Leukemia (AML)*: Lab Hematol, 2012. **18**: 1-10.

75. Imamura T, Morimoto A, Takanashi M, Hibi S, Sugimoto T, Ishii E, Imashuku S: *Frequent co-expression of HoxA9 and Meis1 genes in infant acute lymphoblastic leukaemia with MLL rearrangement*: Br J Haematol, 2002. **119**: 119-121.

76. Ishikawa A, Sasaki M, Ohira S, Ohta T, Oda K, Nimura Y, Chen MF, Jan YY, Yeh TS, Nakanuma Y: *Aberrant expression of CDX2 is closely related to the intestinal metaplasia and MUC2 expression in intraductal papillary neoplasm of the liver in hepatolithiasis.* Lab Invest: 2004. **84**: 629-638.

77. Ishikawa M, Yagasaki F, Okamura D, Maeda T, Sugahara Y, Jinnai I, Bessho M: *A novel gene, ANKRD28 on 3p25, is fused with NUP98 on 11p15 in a cryptic 3-way translocation of t(3;5;11)(p25;q35;p15) in an adult patient with myelodysplastic syndrome/acute myelogenous leukemia*: Int J Hematol, 2007. **86**: 238-245.

78. Iwama A, Oguro H, Negishi M, Kato Y, Morita Y, Tsukui H, Ema H, Kamijo T, Katoh-Fukui Y, Koseki H, van Lohuizen M, Nakauchi H: *Enhanced self-renewal of hematopoietic stem cells mediated by the polycomb gene product Bmi-1* : Immunity, 2004. **21**: 843-851.

79. Iwasaki H, Mizuno S, Arinobu Y, Ozawa H, Mori Y, Shigematsu H, Takatsu K, Tenen DG, Akashi K: *The order of expression of transcription factors di-*

rects hierarchical specification of hematopoietic lineages: Genes Dev, 2006. **20**: 3010-3021.

80. Jacob B, Osato M, Yamashita N, Wang CQ, Taniuchi I, Littman DR, Asou N, Ito Y: *Stem cell exhaustion due to Runx1 deficiency is prevented by Evi5 activation in leukemogenesis*: Blood, 2010. **115**: 1610-1620.

81. Jagadeeswaran G, Zheng Y, Sumathipala N, Jiang H, Arrese EL, Soulages JL, Zhang W, Sunkar R: *Deep sequencing of small RNA libraries reveals dynamic regulation of conserved and novel microRNAs and microRNA-stars during silkworm development*: BMC Genomics, 2010. **11**: 52.

82. Johnson SM, Grosshans H, Shingara J, Byrom M, Jarvis R, Cheng A, Labourier E, Reinert KL, Brown D, Slack FJ: *RAS is regulated by the let-7 microRNA family*: Cell, 2005. **120**: 635-647.

83. Jones CM, Dale L, Hogan BL, Wright CV, Smith JC: *Bone morphogenetic protein-4 (BMP-4) acts during gastrula stages to cause ventralization of Xenopus embryos*: Development, 1996. **122**: 1545-1554.

84. Kamps MP, Look AT, Baltimore D: *The human t(1;19) translocation in pre-B ALL produces multiple nuclear E2A-Pbx1 fusion proteins with differing transforming potentials*: Genes Dev, 1991. **5**: 358-368.

85. Kim VN: *MicroRNA biogenesis: coordinated cropping and dicing*: Nat Rev Mol Cell Biol, 2005. **6**: 376-385.

86. Kling, PJ, Taing KM, Dvorak B, Woodward SS, Philipps AF: *Insulin-like growth factor-I stimulates erythropoiesis when administered enterally*: Growth Factors, 2006. **24**: 218-223.

87. Kloosterman WP, Plasterk RH:*The diverse functions of microRNAs in animal development and disease*: Dev Cell, 2006. **11**: 441-450.

88. Kondo M, Weissman IL, Akashi K: *Identification of clonogenic common lymphoid progenitors in mouse bone marrow*: Cell, 1997. **91**: 661-672.

89. Kongsuwan K, Allen J, Adams JM: *Expression of Hox-2.4 homeobox gene directed by proviral insertion in a myeloid leukemia*: Nucleic Acids Res, 1989. **17**: 1881-1892.

90. Kozomara A, Griffiths-Jones S: *miRBase: integrating microRNA annotation and deep-sequencing data*: Nucleic Acids Res, 2011. **39**: D152-157.

91. Kroeze LI, Nikoloski G, da Silva-Coelho P, van Hoogen P, Stevens-Linders E, Kuiper RP, Schnittger S, Haferlach T, Pahl HL, van der Reijden BA, Jansen JH: *Genetic defects in PRC2 components other than EZH2 are not common in myeloid malignancies*: Blood, 2012. **119**: 1318-1319.

92. Kroon E, Krosl J, Thorsteinsdottir U, Baban S, Buchberg AM, Sauvageau G: *Hoxa9 transforms primary bone marrow cells through specific collaboration with Meis1a but not Pbx1b*: EMBO J, 1998. **17**: 3714-3725.

93. Krumlauf R: *Hox genes in vertebrate development*: Cell, 1994. **78**: 191-201.

94. Krutzfeldt J, Rajewsky N, Braich R, Rajeev KG, Tuschl T, Manoharan M, Stoffel M: *Silencing of microRNAs in vivo with 'antagomirs'*: Nature, 2005. **438**: 685-689.

95. Kumaravelu P, Hook L, Morrison AM, Ure J, Zhao S, Zuyev S, Ansell J, Medvinsky A: *Quantitative developmental anatomy of definitive haematopoietic stem cells/long-term repopulating units (HSC/RUs): role of the aorta-gonad-mesonephros (AGM) region and the yolk sac in colonisation of the mouse embryonic liver*: Development, 2002. **129**: 4891-4899.

96. Ladher R, Mohun TJ, Smith JC, Snape AM: *Xom: a Xenopus homeobox gene that mediates the early effects of BMP-4*: Development, 1996. **122**: 2385-2394.

97. Lai CY, Yu SL, Hsieh MH, Chen CH, Chen HY, Wen CC, Huang YH, Hsiao PC, Hsiao CK, Liu CM, Yang PC, Hwu HG, Chen WJ: *MicroRNA expression aberration as potential peripheral blood biomarkers for schizophrenia*: PLoS One, 2011. **6**: e21635.

98. Lai KW, Koh KX, Loh M, Tada K, Subramaniam MM, Lim XY, Vaithilingam A, Salto-Tellez M, Iacopetta B, Ito Y, Soong R: *MicroRNA-130b regulates the tumour suppressor RUNX3 in gastric cancer*: Eur J Cancer, 2010. **46**: 1456-1463.

99. Lawrence HJ, Sauvageau G, Humphries RK, Largman C: *The role of HOX homeobox genes in normal and leukemic hematopoiesis*: Stem Cells, 1996. **14**: 281-291.

100. Lawrence PA, Morata G: *Homeobox genes: their function in Drosophila segmentation and pattern formation*: Cell, 1994. **78**: 181-189.

101. LeBrun DP, Cleary ML: *Fusion with E2A alters the transcriptional properties of the homeodomain protein PBX1 in t(1;19) leukemias*: Oncogene, 1994. **9**: 1641-1647.

102. Lee RC, Feinbaum RL, Ambros V: *The C. elegans heterochronic gene lin-4 encodes small RNAs with antisense complementarity to lin-14*: Cell, 1993. **75**: 843-854.

103. Lewis BP, Burge CB, Bartel DP: *Conserved seed pairing, often flanked by adenosines, indicates that thousands of human genes are microRNA targets*: Cell, 2005. **120**: 15-20.

104. Lewis BP, Shih IH, Jones-Rhoades MW, Bartel DP, Burge CB: *Prediction of mammalian microRNA targets*: Cell, 2003. **115**: 787-798.

105. Lewis EB: *A gene complex controlling segmentation in Drosophila*: Nature, 1978. **276**: 565-570.

106. Li M, Collins R, Jiao Y, Ouillette P, Bixby D, Erba H, Vogelstein B, Kinzler KW, Papadopoulos N, Malek SN: *Somatic mutations in the transcriptional corepressor gene BCORL1 in adult acute myelogenous leukemia*: Blood, 2011. **118**: 5914-5917.

107. Lim LP, Glasner ME, Yekta S, Burge CB, Bartel DP: *Vertebrate microRNA genes*: Science, 2003. **299**: 1540.

108. Lin H, Grosschedl R: *Failure of B-cell differentiation in mice lacking the transcription factor EBF*: Nature, 1995. **376**: 263-267.

109. Lin YW, Slape C, Zhang Z, Aplan PD: *NUP98-HOXD13 transgenic mice develop a highly penetrant, severe myelodysplastic syndrome that progresses to acute leukemia*: Blood, 2005. **106**: 287-295.

110. Liu, AM, Yao TJ, Wang W, Wong KF, Lee NP, Fan ST, Poon RT, Gao C, Luk JM: *Circulating miR-15b and miR-130b in serum as potential markers for detecting hepatocellular carcinoma: a retrospective cohort study*: BMJ Open, 2012. **2**: e000825.

111. Liu H, Cheng EH, Hsieh JJ: *MLL fusions: pathways to leukemia*: Cancer Biol Ther, 2009. **8**: 1204-1211.

112. Lowenberg B, Downing JR, Burnett A: *Acute myeloid leukemia*: N Engl J Med, 1999. **341**: 1051-1062.

113. Lu Y, Thomson JM, Wong HY, Hammond SM, Hogan BL: *Transgenic over-expression of the microRNA miR-17-92 cluster promotes proliferation and inhibits differentiation of lung epithelial progenitor cells*: Dev Biol, 2007. **310**: 442-453.

114. Lundin C, Horvat A, Karlsson K, Olofsson T, Paulsson K, Johansson B: *t(9;11)(p22;p15) [NUP98/PSIP1] is a poor prognostic marker associated with de novo acute myeloid leukaemia expressing both mature and immature surface antigens*: Leuk Res, 2011. **35**: e75-76.

115. Ma S, Chan YP, Kwan PS, Lee TK, Yan M, Tang KH, Ling MT, Vielkind JR, Guan XY, Chan KW: *MicroRNA-616 induces androgen-independent growth of prostate cancer cells by suppressing expression of tissue factor pathway inhibitor TFPI-2*: Cancer Res, 2011. **71**: 583-592.

116. Ma S, Tang KH, Chan YP, Lee TK, Kwan PS, Castilho A, Ng I, Man K, Wong N, To KF, Zheng BJ, Lai PB, Lo CM, Chan KW, Guan XY: *miR-130b Promotes CD133(+) liver tumor-initiating cell growth and self-renewal via tumor protein 53-induced nuclear protein 1*: Cell Stem Cell, 2010. **7**: 694-707.

117. Maeno M, Mead PE, Kelley C, Xu RH, Kung HF, Suzuki A, Ueno N, Zon LI: *The role of BMP-4 and GATA-2 in the induction and differentiation of hematopoietic mesoderm in Xenopus laevis*: Blood, 1996. **88**: 1965-1972.

118. Magli MC, Barba P, Celetti A, De Vita G, Cillo C, Boncinelli E: *Coordinate regulation of HOX genes in human hematopoietic cells*: Proc Natl Acad Sci USA, 1991. **88**: 6348-6352.

119. Majewski IJ, Blewitt ME, de Graaf CA, McManus EJ, Bahlo M, Hilton AA, Hyland CD, Smyth GK, Corbin JE, Metcalf D, Alexander WS, Hilton DJ: *Polycomb repressive complex 2 (PRC2) restricts hematopoietic stem cell activity*: PLoS Biol, 2008. **6**: e93.

120. Manz MG, Traver D, Miyamoto T, Weissman IL, Akashi K: *Dendritic cell potentials of early lymphoid and myeloid progenitors*: Blood, 2001. **97**: 3333-3341.

121. Mark M, Rijli FM, Chambon P: *Homeobox genes in embryogenesis and pathogenesis*: Pediatr Res, 1997. **42**: 421-429.

122. Martin-Perez D, Sanchez E, Maestre L, Suela J, Vargiu P, Di Lisio L, Martinez N, Alves J, Piris MA, Sanchez-Beato M: *Deregulated expression of the polycomb-group protein SUZ12 target genes characterizes mantle cell lymphoma*: Am J Pathol, 2010. **177**: 930-942.

123. Maziere P, Enright AJ: *Prediction of microRNA targets.* Drug Discov Today: 2007. **12**: 452-458.

124. McDaneld TG, Smith TP, Doumit ME, Miles JR, Coutinho LL, Sonstegard TS, Matukumalli LK, Nonneman DJ, Wiedmann RT: *MicroRNA transcriptome profiles during swine skeletal muscle development*: BMC Genomics, 2009. **10**: 77.

125. McGinnis W, Garber RL, Wirz J, Kuroiwa A, Gehring WJ: *A homologous protein-coding sequence in Drosophila homeotic genes and its conservation in other metazoans*: Cell, 1984. **37**: 403-408.

126. Mead PE, Kelley CM, Hahn PS, Piedad O, Zon LI: *SCL specifies hematopoietic mesoderm in Xenopus embryos*: Development, 1998. **125**: 2611-2620.

127. Medvinsky A, Dzierzak E: *Definitive hematopoiesis is autonomously initiated by the AGM region*: Cell, 1996. **86**: 897-906.

128. miRBase: http://www.mirbase.org/ (2012/11/31).

129. Miyake N, Brun AC, Magnusson M, Miyake K, Scadden DT, Karlsson S: *HOXB4-induced self-renewal of hematopoietic stem cells is significantly enhanced by p21 deficiency*: Stem Cells, 2006. **24**: 653-661.

130. Moens CB, Selleri L: *Hox cofactors in vertebrate development*: Dev Biol, 2006. **291**: 193-206.

131. Moore MA, Metcalf D: *Ontogeny of the hematopoietic system:yolk sac origin of in vivo and in vitro colony forming cells in the developing mouse embryo*: Br J Haematol., 1970. **18**: 279-296.

132. Morerio C, Acquila M, Rosanda C, Rapella A, Tassano E, Micalizzi C, Panarello C: *t(9;11)(p22;p15) with NUP98-LEDGF fusion gene in pediatric acute myeloid leukemia*: Leuk Res, 2005. **29**: 467-470.

133. Moretti PA, Davidson AJ, Baker E, Lilley B, Zon LI, D'Andrea RJ: *Molecular cloning of a human Vent-like homeobox gene*: Genomics, 2001. **76**: 21-29.

134. Morrison SJ, Weissman IL: *The long-term repopulating subset of hematopoietic stem cells is deterministic and isolatable by phenotype*: Immunity, 1994. **1**: 661-673.

135. Moskow JJ, Bullrich F, Huebner K, Daar IO, Buchberg AM: *Meis1, a PBX1-related homeobox gene involved in myeloid leukemia in BXH-2 mice*: Mol Cell Biol, 1995. **15**: 5434-5443.

136. MultAlin: http://multalin.toulouse.inra.fr/multalin/ (2011-11-25).

137. Myers C, Charboneau A, Cheung I, Hanks D, Boudreau N: *Sustained expression of homeobox D10 inhibits angiogenesis*: Am J Pathol, 2002. **161**: 2099-2109.

138. Nakamura T: *NUP98 fusion in human leukemia: dysregulation of the nuclear pore and homeodomain proteins*: Int J Hematol, 2005. **82**: 21-27.

139. Nutt SL, Heavey B, Rolink AG, Busslinger M: *Commitment to the B-lymphoid lineage depends on the transcription factor Pax5*: Nature, 1999. **401**: 556-562.

140. Olena AF, Patton JG: *Genomic organization of microRNAs*: J Cell Physiol, 2010. **222**: 540-545.

141. Onichtchouk D, Glinka A, Niehrs C: *Requirement for Xvent-1 and Xvent-2 gene function in dorsoventral patterning of Xenopus mesoderm*:Development, 1998. **125**: 1447-1456.

142. Orkin SH: *Diversification of haematopoietic stem cells to specific lineages*: Nat Rev Genet, 2000. **1**: 57-64.

143. Orkin SH, Zon LI: *Hematopoiesis: an evolving paradigm for stem cell biology*: Cell, 2008. **132**: 631-644.

144. Ottersbach K, Dzierzak E: *The placenta as a hematopoietic organ*: Int J Dev Biol., 2010. **54**: 1099-1106.

145. Owens BM, Hawley RG: *HOX and non-HOX homeobox genes in leukemic hematopoiesis*: Stem Cells, 2002. **20**: 364-379.

146. Papalopulu N, Kintner C: *A Xenopus gene, Xbr-1, defines a novel class of homeobox genes and is expressed in the dorsal ciliary margin of the eye*: Dev Biol, 1996. **174**: 104-114.

147. Passegue E, Jamieson CH, Ailles AE, Weissman IL: *Normal and leukemic hematopoiesis: are leukemias a stem cell disorder or a reacquisition of stem cell characteristics?* : Proc Natl Acad Sci USA, 2003. **100 Suppl 1**: p. 11842-11849.

148. Paz H, Lynch MR, Bogue CW, Gasson JC: *The homeobox gene Hhex regulates the earliest stages of definitive hematopoiesis*: Blood, 2010. **116**: 1254-1262.

149. Peterson LF, Zhang DE: *The 8;21 translocation in leukemogenesis*: Oncogene, 2004. **23**: 4255-4262.

150. Pizzatti L, Binato R, Cofre J, Gomes BE, Dobbin J, Haussmann ME, D'Azambuja D, Bouzas LF, Abdelhay E: *SUZ12 is a candidate target of the non-canonical WNT pathway in the progression of chronic myeloid leukemia*: Genes Chromosomes Cancer, 2010. **49**: 107-118.

151. PubMed: http://www.ncbi.nlm.nih.gov/nuccore/NM_014468.2 (19.01.2012).

152. Querfurth E, Schuster M, Kulessa H, Crispino JD, Doderlein G, Orkin SH, Graf T, Nerlov C: *Antagonism between C/EBPbeta and FOG in eosinophil lineage commitment of multipotent hematopoietic progenitors.* Genes Dev, 2000. **14**: 2515-2525.

153. Rastegar S, Friedle H, Frommer G, Knochel W: *Transcriptional regulation of Xvent homeobox genes*: Mech Dev, 1999. **81**: 139-149.

154. Rawat VP, Cusan M, Deshpande A, Hiddemann W, Quintanilla-Martinez L, Humphries RK, Bohlander SK, Feuring-Buske M, Buske C: *Ectopic expression of the homeobox gene Cdx2 is the transforming event in a mouse model of t(12;13)(p13;q12) acute myeloid leukemia*: Proc Natl Acad Sci USA, 2004. **101**: 817-822.

155. Rawat VP, Arseni N, Ahmed F, Mulaw MA, Thoene S, Heilmeier B, Sadlon T, D'Andrea RJ, Hiddemann W, Bohlander SK, Buske C, Feuring-Buske M: *The vent-like homeobox gene VENTX promotes human myeloid differentiation and is highly expressed in acute myeloid leukemia.* Proc Natl Acad Sci USA, 2010. **107**: 16946-16951

156. Reya T, Clevers H: *Wnt signalling in stem cells and cancer*: Nature, 2005. **434**: 843-850.

157. Reya T, Duncan AW, Ailles L, Domen J, Scherer DC, Willert K, Hintz L, Nusse R, Weissman IL: *A role for Wnt signalling in self-renewal of haematopoietic stem cells*: Nature, 2003. **423**: 409-414.

158. Reya T, Morrison SJ, Clarke MF, Weissman IL: *Stem cells, cancer, and cancer stem cells*: Nature, 2001. **414**: 105-111.

159. Reya T, O'Riordan M, Okamura R, Devaney E, Willert K, Nusse R, Grosschedl R: *Wnt signaling regulates B lymphocyte proliferation through a LEF-1 dependent mechanism*: Immunity, 2000. **13**: 15-24.

160. Rice KL, Licht JD: *HOX deregulation in acute myeloid leukemia*: J Clin Invest, 2007. **117**: 865-868.

161. Ro S, Park C, Young D, Sanders KM, Yan W: *Tissue-dependent paired expression of miRNAs*: Nucleic Acids Res, 2007. **35**(17): 5944-5953.

162. Rodriguez A, Griffiths-Jones S, Ashurst JL, Bradley A: *Identification of mammalian microRNA host genes and transcription units*: Genome Res, 2004. **14**: 1902-1910.

163. Rossi DJ, Weissman IL: *Pten, tumorigenesis, and stem cell self-renewal*: Cell, 2006. **125**: 229-231.

164. Sauvageau G, Lansdorp PM, Eaves CJ, Hogge DE, Dragowska WH, Reid DS, Largman C, Lawrence HJ, Humphries RK: *Differential expression of homeobox genes in functionally distinct CD34+ subpopulations of human bone marrow cells*: Proc Natl Acad Sci USA, 1994. **91**: 12223-12227.

165. Schmidt JE, von Dassow G, Kimelman D: *Regulation of dorsal-ventral patterning: the ventralizing effects of the novel Xenopus homeobox gene Vox*: Development, 1996. **122**: 1711-1721.

166. Schuler-Metz A, Knochel S, Kaufmann E, Knochel W: *The homeodomain transcription factor Xvent-2 mediates autocatalytic regulation of BMP-4 expression in Xenopus embryos*: J Biol Chem, 2000. **275**: 34365-34374.

167. Shen WF, Montgomery JC, Rozenfeld S, Moskow JJ, Lawrence HJ, Buchberg AM, Largman C: *AbdB-like Hox proteins stabilize DNA binding by the Meis1 homeodomain proteins*: Mol Cell Biol, 1997. **17**: 6448-6458.

168. Shimon I, Shpilberg O: *The insulin-like growth factor system in regulation of normal and malignant hematopoiesis*: Leuk Res, 1995. **19**: 233-240.

169. Siomi H, Siomi MC: *On the road to reading the RNA-interference code*: Nature, 2009. **457**: 396-404.

170. Sirulnik A, Melnick A, Zelent A, Licht JD: *Molecular pathogenesis of acute promyelocytic leukaemia and APL variants*: Best Pract Res Clin Haematol, 2003. **16**: 387-408.

171. Sparmann A, van Lohuizen M: *Polycomb silencers control cell fate, development and cancer*: Nat Rev Cancer, 2006. **6**: 846-856.

172. Streicher KL, Zhu W, Lehmann KP, Georgantas RW, Morehouse CA, Brohawn P, Carrasco RA, Xiao Z, Tice DA, Higgs BW, Richman L, Jallal B, Ranade K, Yao Y: *A novel oncogenic role for the miRNA-506-514 cluster in initiating melanocyte transformation and promoting melanoma growth*: Oncogene, 2012. **31**: 1558-1570.

173. Su X, Drabkin H, Clappier E, Morgado E, Busson M, Romana S, Soulier J, Berger R, Bernard OA, Lavau C: *Transforming potential of the T-cell acute lymphoblastic leukemia-associated homeobox genes HOXA13, TLX1, and TLX3*: Genes Chromosomes Cancer, 2006. **45**: 846-855.

174. Sung KW, Choi J, Hwang YK, Lee SJ, Kim HJ, Kim JY, Cho EJ, Yoo KH, Koo HH: *Overexpression of X-linked inhibitor of apoptosis protein (XIAP) is an independent unfavorable prognostic factor in childhood de novo acute myeloid leukemia*: J Korean Med Sci, 2009. **24**: 605-613.

175. Suresh S, McCallum L, Lu W, Lazar N, Perbal B, Irvine AE: *MicroRNAs 130a/b are regulated by BCR-ABL and downregulate expression of CCN3 in CML*: J Cell Commun Signal, 2011. **5**: 183-191.

176. Taketani T, Taki T, Ono R, Kobayashi Y, Ida K, Hayashi Y: *The chromosome translocation t(7;11)(p15;p15) in acute myeloid leukemia results in fusion of the NUP98 gene with a HOXA cluster gene, HOXA13, but not HOXA9*: Genes Chromosomes Cancer, 2002. **34**: 437-443.

177. Tanzer A, Amemiya CT, Kim CB, Stadler PF: *Evolution of microRNAs located within Hox gene clusters*: J Exp Zool B Mol Dev Evol, 2005. **304**: 75-85.

178. TargetScanHuman Custom: http://www.targetscan.org/vert_50/seedmatch.html (2012-03-07).

179. Tessel MA, Benham AL, Krett NL, Rosen ST, Gunaratne PH: *Role for microRNAs in regulating glucocorticoid response and resistance in multiple myeloma*: Horm Cancer, 2011. **2**: 182-189.

180. Thomson GH: *Antagonism within and around the organizer: BMP inhibitors in vertebrate body patterning*: Trends Genet, 1997. **13**: 209-211.

181. Thorsteinsdottir U, Sauvageau G, Hough MR, Dragowska W, Lansdorp PM, Lawrence HJ, Largman C, Humphries RK: *Overexpression of HOXA10 in murine hematopoietic cells perturbs both myeloid and lymphoid differentiation and leads to acute myeloid leukemia*: Mol Cell Biol, 1997. **17**: 495-505.

182. Tiacci E, Grossmann V, Martelli MP, Kohlmann A, Haferlach T, Falini B:*The corepressors BCOR and BCORL1: two novel players in acute myeloid leukemia*: Haematologica, 2011. **97**: 3-5.

183. Tickenbrock L, Hehn S, Sargin B, Choudhary C, Baumer N, Buerger H, Schulte B, Muller O, Berdel WE, Muller-Tidow C, Serve H: *Activation of Wnt signalling in acute myeloid leukemia by induction of Frizzled-4*: Int J Oncol, 2008. **33**: 1215-1221.

184. Tong JL, Zhang CP, Nie F, Xu XT, Zhu MM, Xiao SD, Ran ZH: *MicroRNA 506 regulates expression of PPAR alpha in hydroxycamptothecin-resistant human colon cancer cells*: FEBS Lett, 2011. **585**: 3560-3568.

185. Tonks A, Pearn L, Musson M, Gilkes A, Mills KI, Burnett AK, Darley RL: *Transcriptional dysregulation mediated by RUNX1-RUNX1T1 in normal human progenitor cells and in acute myeloid leukaemia*: Leukemia, 2007. **21**: 2495-2505.

186. Tsang A, Visvader JE, Turner CA, Fujiwara Y, Yu C, Weiss MJ, Crossley M, Orkin SH: *FOG, a multitype zinc finger protein, acts as a cofactor for transcription factor GATA-1 in erythroid and megakaryocytic differentiation*: Cell, 1997. **90**: 109-119.

187. USCS Genome Browser: http://genome.ucsc.edu/ (2011-12-07).

188. Vardiman JW, Thiele J, Arber DA, Brunning RD, Borowitz MJ, Porwit A, Harris NL, Le Beau MM, Hellstrom-Lindberg E, Tefferi A, Bloomfield CD: *The 2008 revision of the World Health Organization (WHO) classification of myeloid neoplasms and acute leukemia: rationale and important changes*: Blood, 2009. **114**: 937-951.

189. Vigorito E, Perks KL, Abreu-Goodger C, Bunting S, Xiang Z, Kohlhaas S, Das PP, Miska EA, Rodriguez A, Bradley A, Smith KG, Rada C, Enright AJ,

Toellner KM, Maclennan IC, Turner M: *microRNA-155 regulates the generation of immunoglobulin class-switched plasma cells*: Immunity, 2007. **27**: 847-859.

190. Wang L, Chen S, Xue M, Zhong J, Wang X, Gan L, Lam EK, Liu X, Zhang J, Zhou T, Yu J, Jin H, Si J: *Homeobox D10 gene, a candidate tumor suppressor, is downregulated through promoter hypermethylation and associated with gastric carcinogenesis:* Mol Med, 2011. **18**: 389-400.

191. Winnier G, Blessing M, Labosky PA, Hogan BL: *Bone morphogenetic protein-4 is required for mesoderm formation and patterning in the mouse*: Genes Dev, 1995. **9**: 2105-2116.

192. Wu X, Gao H, Ke W, Hager M, Xiao S, Freeman MR, Zhu Z: *VentX transactivates p53 and p16ink4a to regulate cellular senescence*: J Biol Chem, 2010. **286**: 12693-12701.

193. Wu X, Gao H, Ke W, Giese RW, Zhu Z: *The homeobox transcription factor VentX controls human macrophage terminal differentiation and proinflammatory activation*: J Clin Invest, 2011. **121**: 2599-2613.

194. Xiong JW: *Molecular and developmental biology of the hemangioblast*: Dev Dyn, 2008. **237**: 1218-1231.

195. Yang C, Cai J, Wang Q, Tang H, Cao J, Wu L, Wang Z: *Epigenetic silencing of miR-130b in ovarian cancer promotes the development of multidrug resistance by targeting colony-stimulating factor 1*:Gynecol Oncol, 2012. **124**: 325-334.

196. Yao Y, Suo AL, Li ZF, Liu LY, Tian T, Ni L, Zhang WG, Nan KJ, Song TS, Huang C: *MicroRNA profiling of human gastric cancer*: Mol Med Report, 2009. **2**: 963-970.

197. Yeung ML, Yasunaga J, Bennasser Y, Dusetti N, Harris D, Ahmad N, Matsuoka M, Jeang KT: *Roles for microRNAs, miR-93 and miR-130b, and tumor protein 53-induced nuclear protein 1 tumor suppressor in cell growth dysregulation by human T-cell lymphotrophic virus 1*: Cancer Res, 2008. **68**: 8976-8985.

198. Yoder MC: *Embryonic hematopoiesis in mice and humans*: Acta Paediatr Suppl, 2002. **91**: 5-8.

199. Yuan X, Liu C, Yang P, He S, Liao Q, Kang S, Zhao Y: *Clustered micro-RNAs' coordination in regulating protein-protein interaction network*: BMC Syst Biol, 2009. **3**: 65.

200. Zamore PD, Haley B: *Ribo-gnome: the big world of small RNAs*: Science, 2005. **309**: 1519-1524.

201. Zhang P, Zhang X, Iwama A, Yu C, Smith KA, Mueller BU, Narravula S, Torbett BE, Orkin SH, Tenen TG: *PU.1 inhibits GATA-1 function and erythroid differentiation by blocking GATA-1 DNA binding*: Blood, 2000. **96**: 2641-2648.

202. Zhao Y, Liu H, Li Y, Wu J, Greenlee AR, Yang C, Jiang Y: *The role of miR-506 in transformed 16HBE cells induced by anti-benzo[a]pyrene-trans-7,8-dihydrodiol-9,10-epoxide*: Toxicol Lett, 2011. **205**: 320-326.

203. Zhu J, Emerson SG: *Hematopoietic cytokines, transcription factors and lineage commitment:* Oncogene, 2002. **21**: 3295-3313.

204. Zhuang Y, Soriano P, Weintraub H: *The helix-loop-helix gene E2A is required for B cell formation*: Cell, 1994. **79**: 875-884.

7. Acknowledgement

I would like to thank my doctoral supervisor, Prof. Dr. Buske, for the opportunity to work on this thesis in his research group.

My special thanks to his wife, PD Dr. Feuring-Buske, who, in many meetings, gave valuable advice on writing this thesis.

I would like to take this opportunity to thank my co-supervisor, Jun. Prof. Dr. Vijay Rawat. I will never forget the day in the laboratory when he told me to 'think positive Alex', words which will stay with me for a long time. His patience and calm when working on scientific projects greatly impressed me.

My thanks also to Heather McMurtrie, who, with infinite patience and kindness, assisted me with my experiments and made an invaluable contribution to this thesis.

I would like to thank Silvia Thoene, who was a great help in evaluating experiments and structuring and developing this thesis.

My thanks to all other staff and former staff of the institute, who were always willing to help.

I thank the International Graduate School in Molecular Medicine, Ulm, whose doctoral grant has enabled me to devote all my time and energy to this thesis.

Finally, I would like to thank my family, friends and girlfriend for their great support.

8. Curriculum vitae

1. Personal information:

Name:	Alexander Grunenberg
Gender:	Male
Date of birth:	03.05.1986
Place of birth:	Essen, Germany
Nationality:	German

2. Education:

1992/08-1996/06	Elementary school Theodor-Angerhausen Schule, Dormagen, Germany
1996/08-2005/06	High school Bettina von Arnim Gymnasium, Dormagen, Germany
2005/06	University Entrance Qualification (Abitur)
2006/09-2008/08	Study of Medicine Semmelweis University, Budapest, Hungary
2008/10-2013/05	Study of Medicine University of Ulm, Ulm, Germany
2013/05	Medical Licensing Examination

3. Academic Degrees:

2013/07	Doctoral Thesis (Promotion), Medicine, University of Ulm, Institute for Experimental Tumor Research, Comprehensive Cancer Center Ulm, Supervisor: Prof. Dr. C. Buske, Co-Supervisor: Prof. Dr. V.P.S. Rawat

4. Employment history:

2010/10-2011/06	Promotionsprogramm Experimentelle Medizin, International Graduate School in Molecular Medicine Ulm